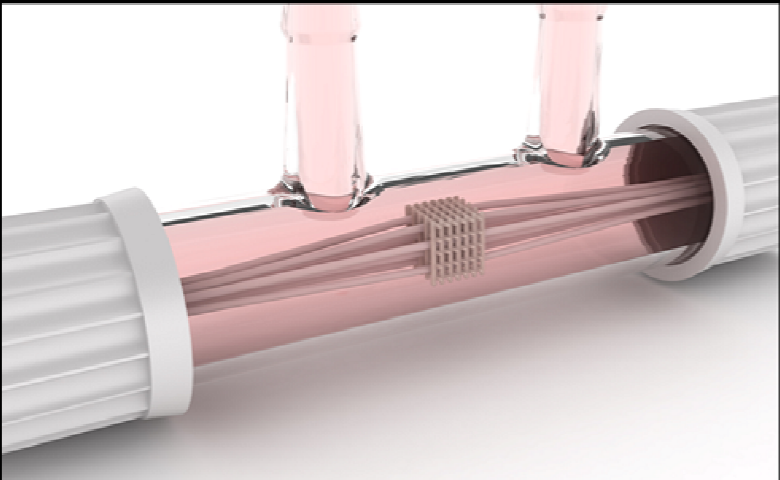


Membrane supported scaffold architectures for tissue engineering



Narasimha Murthy Srivatsa Bettahalli

**Membrane supported scaffold architectures
for
tissue engineering**

Narasimha Murthy Srivatsa Bettahalli

Members of the committee:

Chairman:	Prof. Dr.Ir. J. Huskens	(University of Twente, The Netherlands)
Promoter:	Prof. Dr.-Ing. M. Wessling	(University of Twente, The Netherlands)
Assistant Promoter:	Dr. D. Stamatialis	(University of Twente, The Netherlands)
Members:	Prof. Dr. C.A. van Blitterswijk	(University of Twente, The Netherlands)
	Prof. Dr. D.W. Grijpma	(University of Twente, The Netherlands)
	Prof. Dr. J. Vienken	(Fresenius Medical Care, Germany)
	Dr. C. Legallais	(Université de Technologie, France)

Author - Narasimha Murthy Srivatsa Bettahalli

Title - “Membrane supported scaffold architectures for tissue engineering”

PhD Thesis, University of Twente, Enschede, The Netherlands

The research described in this thesis was financially supported by STW (Utrecht, NL)
(Project number - TKG.6716)



Printed by: Gildeprint Drukkerijen, Enschede, The Netherlands

Cover designed by NM Srivatsa Bettahalli

The front cover shows dual flow glass bioreactor with 3D Free form fabricated scaffold integrated with hollow fibers (set-up artwork by Jonathan B Bennink of Tingle Visuals) and the back cover shows fluorescence microscope image of pre-labeled C2C12 cells cultured dynamically on multilayer cell-electrospun construct in dual flow perfusion bioreactor for 7 days (fluorescent image taken by Hemant Unadkat) and several SEM pictures at the top (PLLA hollow fiber, non-woven electrospun sheet and corrugated fiber) taken by the author.

MEMBRANE SUPPORTED SCAFFOLD ARCHITECTURES FOR TISSUE ENGINEERING

DISSERTATION

to obtain
the degree of doctor at the University of Twente,
on the authority of the rector magnificus,
prof. dr. H. Brinksma,
on account of the decision of the graduation committee,
to be publicly defended
on Friday 4th of February, 2011 at 16.45

by

Narasimha Murthy Srivatsa Bettahalli

born on March 31st, 1978
in Bangalore, India

Promoter: Prof. Dr. –Ing. M. Wessling

Assistant Promoter: Dr. D. Stamatialis

Copyright©: 2011, NMS Bettahalli, Enschede, The Netherlands.

Neither this book nor its parts may be reproduced without written permission of the author.

ISBN: 978-90-365-3151-1

DOI number: 10.3990/1.9789036531511 (<http://dx.doi.org/10.3990/1.9789036531511>)

Sanskrit shanti mantra

!!! Om Sahana Bhavatu, Sahanao Bhunaktu
Sahaveeryam Karvaa vahai
Tejaswee Naava Dheeta Mastu Ma Vidvishaa vahai
Om Shanti Shanti Shanti !!!

Translation

May He protect both of us, May He nourish both of us,
May we both acquire the capacity (to study and understand the scriptures),
May our study be brilliant, May we not argue with each other,
Om peace, peace, peace.

.... Dedicated to my entire family, especially my mom and dad

Table of contents

<i>Chapter 1</i>	
General introduction	1 - 36
<i>Chapter 2</i>	
Development of poly (L-lactic acid) hollow fiber membranes for artificial vasculature in tissue engineering scaffolds	37 - 64
<i>Chapter 3</i>	
Integration of hollow fiber membranes with 3D scaffolds improves nutrient supply in-vitro	65 - 98
<i>Chapter 4</i>	
Engineering multilayer tissue grafts capable of multi cellular organisation	99 - 132
<i>Chapter 5</i>	
Microstructured fibers for improving cell seeding and cell attachment in tissue engineering scaffolds	133 - 154
<i>Chapter 6</i>	
General conclusions and Outlook	155 - 168
<i>Summary / Samenvatting</i>	169 - 176
<i>Acknowledgements</i>	
<i>Curriculum vitae</i>	

Chapter 1

General introduction

Every person is a god in embryo. Its only desire is to be born.

(Deepak chopra)

Introduction

1. Tissue Engineering - general

Tissue engineering is a multidisciplinary field involving principles of engineering and life sciences to improve the health and quality of life for millions of people worldwide by repair, restoring, maintaining, or enhancing tissue and organ function using cells, scaffolds, and growth factors alone or in combination [1-3]. Along with the potential economic benefits from advanced tissue engineering technologies, reduced costs due to the availability of less expensive treatments for major medical problems is obvious, but indirect savings and dramatic improvements in treatment outcomes and quality of life for patients may prove to be even more important. There are several artificial tissues that are already being used for medical treatment (with limitations) which include fabricated skin, cartilage, blood vessels, bone, ligament and tendon [4-6]. It is also hoped that at least some of the whole organs like, liver, lung, kidney, pancreas, breast, intestine, etc. will become available off-the-shelf for treatment in the near future [7, 8].

Besides the therapeutic application where the tissue is either grown in a patient (*in-vivo*) or outside the patient (*in-vitro*) and then transplanted to the patient, tissue engineering can have diagnostic applications where the tissue is made *in-vitro* and used for testing drug metabolism and uptake, toxicity, and pathogenicity [9-12]. The foundation of tissue engineering / regenerative medicine for either therapeutic or diagnostic applications is the ability to exploit living cells in a variety of ways.

A tissue engineer first has to consider the function of the tissue - must it be strong? Elastic? Should it release certain proteins, like insulin from the pancreas, or filter toxins, like the kidneys? Then a 3D support must be designed that, when combined with cells, will eventually duplicate those functions, and continue to function properly in the body for years to come. Depending on the type of tissue, the design process can involve a variety of disciplines including mechanical / chemical engineering, molecular biology, physiology, medicine, polymer chemistry, and nanotechnology.

A common approach for *in-vitro* tissue engineering is the assembly of a hybrid construct consisting of a porous biodegradable matrix or scaffold to which cells can physically adhere after seeding. This *in-vitro* tissue precursor is often combined with bioactive molecules to stimulate proliferation and/or differentiation during the *in-vitro* culture period. Finally, the hybrid construct is implanted into the defect site to induce and direct the growth of new tissue of interest as the scaffold material degrades (Figure 1). Hence, tissue engineering research includes the following areas:

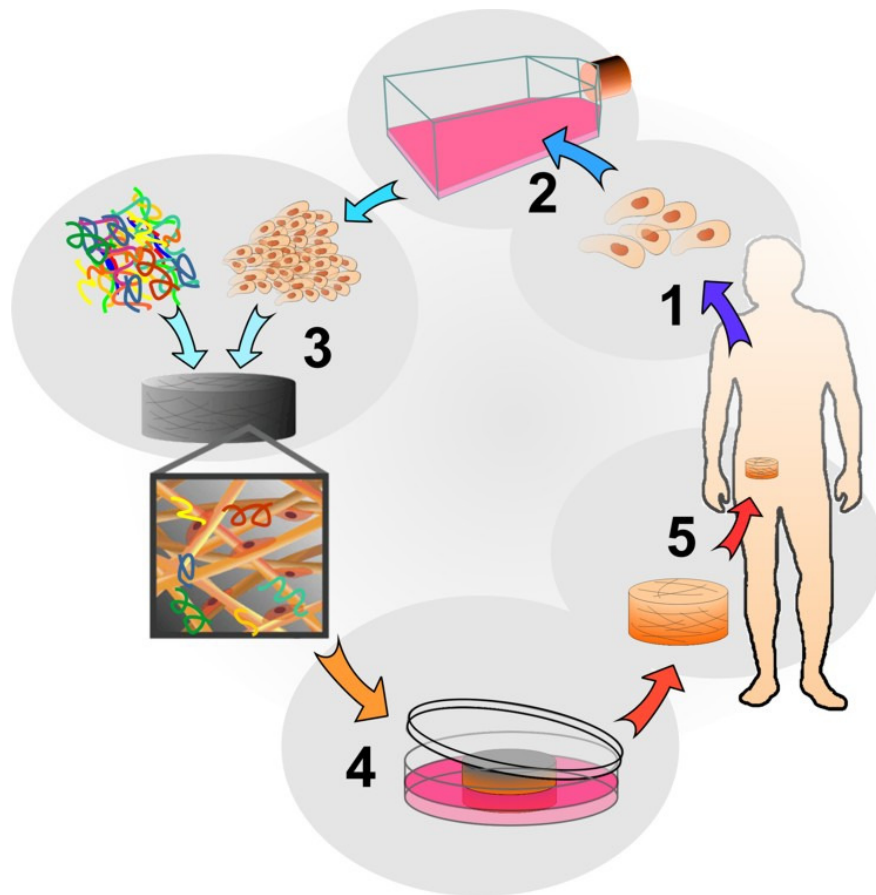


Figure 1. Tissue engineering approach: 1 – harvesting cells: 2 – expansion and/or differentiation of cells 3 – seed onto an appropriate scaffold with suitable growth factors 4 - place in static or dynamic culture system 5 - re-implant engineered construct. Adapted from Imperial college website.

Biomaterials

Biomaterials can be defined as substances in therapeutic or diagnostic systems that are in contact with biological fluids [13]. Tissue engineering includes novel biomaterials that are designed as *scaffolds* to direct the organization, growth, and differentiation of cells in the process of forming functional tissue by providing both physical and chemical cues. For instance, for cardiovascular implants the devices have certain size and surface requirements in order to avoid clotting [4], Cells attach to the scaffolds and reorganize themselves to form functional tissue by proliferating, synthesizing extracellular matrix, and migrating along the scaffold. This reorganization can begin to occur outside of the body in a bioreactor and then continue after implantation into a patient.

The number of biomaterials used for tissue engineering is vast. They can be categorized based on their application: for hard and soft tissue engineering or divided into natural and synthetic biomaterials [14-17] and their composites [18]. Natural biomaterials such as gelatin, agar, fibrin or collagen and synthetic bioresorbable polymers like poly lactide (PLA), poly glycolide (PGLA), poly (ethylene glycol) terephthalate - poly (butylene) terephthalate (PEGT-PBT) and polycaprolactone (PCL) and others have been used extensively for tissue engineering applications currently [16, 19-22].

An intrinsic property related to biomaterials is biocompatibility. Biocompatibility is defined as the biological performance of a certain material in a specific application and its acceptance/suitability for such application if both host and material responses are optimal [23, 24]. The material response focuses on fracture, wear, corrosion, dissolution, swelling and leaching [25, 26]. The degree of biocompatibility is not the same in all biomaterials. Often, material surface properties have to be modified in order to enhance the interaction of material with the host or biological fluid and suppress immunoresponses. Biomaterial surfaces can be modified either physically by methods like plasma etching, corona discharge, UV irradiation, etc. [21, 27] or by covalent attachment [28]. For the latter, chemical grafting, photografting, plasma polymerization, grafting with ionization radiation, self-assembled monolayer formation or biological modification, are some of the strategies being used to control host response and increase biocompatibility [29].

Bioresorbable / biodegradable polymers are designed to degrade within the body and be absorbed naturally once their function have been accomplished [17, 19]. The scaffolds are often made of polymers designed to degrade slowly and safely in the body, disappearing as the cells regenerate specific tissue of interest [22, 30]. Degraded materials can be extremely complex chemically [25, 26], a good scaffold must facilitate cell attachment without provoking an immune response, permit the diffusion of nutrients from the blood (*in-vivo*), and (at least initially) mimic the mechanical properties of the tissue to be engineered [31]. Additionally, the scaffold can be constructed with or designed to release growth factors that can beneficially manipulate cell behavior in culture [32-34].

Scaffolds

In tissue engineering, a scaffold may be defined as, “***a 3D conduit for cells, growth factors and/or signaling molecules which promotes infiltration and phenotypic regulation of the desired cell type, with extracellular matrix formation, resulting in functional repair, or regeneration, of damaged tissue***” [35]. As the scaffold provides the basic foundation for cell-based tissue engineering strategies, its various properties need to be carefully designed and optimized. In addition to 3D shape, scaffolds need to be porous. Pore size, porosity and pore interconnectivity are crucial scaffold parameters. The size of interconnections between pores should be suitably large and with straight path/access for cell infiltration and to support ECM deposition of desired tissue. It is preferable that scaffolds for tissue engineering have 100% interconnecting pore volume, thereby also maximizing the diffusion and exchange of nutrients throughout the entire scaffold pore volume [4, 36-38]. Micro-pores (*i.e.* <20 μ m) influence cell function (*e.g.* cell attachment), whereas macro-pores (*i.e.* >50 μ m) influence tissue function, for example, pores 50-400 μ m in size are typically suggested for bone in-growth in relation to vascularity [39].

With the recent exponential growth of the field of tissue engineering [40, 41], numerous scaffold materials and designs have been described in literature. Discussion of all different type of scaffold is beyond of scope of this thesis. Hence only free form fabricated (FFF) scaffold or rapid prototyping and electro spun (ES) mesh, used as scaffold in this thesis are briefly discussed.

Rapid prototyping enables scaffolds to be fabricated with precise control over micro- and macrostructure. Rapid prototyping is capable of directly producing complex, 3D scaffolds by joining liquids or by melt extrusion (bioplotter), powders (stereo-lithography), and sheet materials (fused by compression) one layer at a time using computer-aided design [36, 41, 42]. Rapid prototyping offers the potential to precisely control the morphology, geometry, and overall shape of the scaffold and may enable the creation of 3D scaffolds that matches the anatomical defects.

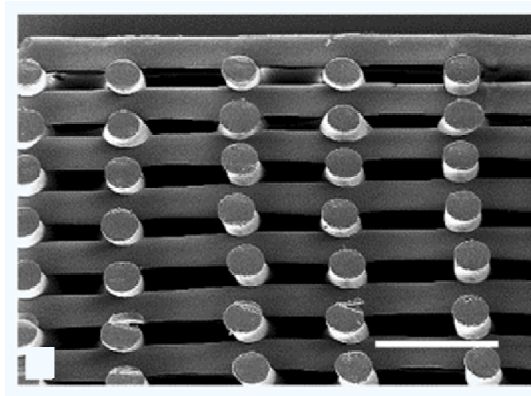


Figure 2. SEM image of free form fabricated scaffold (orientation = 0-90)

Electro-spinning process (ESP) is a method to fabricate nonwoven mesh as scaffold to mimic collagen fibrils in natural tissue matrix [43] with fiber size in the nano to micrometer scale [44-47] with different fiber surface morphology [48]. ESP utilizes an electrostatic field to control the formation and deposition of polymer nanofibers [49-51]. The fibrous mesh also attributes in spatial arrangement (random or aligned), high porosity, mechanical property and increased surface area [52, 53] which can be controlled for production of efficient, reproducible, rapid and inexpensive sheets.

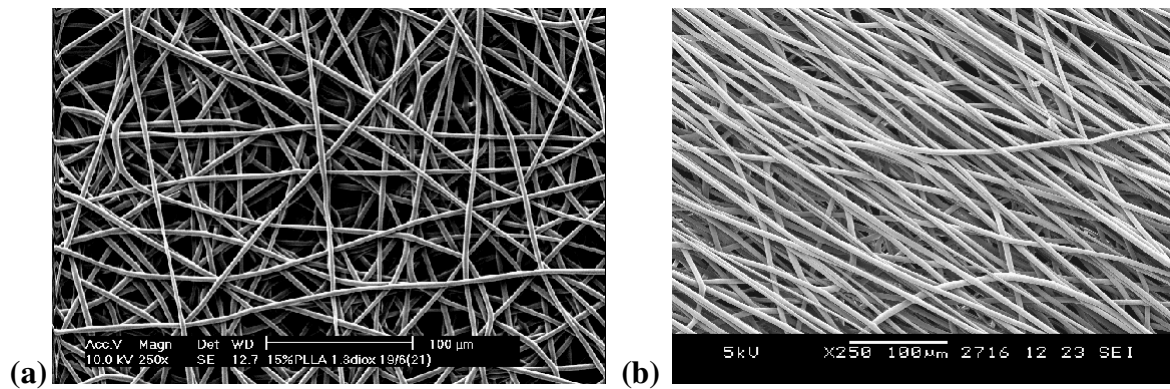


Figure 3. SEM images of electro-spun sheet (a) non-woven and (b) aligned

Cells

Tissue engineering includes methodologies for the proliferation and differentiation of cells. In fact, use of various cell sources such as xenogeneic cells [54, 55], allogeneic cells [56, 57], autologous cells [58, 59], stem cells and genetically engineered cells have been reported [60]. The important thing is that the donor / source immune system markers are closely matched to the host. Xenogeneic cell therapy is the use of viable animal somatic cell preparations suitably adapted for the transplantation, implantation, and infusion into human recipients [55]. The allogeneic stem cell isolation is a procedure in which the bone marrow stromal cells are harvested from healthy bone marrow or peripheral blood stem cells from a donor [57], whereas, autologous cells are cells that are harvested from the patient himself. The use of autologous cells in tissue engineering has the benefit of avoiding an immunologic response. The best source for autologous cells is from the organ that needs repair or replacement because those cells already have the genetic coding for the organ. Recently, stem cell research has emerged with profound importance which includes undifferentiated cell source from embryonic, fetal, or adult sources, human and non-human. It includes research in which stem cells are isolated, derived or cultured for purposes such as developing cell or tissue therapies, studying cellular differentiation, research to understand the factors necessary to direct cell specialization to specific pathways, and other developmental studies.

Biomolecules

Biomolecules (mostly secreted by the cells themselves or produced artificially in laboratory) like growth factors, differentiation factors, adhesion proteins, angiogenic factors and/or morphogenic proteins which enhance the cell proliferation and/or differentiation, are generally incorporated within the matrix / scaffold [61-63]. These include fibronectin and vitronectin which are adhesion proteins that impart biological recognition ability to material surfaces by coating on synthetic scaffold [63, 64], bone morphogenetic proteins (BMPs) which are used in healing acute bone fractures [65] and angiogenesis-stimulating molecules which are produced through recombinant DNA technology and shown to promote growth of new blood vessels [66]. Research is in progress to identify the administration of growth promoter which needs to be standardized, with respect to their concentration and duration of exposure (For complex organs multiple factors may be needed) so that precise timing is identified when to replace one factor by another.

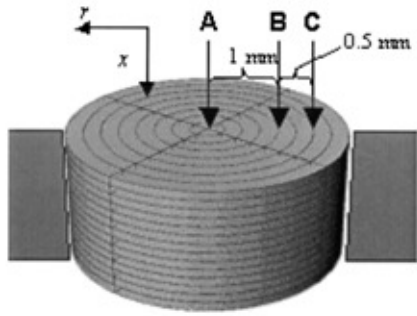
Physiological aspects in tissue design

Biomechanical aspects include properties of native tissues, identification of minimum mechanical properties required of engineered tissues and/or mechanical signals regulating the efficacy and safety of engineered tissues [67, 68]. Engineering design aspects include 2D cell expansion, 3D tissue growth, scaffold fabrication methods, bioreactors, cell and/or tissue storage and shipping (biological packaging) etc. [69-71]. Tissue-engineered cartilage, for example, becomes larger and contains more collagen and other proteins that form a suitable extracellular matrix if it is cultured in rotating vessels that expose the developing tissue to variations in fluid forces. Cartilage cultured in this way contains extracellular matrix proteins that make it stiffer, more durable and more responsive physiologically to external forces. Likewise, it has been reported that osteoblasts cultured on a base of collagen beads being stirred in a bioreactor make more bone minerals than they would do when they are grown in a fiat, stationary dish [72, 73]. Further, Niklason L.E. et.al has also demonstrated that tissue-engineered small arteries made of endothelial cells (blood vessel lining) and smooth muscle cells shaped into tubes develop mechanical properties more akin to natural blood vessels if they have medium pulsed through them to imitate the blood pressure generated by a beating heart [74]. Several other research groups are developing ways to grow skeletal and cardiac muscle tissues that become stronger as they respond to physical stress.

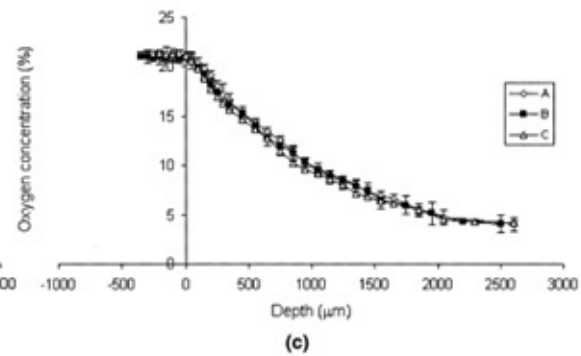
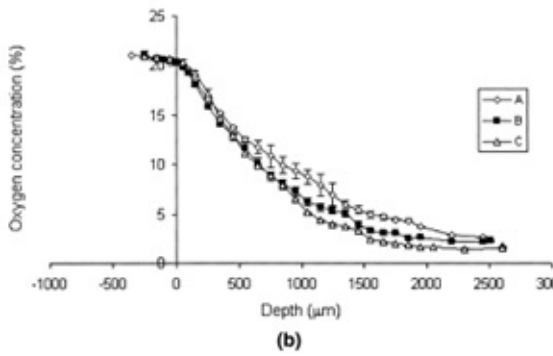
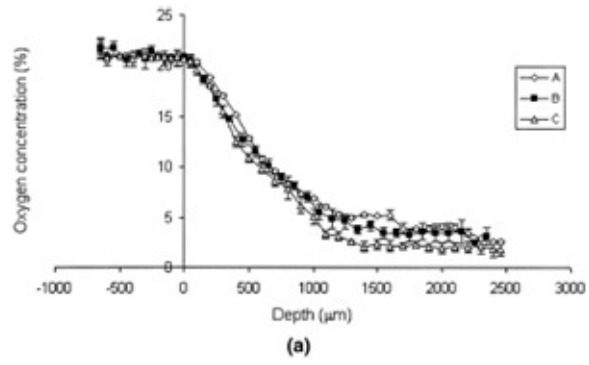
2. Limitations in tissue engineering

Using all the above sophisticated techniques in various combinations, tissue engineering has resulted in the *in-vitro* growth of tissues with thickness of less than 500 μ m from the external surface [75, 76]. The major limitation in engineering large tissues of clinical relevance is the cell density and thickness of the growing tissue which gives rise to diffusion constraints. The pioneering cells cannot migrate deep into the scaffold because of the lack of nutrients and oxygen and insufficient removal of waste products. In fact cell colonization at the scaffold periphery is consuming, or acting as an effective barrier to the diffusion of oxygen and nutrients into the interior of the scaffold [69, 77-80]. For example Figure 4 show the spatial oxygen concentration and cell distribution (as reported by Malda et al. [80]) within cylindrical free form fabricated scaffold (4mm height and 4mm diameter) seeded with cartilaginous cells and cultured for 14, 21 and 41days. The plot show that the oxygen concentration drops from 25% dissolved oxygen at the surface to less than 5% at a depth of 1mm inside the scaffold (80% decrease in oxygen concentration). Similarly the plot shows that the cell density also decreases by more than 80% at a depth of 800-1200 μ m from the surface of the scaffold (although cartilaginous cells are known to sustain and proliferate in avascular environment naturally).

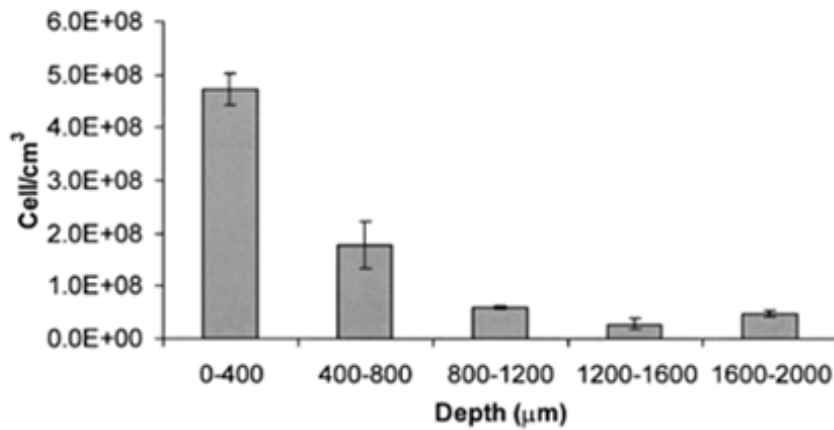
Hence, currently only avascular or thin sheets of tissues are being successfully engineered such as cartilage, skin graft, cardiovascular valves, ligaments, tendons etc. [4-6]. Tendon, ligament or skin is a relatively thin or 2D tissue, thereby explaining the success of producing this tissue with conventional scaffold fabrication techniques [81-83]. Further, the low oxygen requirement of cartilage may be the reason why only this tissue has been successfully grown *in-vitro* to thick cross-sections i.e. approximately 1mm using conventional scaffold fabrication techniques [76, 84]. For example, in case of bone tissue engineering, the high rates of nutrient and oxygen transfer at the surface of the scaffold promote the mineralization on the scaffold surface, further limiting the mass transfer to the interior of the scaffold [5, 6, 77]. Similarly, most other 3D tissues require a high oxygen and nutrient concentration, whereas human body supplies its tissues with adequate concentrations of oxygen and nutrients via blood through capillary network.



Schematic representation of the construct, the sample location A, B and C



Oxygen concentration within cartilaginous constructs cultured for (a) 14 (b) 27 (c) 41 days on 3dF scaffold



Cell distribution within construct cultured for 28 days

Figure 4. Plot of oxygen concentration and cell distribution in 3D free form fabricated scaffold cultured with cartilaginous cells as reported by Malda et. al. (Plot adapted from [80])

Most of the tissue/organs in our body are usually composed of multiple layers of various cell types. The cells are arranged in an elaborate and hierarchical order to achieve specific function and to mutually regulate the cellular activity by soluble bioactive molecules, cell–cell or cell–ECM interactions [85-87]. Figure 5 show highly organized cellular arrangement in bone and blood vessels.

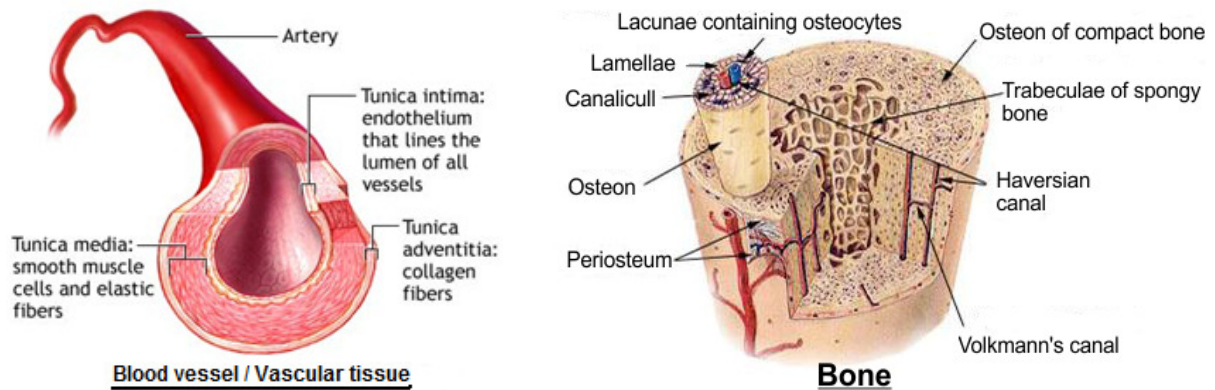


Figure 5. Illustration of multi-cellular organization in natural human tissue

This elaborate structure also provides individual cells with a defined microenvironment, where the cells experience specific cues and show corresponding responses towards tissue function. Hence **a system to mimic capillary network and overcome diffusion limitations within large tissue construct has to be engineered.**

3. Requirement of vascularization in tissue engineering

Vasculature is, along with the lymphatic and the nervous system, embedded into almost every tissues and organs. It is a critical template for the exchange of gas, nutrients, cells or molecules and a regulator of tissue development. Most tissues are highly vascularized with the blood vessels to supply the individual cells with nutrients and oxygen. For tissue to grow beyond 100-200 μm , new blood vessel formation is required [80, 88, 89]. The same can be said about tissue engineered constructs. Angiogenesis is the primary requirement for generation of an appreciable mass of most tissues, but initiation and control of angiogenesis remain a major technical challenge to tissue engineering [90-92]. During *in-vitro* culture, large volumes of porous tissue engineered constructs can be supplied with nutrients for instance in bioreactors [93-97]. However, after implantation of tissue constructs, the supply of oxygen and nutrients to the implant is limited by diffusion processes and the speed of ingrowth of host vessels. In active tissue, sufficient diffusion is confined to 100-200 μm from the next capillary, and the formation of host vessels within the construct takes time [98]. This means that insufficient vascularization can lead to nutrient deficiencies and/or hypoxia in the tissue. Moreover, nutrient and oxygen gradients will be present in the outer regions of the tissue, which could result in non-uniform cell differentiation and integration [80]. **An engineering solution to supply oxygen and essential nutrients to the growing tissue may be to use hollow fiber membrane bioreactor;** so that the hollow fiber membrane embedded in-between reduces the diffusion distance while mimicking the blood capillary system [99-102]. Evidence of endothelial cells growing on porous polymeric (PES) hollow fiber membranes has been reported [103], illustrating **the possibility to connect hollow fiber to host vascular system to enhance capillary in-growth *in-vivo*.**

4. Bioreactors for tissue engineering

While tissue engineering has grown into a field of intense research in recent years, the bioreactor is placed central to the tissue culture process providing the pre-defined chemical, biochemical, physical and mechanical environments for the seeded scaffolds, in which cells proliferate and differentiate to form neo-tissues [69, 70]. Bioreactors focus on, first, the *in-vitro* construction of transplantable vital tissues [104-106] and, second, on the development of *in-vitro* models that are superior to conventional monolayer or suspension cell cultures with sophisticated and specialized culture techniques that may contribute to realize cultivation of tissue *in-vitro*, bioreactors can support tissue engineering that ultimately leads to true three dimensional cultures which more closely resemble the human *in-vivo* situation [107]. Bioreactors are also essential in tissue engineering because they also enable systematic studies of the responses of living tissues to various mechanical and biochemical cues [108]. Bioreactor as such can be broadly divided into (a) Static and (b) Dynamic bio reactors. Sub-classification of bioreactor (Figure 6) depends on the geometry and/or special function customized for particular tissue growth.


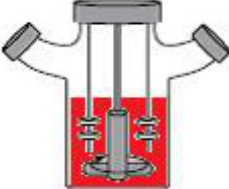

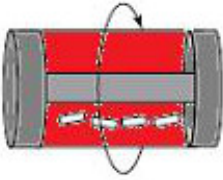


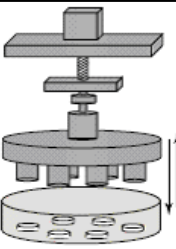
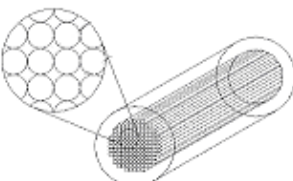
Static bioreactor		Dynamic Bioreactor	
Schematic	Application	Schematic	Application
 <p>T-flask</p>	Cell expansion and Proliferation of thin cell sheet (2D culture) (Diffusion)	 <p>Spinner flask</p>	Cell seeding and proliferation of small 3D constructs (Forced diffusion with mixed reactor conditions)
 <p>Culture wells</p>	Proliferation of small 3D constructs (Diffusion)	 <p>Rotating wall bioreactor</p>	Cell seeding and proliferation of small 3D constructs (Forced diffusion with mixed reactor conditions) [109]
 <p>Petridish</p>	Cell seeding and proliferation of 3D constructs (Diffusion)	 <p>Perfusion bioreactor</p>	Cell expansion, seeding and proliferation of 3D constructs (Forced diffusion with plug flow reactor conditions) [110]
 <p>Mechanical stimulation bioreactor</p>	Stimulation to induce cell proliferation and differentiation (Shear stress) (Can also be used along with dynamic bioreactor system)	 <p>Hollow fiber perfusion bioreactor</p>	Cell expansion (Forced diffusion with low shear stress)

Figure 6. Various tissue culture systems broadly classified under static and dynamic culture techniques

Critical aspects of a bioreactor design for Tissue Engineering

Bioreactors designed for tissue engineering are built to suit different constraints such as (a) small scale and large scale cell proliferation (e.g. lab experiments to organ therapy), (b) *in-vitro* development of 3D tissue constructs from isolated and proliferated cells (e.g. skin, blood vessel) and (c) organ support device (e.g. artificial liver, kidney) [111-113].

The critical common design aspects of these bioreactors are to provide controlled environmental conditions such as oxygen tension, pH, temperature and mechanical simulation (mimicking *in-vivo* conditions). Such bioreactors should also allow aseptic and automated feeding and sampling operations along with biosensors to regulate and maintain culture. Along-with these common requirements specific criteria for 3D tissue constructs based on scaffold configuration and cell type including ease of culturing (mono or hetero cell type) and efficient nutrient supply to avoid necrosis and hypo/hyper-oxia within the developing tissue [80, 112].

Furthermore, a bioreactor system should allow for automated processing steps and possibly mobile and/or installable at hospitals. This is essential not only for controlled, reproducible, statistically relevant basic studies but also for the future routine manufacturing of tissues for clinical application [114, 115]. Besides these global requirements, specific key criteria for 3D tissue constructs based on cells and scaffolds interactions have to be met, including the proliferation of cells, seeding of cells on macro-porous scaffolds, nutrient (particularly oxygen) supply within the resulting tissue, and mechanical stimulation of the developing tissues [115].

Proliferation of cells is the first step in establishing a tissue culture. Usually, only a small number of cells can be obtained from a biopsy specimen, hence expansion of up to several orders of magnitude is required. Normally static bioreactors such as culture dishes (e.g., petri-dishes, well plates, and T-flasks) are generally used for cell expansion, wherein a maximum of approximately 8 - 10 generations cell expansion is achievable with several sub-cultivations and large surface area. Recent studies have shown that micro-carrier cultures performed in well mixed/ plug flow bioreactors can significantly improve cell expansion [115, 116]. The expansion is quite often accompanied by the dedifferentiation which is a major negative point to be taken care while proliferation of cells. For example, proliferating chondrocytes show a decreased expression level of collagen type II [78, 117].

High cell density and homogenous seeding on macro-porous scaffold is an important step in establishing 3D tissue culture. Although high cell density have been associated with enhanced tissue formation like cardiac tissue formation, bone mineralization and cartilage matrix production [118-120]; inhomogeneous distribution of cells within the scaffold significantly affects the tissue culture properties. Several techniques for seeding have been discussed by Martin et al [84, 114]. Critical aspect of large tissue construct depends on the efficacy of mass transfer (e.g., oxygen and nutrient supply, and removal of toxic metabolites) as the growing tissues do not have their own blood supply and nutrients have to be transferred by diffusion [84, 121]. Bioreactors improve cell survival and/or homogeneity of cell seeding, for instance, constructs can be cultivated suspended in culture medium in spinner flasks. Convective flow allows continuous mixing of the medium surrounding the constructs [97]. However, only external mass- transfer limitations can be reduced in spinner flasks or stirred tank bioreactors [93]. Bioreactors that perfuse medium through porous scaffolds allow the reduction of internal mass-transfer limitations and the exertion of mechanical forces by fluid flow [122, 123]. Although research in design and functional properties of perfusion bioreactors for tissue engineered blood vessels [124, 125], heart valves [126, 127], cartilage [128, 129], and mineralized matrix deposition by bone cells [95, 130, 131] are reported, there are still some challenges. Perfusion bioreactors can offer greater control of mass transport than other conventional convective systems, but there still remains the potential for flow to follow a preferential path through the construct (particularly for scaffolds with a wide pore size distribution or if the tissue develops non-uniformly), leaving other regions poorly nourished [132]. Furthermore, optimizing a perfusion system may include retention of newly synthesized ECM components within the construct and fluid-induced shear stresses within the scaffold pores.

Alternative to conventional cell culture system - Hollow-fiber bioreactor technology

The hollow-fiber bioreactor concept makes use of semi-permeable membranes. Semi-permeable membranes are selectively permeable for molecules of different size, permeability being dependent on pore-size. Membranes are generally used to separate two independent compartments (cell and medium compartment). Thus, delivery to, removal from and retention of substances within cell compartment can be realized. Figure 7 illustrates the use of a semi-permeable membrane in a membrane bioreactor to culture cells.

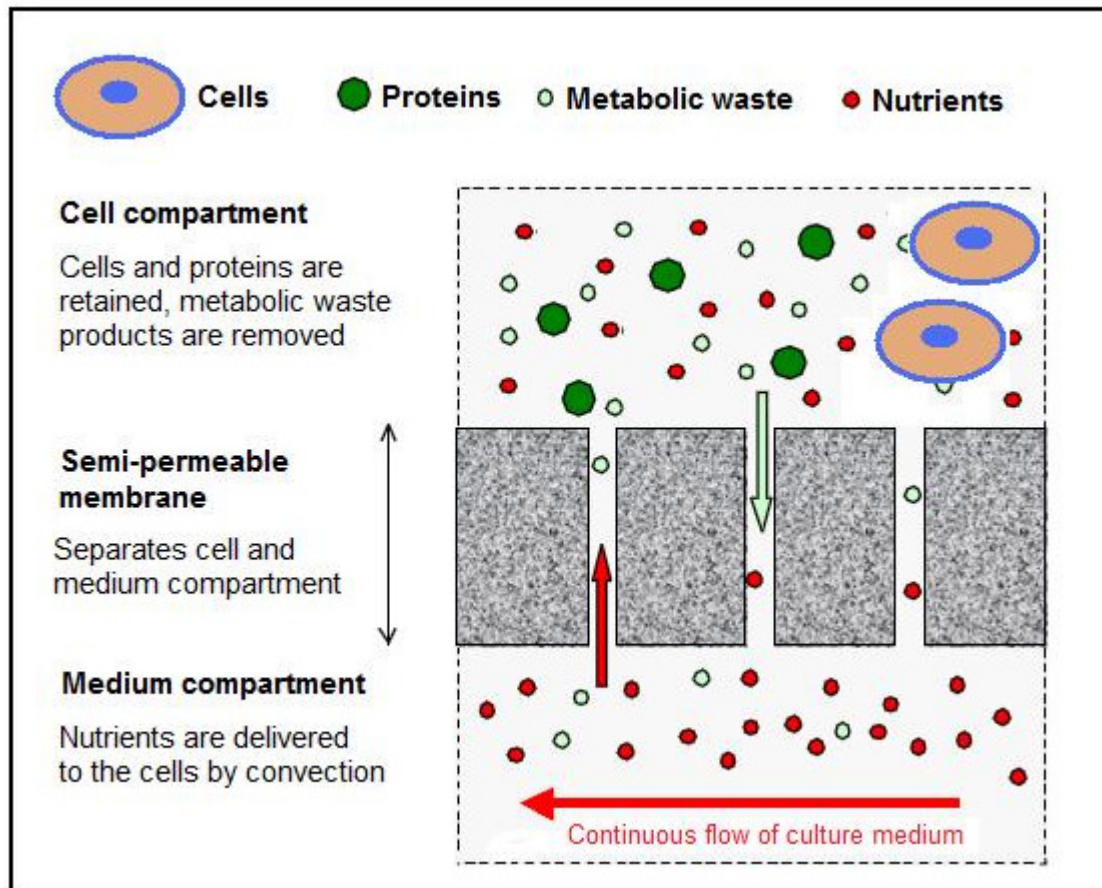


Figure 7. Schematic of the principle use of semi-permeable membranes in hollow fiber bioreactors to culture cells *in-vitro*. The membranes allow passage (medium, growth factor proteins, metabolic waste etc.) or retention of molecules (e.g. cells, extra cellular matrix, growth factors, proteins etc.) depending on their pore-size.

Semi-permeable membranes find broad usage in medical applications [14], e.g. in artificial kidneys to treat acute and chronic renal failure [133, 134] or in artificial livers, to gap the time after organ failure until transplantation can be performed [135-138]. During open heart surgery, oxygenators containing oxygenation membranes ensure optimal supply with oxygen to the patient [139, 140]. Cells can be encapsulated in membrane tubes and are thus isolated from the immune system of the host after transplantation. Immuno-isolated cells allow controlled release of therapeutics, e.g. aiming at new therapeutic options for chronic pain patients, patients with endocrine disorders, diseases of the central nervous system and other diseases [141-143]. Table 1 shows various polymeric membranes available commercially to culture cells in small scale for research purpose to pilot and industrial scale cell culture mainly for cell expansion.

Table 1. *Commercially available membrane based cell culture devices*

	Oxygenation	Perfusion	Culture samples	Microscope	Sample aspiration
Transwells™	No oxygenation	Not possible	Inserts for culture well plate	Depends on type of membrane	Sampling by a pipet
miniPERM	Silicone flat membrane	Not possible	40ml	Not possible	Sampling port for syringe
CELLine	Silicon membrane – T-flask - base	Not possible	5 - 15ml	Not possible	Sampling port for syringe
Tecnomouse	Silicone flat membrane	Necessary	8 - 10ml	Visual control but no microscopy	Sampling port for syringe
FiberCell	High flux Polysulfone HF	Necessary	2.5 – 150ml	Visual control but no microscopy	Recirculation port for syringe

Polymeric membranes have also been widely used for numerous applications in the biotechnological and biomedical area, since Loeb and Sourirajan discovered a method to prepare asymmetric membranes [144, 145]. Biocompatible polymeric porous hollow fibers from poly-ether-sulfone (PES) [146, 147] and poly-ether-imide (PEI)[148] are commercial available, which are used in life supporting medical devices such as haemodialysis, artificial liver etc.. They have also been used to study different cellular activity and cell expansion [149, 150]. But, to have a completely implantable tissue engineered construct there is a requirement for biodegradable hollow fiber which may also have the ability to connect to the host vasculature after implantation. Further, since the cell culture medium contains high amount of proteins (like serum, growth factors and other bio-molecules) the membranes should be of microfiltration range suitable to permeate complete medium components to the cells.

Previously, research has been carried out to fabricate small length hollow fiber from biodegradable material like PLLA for drug delivery applications [151], wherein the material degrades over time for controlled release. Only recently, poly(lactic-co-glycolic acid) (PLGA) [152] hollow fiber fabrication method has been reported to act as scaffolds for tissue

culturing. Hence, **fabrication of implantable, mechanically strong, porous biodegradable hollow fibers with high cell culture medium permeance to deliver nutrient to the proliferating cells *in-vitro* when incorporated in tissue engineering scaffolds.**

Generally, hollow fibers can be fabricated via phase separation. There, a viscous polymer solution containing the polymer, solvent and sometimes additives (e.g. a second polymer or and non solvent) is pumped through a spinneret (see Figure 8). A bore injection fluid is simultaneously pumped through the inner tube of the spinneret. After a short residence time in the air or a controlled atmosphere, the fiber is immersed in a non solvent bath where coagulation occurs. During the fabrication process, three parameters control the morphology of the fibers to a great extent: composition of the polymer solution(s), composition of the bore liquid and air gap conditions. Other parameter, such as composition and temperature of the coagulation bath, spinning speed and post treatment are important as well.

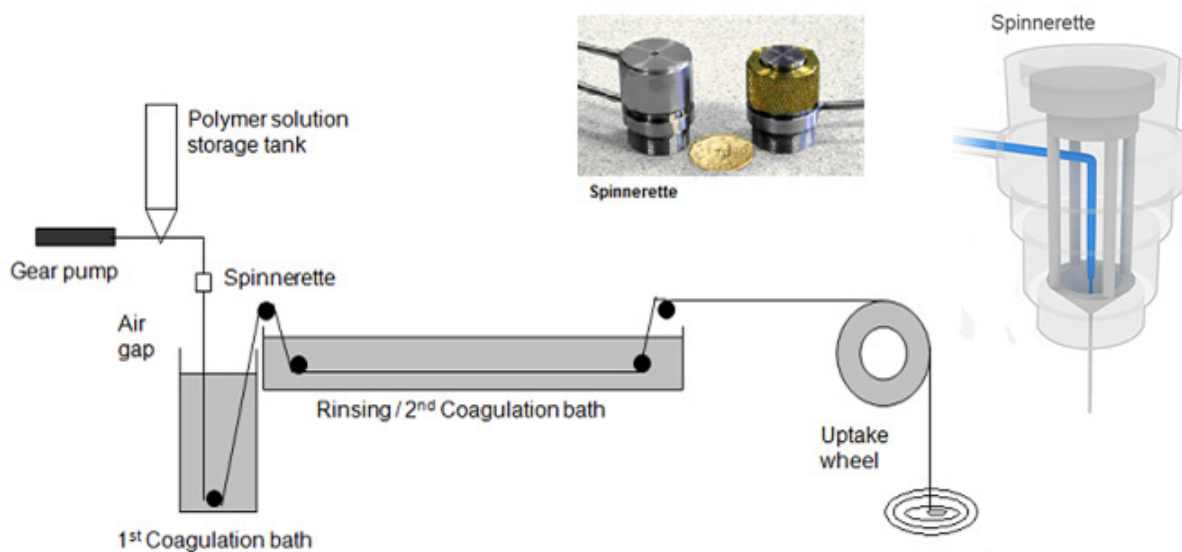


Figure 8. Schematic of hollow fiber spinning set-up

In batch culture, depletion of key nutrients, accumulation of toxic by-products such as ammonia and lactate or changes of pH and osmolarity can lead to cell death, thus limiting the theoretical maximum cell density [99, 101]. This limitation can be overcome by maintaining a

steady-state level of nutrients and metabolites by the use of a hollow-fiber bioreactor system, that can, in principle, support the cultivation of large numbers of mammalian cells.

The use of hollow fiber bioreactors as bio-artificial liver device producing enzymes [153] was first demonstrated by Wolf and Munkelt in 1975 [154], who cultured hepatocytes in the extra-capillary space of a hollow fiber bioreactor derived from the original design of Knazek et al., [155].

The principle of a hollow-fiber bioreactor based on hemodialysis modules was first described by Knazek et al, [155]. Based on his design even flat-bed hollow-fiber cell culture systems are described with even distribution of fibers in 2D plane enabling controlled amount of medium permeation [156]. Hollow-fiber membranes are potted in a shell, thus creating a medium and a cell compartment which are separated by the membranes (see Figure. 9). Cells are typically inoculated outside the hollow-fibers in the extra-capillary space. Culture medium is recirculated through the capillaries resulting in a continuous delivery of nutrients to the cells and removal of metabolic by-products.

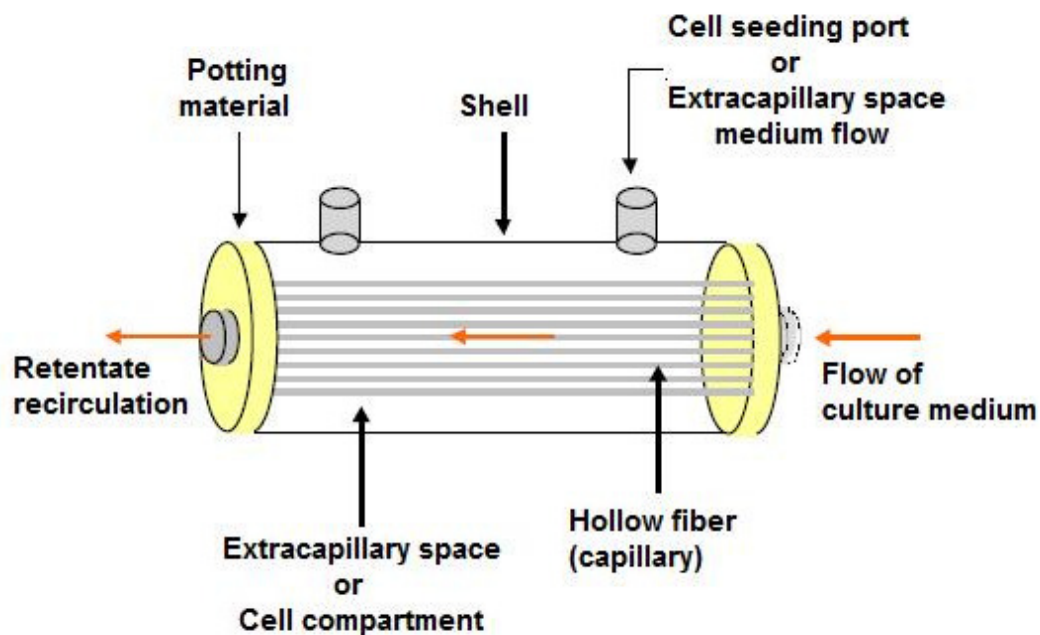


Figure 9. Principle of a hollow-fiber membrane bioreactor

In addition, sufficient oxygenation of the cell culture can to be ensured by using dedicated oxygenation membranes for optimal supply of oxygen. Hollow-fiber bioreactor technology enables increased cell densities compared to conventional cell culture procedures, leading to three-dimensional structures [157, 158] with increased concentrations of self secreted bio-molecules, thus offering a unique cell culture environment not available in traditional low density or monolayer culture. Hence, **integration of porous and semi-permeable hollow fiber membranes with 3D tissue engineering scaffold / construct can thus serve similar functions to that of arteries and veins *in-vivo*.**

5. Aims and outline of this thesis

The main goal of this thesis is to investigate the use of semi-permeable membranes to overcome transport limitation in *in-vitro* 3D tissue engineering constructs.

Study direction of the present work was to improve conventional culture systems with regard to

- Continuous supply with nutrients and oxygen to the cultured cells
- Continuous detoxification of the culture
- Support three dimensional growth of cells and controlled delivery of complete medium substances to the cells at physiological condition
- Viability of the cultured cells with low disturbance of the culture (low shear stress)
- multicellular organization to mimic natural tissue
- Easily sterilizable construct and closed culture system to avoid contamination
- Small culture volume for even distribution and increase efficiency

Hence, in **chapter 2** we investigate the development of bio-degradable porous Poly lactic acid (PLLA) hollow fiber using a miniaturized spinning setup. Further we demonstrate the suitability of the produced fiber for *in-vitro* tissue engineering application mimicking vascularization by complete proliferation medium permeability.

Chapter 3 investigates the integration of HF membrane with in 3D tissue construct to overcome nutrient limitation. The optimum number of hollow fiber and its spatial distribution was tested for one specific scaffold and cell type. We developed multilayer constructs by rolling of pre-seeded ES sheet (**Chapter 4**). The rolling of pre-seeded ES sheet, which mimics *in-vivo* like microenvironment, with controlled cell seeding density, uniform cell distribution and manipulated cell type distribution with specific thickness or number of layers according to tissue of interest, is achievable within this illustrated scaffold organization. In addition we can manipulate the degree of cell-cell interaction or even cell migration in this system.

Further, the effect of surface topography on cell seeding or adhesion and proliferation in static and dynamic culture conditions is investigated. An improved efficiency of cell seeding and

proliferation in static and reduced effect of shear stress to the cells in dynamic culture conditions was assessed in **chapter 5**.

In **chapter 6**, general conclusions arising from this thesis are discussed. It also outlines some future perspectives.

References

- [1] Langer R, Vacanti JP. Tissue engineering. *Science*. 1993;260 (5110):920-6.
- [2] Laurencin CT, Ambrosio AMA, Borden MD, Cooper JA. Annual Review of Biomedical Engineering. *Annual Review of Biomedical Engineering*. 1999;1:19-46.
- [3] Stock UA, Vacanti JP. TISSUE ENGINEERING: Current State and Prospects. *Annual Review of Medicine*. 2001;52:443-51.
- [4] Sachlos E, Czernuszka JT. Making tissue engineering scaffolds work. Review on the application of solid free form fabrication to the production of tissue engineering scaffolds. *European Cells and Materials*. 2003;5:29-40.
- [5] Porter JR, Ruckh TT, Popat KC. Bone Tissue Engineering: A Review in Bone Biomimetics and Drug Delivery Strategies
Biotechnol Prog. 2009;25(6):1539-60.
- [6] Salgado AJ, Coutinho OP, Reis RL. Bone Tissue Engineering: State of the Art and Future Trends. *Macromol Biosci*. 2004;4:743–65.
- [7] Pearson B, Ph.D., R. G., Bhandari R, Quirk RA, Shakesheff PKM. Recent Advances in Tissue Engineering: An Invited Review. 2002;12:33.
- [8] Oh S, Oh N, Appleford M, Ong JL. Bioceramics for Tissue Engineering Applications – A Review. *American Journal of Biochemistry and Biotechnology*. 2006;2(2):49-56.
- [9] Cho E, WJ. L. Human stem cells, chromatin, and tissue engineering: boosting relevancy in developmental toxicity testing. *Birth Defects Res C Embryo Today*. 2007;81(1):20-40.
- [10] Miranda JP, Rodrigues A, Tostões RM, Leite S, Zimmerman H, Carrondo MJT, et al. Extending Hepatocyte Functionality for Drug-Testing Applications Using High-Viscosity Alginate–Encapsulated Three-Dimensional Cultures in Bioreactors. *Tissue Engineering Part C: Methods*. Epub Date - April 6 2010.
- [11] Holmes AM, Creton S, Chapman K. Working in partnership to advance the 3Rs in toxicity testing. *Toxicology*. 2010;267:14-9.
- [12] Bhogal N, Grindon C, Combes R, Balls M. Toxicity testing: creating a revolution based on new technologies. *Trends in Biotechnology*. 2005;23:299-307.
- [13] Peppas NA, Langer R. New challenges in biomaterials. *Science*. 1994:1715-20.

[14] Stamatialis DF, Papenburg BJ, Gironès M, Saiful S, Bettahalli SNM, Schmitmeier S, et al. Medical applications of membranes: Drug delivery, artificial organs and tissue engineering. *Journal of Membrane Science*. 2008;308:1-34.

[15] Agrawal CM, Ray RB. Biodegradable polymeric scaffolds for musculoskeletal tissue engineering. *Journal of Biomedical Materials Research* 2001;55(2):141-50.

[16] Gunatillake PA, Adhikari R. Biodegradable Synthetic Polymers for Tissue Engineering. *European Cells and Materials*. 2003;5:1-16.

[17] Freed LE, Marquis JC, Nohria A, Emmanuel J, Mikos AG, Langer R. Neocartilage formation in vitro and in vivo using cells cultured on synthetic biodegradable polymers. *J Biomed Mater Res* 1993;27(1):11-23.

[18] Ramakrishna S, Mayer J, Wintermantel E, Leong KW. Biomedical applications of polymercomposite materials: a review. *Composites Science and Technology* 2001;61(9):1189-224.

[19] Hench LL, Jones JR. *Biomaterials, artificial organs and tissue engineering*. Boca Raton: CRC Press; 2005.

[20] Black J. *Biological performance of materials: Fundamentals of Biocompatibility*. Boca Raton: Taylor & Francis; 2006.

[21] Reis RL, San Roman J. *Biodegradable systems in tissue engineering and regenerative medicine*. Boca Raton: CRC Press; 2005.

[22] Nair LS, Laurencin CT. Biodegradable polymers as biomaterials. *Progress in Polymer Science*.32:762-98.

[23] Williams DF. On the mechanisms of biocompatibility. *Biomaterials*. 2008;29(20).

[24] Anderson JM, Langone JJ. Issues and perspectives on the biocompatibility and immunotoxicity evaluation of implanted controlled release systems. *J Control Release*. 1999;57(2):107-13.

[25] Fu K, Pack DW, Klibanov AM, Langer R. Visual evidence of acidic environment within degrading poly(lactic-co-glycolic acid) (PLGA) microspheres. *Pharm Res*. 2000;17(1) 100-6.

[26] Wang PY. Compressed poly(vinyl alcohol)-polycaprolactone admixture as a model to evaluate erodible implants for sustained drug delivery. *J Biomed Mater Res*. 1989;23(1).

[27] Olde Riekerink MB, Claase MB, Engbers GH, Grijpma DW, J. F. Gas plasma etching of PEO/PBT segmented block copolymer films. *J Biomed Mater Res A*. 2003;65(4):417-28.

- [28] Deschamps AA, Claase MB, Sleijster WJ, de Bruijn JD, Grijpma DW, J. F. Design of segmented poly(ether ester) materials and structures for the tissue engineering of bone. *J Control Release* 2002;78(1-3):175-86.
- [29] Mahmood TA, de Jong R, Riesle J, Langer R, CA. vB. Adhesion mediated signal transduction in human articular chondrocytes: the influence of biomaterial chemistry and tenascin-C. *Exp Cell Res.* 2004;301(2).
- [30] Beumer GJ, van Blitterswijk CA, M. P. Degradative behaviour of polymeric matrices in (sub)dermal and muscle tissue of the rat: a quantitative study. *Biomaterials.* 1994;15(7):551-9.
- [31] Hutmacher DW, Schantz T, Zein I, Ng KW, Teoh SH, KC. T. Mechanical properties and cell cultural response of polycaprolactone scaffolds designed and fabricated via fused deposition modeling. *J Biomed Mater Res.* 2001;55(2):203-16.
- [32] Babensee JE, McIntire LV, Mikos AG. Growth factor delivery for tissue engineering. *Pharm Res.* 2000;17(5):497-504.
- [33] Bezemer JM, Grijpma DW, Dijkstra PJ, van Blitterswijk CA, J. F. A controlled release system for proteins based on poly(ether ester) block-copolymers: polymer network characterization. *J Control Release.* 1999;62(3):393-405.
- [34] van Dijkhuizen-Radersma R, Peters FL, Stienstra NA, Grijpma DW, Feijen J, de Groot K, et al. Control of vitamin B12 release from poly(ethylene glycol)/poly(butylene terephthalate) multiblock copolymers. *Biomaterials.* 2002;23(6).
- [35] Woodfield TBF, Bezemer JM, Pieper JS, van Blitterswijk CA, . RJ. Scaffolds for tissue engineering of cartilage. *Crit Rev Eukaryot Gene Expr* 2002. 2002;12(3):209-36.
- [36] Hutmacher D. Scaffolds in tissue engineering bone and cartilage. *Biomaterials.* 2000;21(24):2529-43.
- [37] Freed LE, Vunjak-Novakovic G, Biron RJ, Lesnoy DC, Barlow SK, Langer R, et al. Biodegradable Polymer Scaffolds for Tissue Engineering. *Nat Biotech.* 1994;12:689-93.
- [38] Chen G, Ushida T, Tateishi T. Scaffold Design for Tissue Engineering. *Macromol Biosci* 2002;2:67-77.
- [39] Pilliar R. Powder metal-made orthopedic implants with porous surface for fixation by tissue ingrowth. *Clin Orthop.* 176:42-51.
- [40] Lysaght M, Reyes J. The growth of tissue engineering. *Tissue engineering.* 2001;7(5):485-93.
- [41] Moroni L, de Wijn J, van Blitterswijk C. Integrating Novel Technologies to Fabricate Smart Scaffolds. *J Biomater Sci - Polym Ed* 2008;19:543-72.

- [42] Moroni L, de Wijn J, van Blitterswijk C. 3D fiber-deposited scaffolds for tissue engineering: Influence of pores geometry and architecture on dynamic mechanical properties. *Biomaterials*. 2006;27:974-85.
- [43] Pham QP, Sharma U, Mikos AG. Electrospinning of polymeric nanofibers for tissue engineering applications: A review. *Tissue Engineering*. 2006;12:1197-211.
- [44] Reneker DH, Yarin A, Zussman E, Koombhongse S, Kataphinan W. Nanofiber manufacturing: Toward better process control. 2006. p. 7-20.
- [45] Theron SA, Zussman E, Yarin AL. Experimental investigation of the governing parameters in the electrospinning of polymer solutions. *Polymer*. 2004;45:2017-30.
- [46] Tuzlakoglu K, Bolgen N, Salgado AJ, Gomes ME, Piskin E, Reis RL. Nano- and micro-fiber combined scaffolds: A new architecture for bone tissue engineering. *Journal of Materials Science: Materials in Medicine*. 2005;16:1099-104.
- [47] Zussman E, Theron A, Yarin AL. Formation of nanofiber crossbars in electrospinning. *Applied Physics Letters*. 2003;82:973-5.
- [48] Moroni L, Licht R, de Boer J, de Wijn J, van Blitterswijk C. Fiber Diameter and Texture of Electrospun PEOT/PBT Scaffolds Influence Human Mesenchymal Stem Cells Proliferation and Morphology, and the Release of Incorporated Compounds. *Biomaterials* 2006;27:4911-22.
- [49] Frenot A, Chronakis IS. Polymer nanofibers assembled by electrospinning. *Current Opinion in Colloid and Interface Science*. 2003;8:64-75.
- [50] Huang ZM, Zhang YZ, Kotaki M, Ramakrishna S. A review on polymer nanofibers by electrospinning and their applications in nanocomposites. *Composites Science and Technology*. 2003;63:2223-53.
- [51] Reneker DH, Yarin AL, Zussman E, Xu H. Electrospinning of Nanofibers from Polymer Solutions and Melts. 2007. p. 43-195,345-6.
- [52] Neves NM, Campos R, Pedro A, Cunha J, Macedo F, Reis RL. Patterned nanofiber meshes for biomedical applications. 2006. p. 155-8.
- [53] Pham QP, Sharma U, Mikos AG. Electrospun poly (ϵ -caprolactone) microfiber and multilayer nanofiber/microfiber scaffolds: Characterization of scaffolds and measurement of cellular infiltration. *Biomacromolecules*. 2006;7:2796-805.
- [54] Derham C, Ingram J, Fisher J, Homer-Vanniasinkam S, Ingham E. Characterisation of a decellularised xenogeneic scaffold for tissue engineering of small diameter vessels. *European Cells and Materials*. 2006;11(3):46.

- [55] Schmidt D, Stock UA, Hoerstrup SP. Tissue engineering of heart valves using decellularized xenogeneic or polymeric starter matrices. *Philos Trans R Soc Lond B Biol Sci.* 2007;362(1484):1505–12.
- [56] Cutler C, Antin JH. Peripheral Blood Stem Cells for Allogeneic Transplantation: A Review. *STEM CELLS.* 2001;19:108-17.
- [57] Marolt D, Knezevic M, Novakovic GV. Bone tissue engineering with human stem cells-Review. *Stem Cell Research & Therapy.* 2010;1:10.
- [58] Bianco P, PG. R. Stem cells in tissue engineering. *Nature.* 2001;414(6859):118-21.
- [59] Chang YJ SD, Tseng CP, Hsieh TB, Lee DC, Hwang SM. Disparate mesenchyme-lineage tendencies in mesenchymal stem cells from human bone marrow and umbilical cord blood. *Stem Cells.* 2006;24(3):679-85.
- [60] Fodor WL. Tissue engineering and cell based therapies, from the bench to the clinic: The potential to replace, repair and regenerate. *Reprod Biol Endocrinol* 2003;1:102.
- [61] Morstyn G, A.W. B. Hemopoietic growth factors: a review. *Cancer Res.* 1988;48(20):5624-37.
- [62] Discher DE, Mooney DJ, Zandstra PW. Growth Factors, Matrices, and Forces Combine and Control Stem Cells. *Science.* 2009;324(5935) 1673 - 7.
- [63] Kiritsy CP, Lynch SE. Role of Growth Factors in Cutaneous Wound Healing: A Review. *Critical Reviews in Oral Biology & Medicine.* 1993;4:729-60.
- [64] Wu MH, Ustinova E, Granger HJ. Integrin binding to fibronectin and vitronectin maintains the barrier function of isolated porcine coronary venules. *J Physiol.* 2001;532:785-91.
- [65] Capra P, Conti B. The role of Bone Morphogenetic Proteins (BMPs) in bone tissue engineering: A mini review. *Scientifica Acta.* 2009;3(1):25-32.
- [66] Ahrendt G, Chickering DE, Ranieri JP. Angiogenic Growth Factors: A Review for Tissue Engineering. *Tissue engineering.* 1998;4:117-30.
- [67] Oddou C, Pierre J. Biomechanical aspects in tissue engineering. *Clinical Hemorheology and Microcirculation.* 2005;33:189-95.
- [68] Martin I, Obradovic B, Treppo S, Grodzinsky AJ, Langer R, Freed LE, et al. Modulation of the mechanical properties of tissue engineered cartilage. *Biorheology.* 2000;37:141.
- [69] Martin I, Wendt D, Heberer M. The role of bioreactors in tissue engineering. *Trends Biotechnology.* 2004;22:80-6.

[70] Pei M, Solchaga LA, Seidel J, Zeng L, Vunjak-Novakovic G, Caplan AI, et al. Bioreactors mediate the effectiveness of tissue engineering scaffolds. *The FASEB journal : official publication of the Federation of American Societies for Experimental Biology*. 2002;16:1691-4.

[71] Bancroft GN, Sikavitsas VI, Mikos AG. Design of a flow perfusion bioreactor system for bone tissue-engineering applications. *Tissue Engineering*. 2003;9:549-54.

[72] Zhang Y-L, Frangos JA, Chachisvilis M. Mechanical stimulus alters conformation of type 1 parathyroid hormone receptor in bone cells. *American journal of physiology Cell physiology*. 2009;296(6):1391-9.

[73] Frangos JA, McIntire LV, Eskin SG. Biotechnology and bioengineering. Shear stress induced stimulation of mammalian cell metabolism. 1988;32(8):1053-60.

[74] Niklason LE, Poh M, Boyer M, Solan A, Dahl SL, Pedrotty D. Blood vessels engineered from human cells. *Lancet*. 2005;365:2122-24.

[75] Ishaug-Riley SL, Crane GM, Gurlek A, Miller MJ, Yasko AW, Yaszemski MJ, et al. Ectopic bone formation by marrow stromal osteoblast transplantation using poly(DL-lactic-co-glycolic acid) foams implanted into the rat mesentery.

8. *J Biomed Mater Res*. 1997;36:1-13.

[76] Freed LE, G V-N. Culture of organized cell communities. *Adv Drug Deliver Rev*. 1998;33:15-30.

[77] Martin I, Padera RF, Vunjak-Novakovic G, LE F. In vitro differentiation of chick embryo bone marrow stromal cells into cartilaginous and bone-like tissues. *J Orthopaed Res* 1998;16:181-9.

[78] Malda J, Martens DE, Geffen v, Tramper J, van Blitterswijk CA, Riesle J. Low oxygen tension stimulates redifferentiation of dedifferentiated adult human nasal chondrocytes. *Osteoarthritis Cartilage*. 2004;12:306-131.

[79] Malda J, Martens DE, Tramper J, van Blitterswijk CA, Riesle J. Cartilage tissue engineering: Controversy in the effect of oxygen. *Critical Reviews In Biotechnology*. 2003;23:175-94.

[80] Malda J, Rouwkema J, Martens DE, le Comte EP, Kooy FK, Tramper J, et al. Oxygen gradients in tissue-engineered Pegt/Pbt cartilaginous constructs: Measurement and modeling. *Biotechnology and Bioengineering*. 2004;86:9-18.

[81] Eaglstein WH, V F. Tissue engineering and the development of Apligraf, A human skin equivalent. *Clin Ther* 1997;19:894-905.

- [82] Shevchenko RV, James SL, James SE. A review of tissue-engineered skin bioconstructs available for skin reconstruction. *Journal of The Royal Society Interface*. 2010;7:229-58.
- [83] Priya SG, Jungvid H, Kumar A. Skin tissue engineering for tissue repair and regeneration. *Tissue engineering Part B, Reviews* 01/04/2008; 14(1):105-18. 2008;14(1):105-18.
- [84] Woodfield TBF, Van Blitterswijk CA, De Wijn J, Sims TJ, Hollander AP, Riesle J. Polymer scaffolds fabricated with pore-size gradients as a model for studying the zonal organization within tissue-engineered cartilage constructs. *Tissue Engineering*. 2005;11:1297.
- [85] Fukuhara S, Tomita S, Yamashiro S, Morisaki T, Yutani C, Kitamura S, et al. Direct cell-cell interaction of cardiomyocytes is key for bone marrow stromal cells to go into cardiac lineage in vitro. *Journal of Thoracic and Cardiovascular Surgery*. 2003;125:1470-80.
- [86] Kleinman HK, Philp D, Hoffman MP. Role of the extracellular matrix in morphogenesis. *Current Opinion in Biotechnology*. 2003;14:526-32.
- [87] Stahl A, Wenger A, Weber H, Stark GB, Augustin HG, Finkenzeller G. Bi-directional cell contact-dependent regulation of gene expression between endothelial cells and osteoblasts in a three-dimensional spheroidal coculture model. *Biochemical and Biophysical Research Communications*. 2004;322:684-92.
- [88] Carmeliet P, Jain RK. Angiogenesis in cancer and other diseases. *Nature*. 2000;407:249-57.
- [89] Hassan KA, Mervat El A, Nadia M, Mohsin B. Intercapillary distance measurement as an indicator of hypoxia in carcinoma of the cervix uteri. *International journal of radiation oncology, biology, physics*. 1986;12:1329-33.
- [90] Rouwkema J, Boer JD, Blitterswijk CAV. Endothelial Cells Assemble into a 3-Dimensional Prevascular Network in a Bone Tissue Engineering Construct. *Tissue Engineering*. 2006;12:2685-93.
- [91] Rouwkema J, Rivron NC, van Blitterswijk CA. Vascularization in tissue engineering. *Trends Biotechnology*. 2008;26(8):434-41.
- [92] Rivron NC, Liu JJ, Rouwkema J, de Boer J, van Blitterswijk CA. Engineering vascularised tissues in vitro. *Eur Cell Mater*. 2008;15:27-40.
- [93] Sucusky P, Osorio DF, Brown JB, Neitzel GP. Fluid mechanics of a spinner-flask bioreactor. *Biotechnol Bioeng* 2004;85(1):34-46.
- [94] Portner R, Nagel-Heyer S, Goepfert C, Adamietz P, Meenen NM. Bioreactor design for tissue engineering. *Journal of bioscience and bioengineering*. 2005;100:235-43.

- [95] Janssen FW, Oostra J, Oorschot A, van Blitterswijk CA. A perfusion bioreactor system capable of producing clinically relevant volumes of tissue-engineered bone: In-vivo bone formation showing proof of concept. *Biomaterials*. 2006;27:315-23.
- [96] Radisic M, Deen W, Langer R, Vunjak-Novakovic G. Oxygen distribution in channeled cardiac constructs perfused with oxygen carrier supplemented culture medium. 2004. p. 8757-9.
- [97] Sikavitsas V, Bancroft G, Mikos A. Formation of three dimensional cell/polymer constructs for bone tissue engineering in a spinner flask and a rotating wall vessel. *J Biomed Mater Res*. 2002;62:136-48.
- [98] Deleu J, Trueta J. Vascularisation of bone grafts in the anterior chamber of the eye. *J Bone Joint Surg Br*. 1965;47:319.
- [99] Abdullah NS, Das DB, Ye H, Cui ZF. 3D bone tissue growth in hollow fibre membrane bioreactor: Implications of various process parameters on tissue nutrition. *International Journal of Artificial Organs*. 2006;29:841-51.
- [100] Broadhead KW, Biran R, Tresco PA. Hollow fiber membrane diffusive permeability regulates encapsulated cell line biomass, proliferation, and small molecule release. *Biomaterials*. 2002;23:4689-99.
- [101] Ye H, Das DB, Triffitt JT, Cui Z. Modelling nutrient transport in hollow fibre membrane bioreactors for growing three-dimensional bone tissue. *Journal of Membrane Science*. 2006;272:169-78.
- [102] Piret JM, Cooney CL. Model of oxygen transport limitations in hollow fiber bioreactors. *Biotechnology and Bioengineering*. 1991;37:80-92.
- [103] Ungera RE, Petersa K, Huangb Q, Funka A, Paulb D, Kirkpatricka CJ. Vascularization and gene regulation of human endothelial cells growing on porous polyethersulfone (PES) hollow fiber membranes. *Biomaterials*. 2005;26:3461-9.
- [104] Heath CA, Magari SR. Mini-review: Mechanical factors affecting cartilage regeneration in vitro. *Biotechnology and Bioengineering*. 1996;50:430-7.
- [105] Sodian R, Hoerstrup SP, Sperling JS, Daebritz SH, Martin DP, Schoen FJ, et al. Tissue engineering of heart valves: in vitro experiences. *Ann Thorac Surg*. 2000;70:140-4.
- [106] Brown AL, Farhat W, Merguerian P. 22week assessment of bladder acellular matrix as a bladder augmentation material in a porcine model. *Biomaterials*. 2002;23:2179.
- [107] O'Connor KC. three dimensional cultures of prostatic cells: Tissue models for the development of novel anti cancer therapies. *Pharm Res*. 1999;16:486-93.

- [108] Chen H-C, Hu Y-C. Bioreactors for tissue engineering. *Biotechnology letters*. 2006;28(18):1415-23.
- [109] Bilgen B, Chang-Mateu IM, Barabino GA. Characterization of Mixing in a Novel Wavy-Walled Bioreactor for Tissue Engineering. *Biotechnology and Bioengineering* 2005;92(7):907-19.
- [110] Gomes ME, Holtorf HL, Reis RL, Mikos AG. Influence of the porosity of starch-based fiber mesh scaffolds on the proliferation and osteogenic differentiation of bone marrow stromal cells cultured in a flow perfusion bioreactor. *Tissue engineering*. 2006;12(4):801-9.
- [111] Fey-Lamprecht F, Albrecht W, Groth T, Weigel T, Gross U. Morphological studies on the culture of kidney epithelial cells in a fiber-in-fiber bioreactor design with hollow fiber membranes. *J Biomed Mater Res A*. 2002;65(2):144-57.
- [112] Shachar M, Cohen S. Cardiac Tissue Engineering, *Ex-Vivo: Design Principles in Biomaterials and Bioreactors* Heart failure reviews. 2004;8:271-6.
- [113] Lu H-F, Lim WS, Zhang P-C, Chai SM, Yu H, Mao H-Q, et al. Galactosylated Poly(vinylidene difluoride) Hollow Fiber Bioreactor for Hepatocyte Culture. *Tissue engineering*. 2005;11:1667-77.
- [114] Martin I, Wendt D, Heberer M. The role of bioreactors in tissue engineering. *Trends in Biotechnology*. 2004;22:80.
- [115] Nagel-Heyer Leist. S, Ch. L, S, Goepfert. C, Pörtner. R. From biopsy to cartilage-carrier constructs by using microcarrier cultures as sub-process. In *Proceedings of 19th ESACT meeting European Society for Animal Cell Technology (ESACT)*. 2005:139.
- [116] Bardouille C, Lehmann J, Heimann P, Jockusch H. Growth and differentiation of permanent and secondary mouse myogenic cell lines on microcarriers. *Applied Microbiology and Biotechnology*. 2001;55:556.
- [117] C D, Schünke.M, Christesen.K, Kurz.B a. Redifferentiation of dedifferentiated bovine articular chondrocytes in alginate culture under low oxygen tension. *Osteoarthritis Cartilage*. 2002;10:13-22.
- [118] Freed LE, Langer R, Martin I, Pellis NR, Vunjak-Novakovic G. Tissue engineering of cartilage in space. *Proceedings of the National Academy of Sciences of the United States of America*. 1997;94:13885.
- [119] Holy CE, Shoichet MS, Davies JE. Engineering three-dimensional bone tissue in vitro using biodegradable scaffolds: Investigating initial cell-seeding density and culture period. *Journal of Biomedical Materials Research*. 2000;51:376.

- [120] Carrier RL, Papadaki M, Rupnick M, Schoen FJ, Bursac N, Langer R, et al. Cardiac tissue engineering: Cell seeding, cultivation parameters, and tissue construct characterization. *Biotechnology and Bioengineering*. 1999;64:580.
- [121] Kannan RY, Salacinski HJ, Sales K, Butler P, Seifalian AM. The roles of tissue engineering and vascularisation in the development of micro-vascular networks: A review. *Biomaterials*. 2005;26:1857.
- [122] Bancroft G, Sikavitsas V, Mikos A. Design of a flow perfusion bioreactor system for bone tissue engineering applications. *Tissue engineering*. 2003;9:549-54.
- [123] Cioffi M, Kaffer J, Strabel S, Dubini G, Martin I, Wendt D. Computational evaluation of oxygen and shear stress distributions in 3D perfusion culture systems: Macro-scale and micro-structured models. *Journal of Biomechanics*. 2008;41:2918-25.
- [124] Williams C, Wick TM. Perfusion Bioreactor for Small Diameter Tissue-Engineered Arteries. *Tissue engineering*. 2004;10:930-41.
- [125] Visconti R, Mironov V, Kasyanov VA, Yost MJ, Twal W, Trusk T, et al. Cardiovascular Tissue Engineering I. Perfusion Bioreactors: A Review. *J of long term effects of medical implants*. 2006;16(2):104.
- [126] Mol A, Driessen NJB, Rutten MCM, Hoerstrup SP, Bouten CVC, Baaijens FPT. Tissue Engineering of Human Heart Valve Leaflets: A Novel Bioreactor for a Strain-Based Conditioning *Annals of Biomedical engineering*. 2005;33:1778 - 88.
- [127] Mol A, Driessen N, Rutten M, Hoerstrup S, Bouten C, Baaijens F. Tissue Engineering of Human Heart Valve Leaflets: A Novel Bioreactor for a Strain-Based Conditioning Approach. *Annals of Biomedical Engineering*. 2005;33:1778-88.
- [128] Wendt D, Stroebel S, Jakob M, John GT, Martin I. Uniform tissues engineered by seeding and culturing cells in 3D scaffolds under perfusion at defined oxygen tensions. *Biorheology*. 2006;43(3-4):481-8.
- [129] Davisson T, Sah RL, A R. Perfusion increases cell content and matrix synthesis in chondrocyte three-dimensional cultures. *Tissue engineering*. 2002;8(5):807-16.
- [130] Janssen FW, Hofland I, van Oorschot A, Oostra J, Peters H, CA vB. Online measurement of oxygen consumption by goat bone marrow stromal cells in a combined cell-seeding and proliferation perfusion bioreactor. *J Biomed Mater Res A*. 2006;79(2):338-48.
- [131] Bancroft GN, Sikavitsas VI, van den Dolder J, Sheffield TL, Ambrose CG, Jansen JA, et al. Fluid flow increases mineralized matrix deposition in 3D perfusion culture of marrow stromal osteoblasts in a dose-dependent manner. *Proc Natl Acad Sci U S A*. 2002;99(20):12600-5.

- [132] Porter B, Zuel R, Stockman H, Guldberg R, D F. 3-D computational modeling of media flow through scaffolds in a perfusion bioreactor. *J Biomech.* 2005;38(3):543-9.
- [133] Klinkmann H, Vienken J. Membranes for dialysis. *Nephrology Dialysis Transplantation.* 1995;10:39-45.
- [134] Clark WR. Hemodialyzer Membranes and Configurations: A Historical Perspective. *Seminars in Dialysis.* 2000;13:309-11.
- [135] Gerlach J. Development of a hybrid liver support system: a review. *Int J Artif Organs.* 1996;19(11):645-54.
- [136] Gerlach JC. Use of hepatocyte culture for liver support bioreactors. *Adv Exp Med Biol.* 1994;368:165-71.
- [137] Flendrig LM, te Velde AA, Chamuleau RAFM. Semipermeable hollow fiber membranes in hepatocyte bioreactors: a prerequisite for a successful bioartificial liver? . *Artif organs.* 1997;21(11):1177-81.
- [138] De Bartolo L, Salerno S, Curcio E, Piscioneri A, Rende M, Morelli S, et al. Human hepatocyte functions in a crossed hollow fiber membrane bioreactor. *Biomaterials.* 2009;30(13):2531-43.
- [139] Wegner JA. Oxygenator anatomy and function. *J Cardiothor Vasc An.* 1997;11:275.
- [140] De Bartolo L, Salerno S, Morelli S, Giorno L, Rende M, Memoli B, et al. Long-term maintenance of human hepatocytes in oxygen-permeable membrane bioreactor. *Biomaterials.* 2006;27(27):4794-803.
- [141] Tresco PA. Tissue engineering strategies for nervous system repair. In: Seil FJ, editor. *Progress in Brain Research: Elsevier;* 2000. p. 349-63.
- [142] Guenard V, Kleitman N, Morissey T, Bunge R, Aebischer P. Syngenic schwann cells derived from adult nerves seeded in semipermeable guidance channels enhance peripheral nerve regeneration. *J Neuroscience.* 1992;12:3310-20.
- [143] Uludag H, De Vos P, Tresco PA. Technology of mammalian cell encapsulation. *AdvDrugDelivRev.* 2000;42:29-64.
- [144] Loeb S. The Loeb-Sourirajan Membrane: How it Came About. *Synthetic Membranes, A Turbak, ed, ACS Symposium Series-153.* 1981;1.
- [145] Loeb S, Sourirajan S. Sea Water Demineralization by Means of an Osmotic Membrane. *Advances in Chemistry Series.* 1962;38:117.

- [146] Barzin J, Feng C, Khulbe KC, Matsuura T, Madaeni SS, Mirzadeh H. Characterization of polyethersulfone hemodialysis membrane by ultrafiltration and atomic force microscopy. *Journal of Membrane Science*. 2004;237:77-85.
- [147] Su B-h, Fu P, Li Q, Tao Y, Li Z, Zao H-s, et al. Evaluation of polyethersulfone highflux hemodialysis membrane in vitro and in vivo. *Journal of Materials Science: Materials in Medicine*. 2008;19:745-51.
- [148] Lützow K, Weigel T, Lendlein A. Poly(ether imide) Scaffolds as Multifunctional Materials for Potential Applications in Regenerative Medicine. *Artificial Organs*. 2006;30:764-9.
- [149] Unger RE, Huang Q, Peters K, Protzer D, Paul D, Kirkpatrick CJ. Growth of human cells on polyethersulfone (PES) hollow fiber membranes. *Biomaterials*. 2005;26:1877-84.
- [150] Unger RE, Peters K, Huang Q, Funk A, Paul D, Kirkpatrick CJ. Vascularization and gene regulation of human endothelial cells growing on porous polyethersulfone (PES) hollow fiber membranes. *Biomaterials*. 2005;26:3461-9.
- [151] Schakenraad JM, Oosterbaan JA, Nieuwenhuis P, Molenaar I, Olijslager J, Potman W, et al. Biodegradable hollow fiber for the controlled release of drugs. *Biomaterials*. 1988;9:116-20.
- [152] Marianne JE, Julian BC. Poly(lactic-co-glycolic acid) hollow fibre membranes for use as a tissue engineering scaffold. *Biotechnology and Bioengineering*. 2007;96:177-87.
- [153] Kitano H, Ise N. Hollow fiber enzyme reactors. *Trends in Biotechnology*. 2:5-7.
- [154] Wolf C, Munkelt B. Bilirubin conjugate be an artificial liver composed of cultured cells and synthetic capillaries. *TransAmSocArtifInternOrgans*. 1975;21:16-27.
- [155] Knazek RA, Gullino PM, Kohler PO, Dedrick RL. Cell culture on artificial capillaries: An approach to tissue growth in vitro. *Science*. 1972;178(56):65-6.
- [156] Nagel A, Koch S, Valley U, Emmrich F, Marx U. Membrane based cell culture systems – An alternative to in vivo production of monoclonal antibodies. *Dev Biol Stand*. 1999;101:57-64.
- [157] Williams SNO, Callies RM, Brindle KM. Mapping of oxygen tension and cell distribution in a hollow-fiber bioreactor using magnetic resonance imaging. *Biotechnology and Bioengineering*. 1997;56:56-61.
- [158] Neves AA, Brindle KM. Monitoring the Performance of Tissue Engineering Bioreactors Using Magnetic Resonance Imaging and Spectroscopy. In: Chaudhuri J, Al-Rubeai M, editors. *Bioreactors for Tissue Engineering*: Springer Netherlands; 2005. p. 335-52.

Chapter 2

Development of poly (L-lactic acid) hollow fiber membranes for artificial vasculature in tissue engineering scaffolds

N.M.S. Bettahalli, H. Steg, M. Wessling, D. Stamatialis*

MIRA Institute for Biomedical Technology and Technical Medicine, University of Twente,
Membrane Technology Group, Faculty of Science and Technology, PO Box 217, 7500 AE Enschede,
The Netherlands.

If you aren't fired with enthusiasm, you will be fired with enthusiasm.

(Vince Lombardi)

Abstract

In tissue engineering constructs, vascularization within in-vitro cultured tissue is one of the major problems, as proliferating cells act themselves as a barrier for mass transfer. Issues related especially to nutrient and oxygen delivery to the cells limit tissue construct development to smaller than clinically relevant dimensions, which in-turn limits the ability for in-vivo integration.

In this work, we develop highly permeable biodegradable Poly (L-lactic acid) (PLLA) hollow fibers (HF) which when integrated with tissue engineered scaffolds in -vitro can improve nutrient supply to the cells. In fact, we study various fiber spinning parameters to develop the optimum fiber structure. By using 1,4 dioxane as solvent and ethanol as non-solvent at very low temperature (-6°C), we develop fibers with thin dense top-layer and spongy sub-layer. Porogens like Poly-vinylpyrrolidone (PVP) and Poly (ethylene-glycol) (PEG) are added to the dope solution. Subsequent treatment with sodium hypochlorite produces open fiber surface and increased pore interconnectivity. The produced fibers have good mechanical properties. The transport of Bovine serum albumin (BSA) and of cell culture medium supplement with 10% Fetal bovine serum (FBS) through the produced PLLA fiber is high (permeance $\sim 2100 \text{ L}/(\text{m}^2\text{hbar})$) with low retention. In-vitro static and dynamic cell culturing for 3 and 7 days using mouse pre-myoblast (C2C12) cells suggests that the fabricated PLLA hollow fibers are suitable for delivery nutrients to the cells in a tissue engineering scaffold.

Adapted from NMS Bettahalli et.al, Development of poly (L-lactic acid) hollow fiber membranes for artificial vasculature in tissue engineering scaffolds, Accepted at Journal of Membrane Science.

1 Introduction

Tissue engineering is a cell based therapy that has emerged as a thriving and complimentary new field of medical science. It is an interdisciplinary field that applies the principles of engineering and the life sciences to develop biological substitutes that restore, maintain, or improve tissue function [1, 2]. Just a decade ago most scientists believed that human tissue could be replaced only with direct transplants from donors or with fully artificial substitutes made of plastic, ceramics, metal etc. However, innovative and imaginative work in laboratories around the world is demonstrating that creation of bio-hybrid organs is feasible. But before this research will begin to pay off in terms of reliable tissues, tissue engineering must surmount some important hurdles.

In nature, blood vessels carry blood from the heart to the tissues and organs and back to the heart. They form a branched system of arteries and veins which then branch into smaller arterioles and capillaries. In active tissue, sufficient diffusion is confined to 150 - 200 μ m from the nearby capillary [3]. In 3D tissue formation, vascularization of in-vitro culture constructs is one of the major challenges apart from cell differentiation and proliferation up to scaffold design and bioreactor culture.

The mass transfer limitation within the in-vitro 3D cultured constructs could be addressed by utilization of porous biodegradable hollow fibers mimicking the blood arteries when incorporated within the traditional tissue scaffold. As incorporated porous fiber wall itself act as barrier between the proliferating cells and flowing media, perfusion bio-reactor systems could be used to develop 3D tissue of clinical relevance. Hence, implantable mechanically strong porous biodegradable hollow fibers with high cell culture medium permeance and rather low cell adhesion are necessary to deliver nutrient to the cells in tissue engineering scaffolds.

Recently, an interesting study reported the development of biodegradable poly(lactic-co-glycolic acid) (PLGA) hollow fibers for tissue engineering application [4]. Others also developed biodegradable PLLA hollow fiber membranes for drug delivery [5-7] or ultra filtration membrane applications [8]. In the latter, the PLLA membranes have high clean water flux but also high protein retention (~80%). Since the cell culture medium contains high amount of proteins, these membranes would not be suitable for delivering the medium to the cells.

In this study by tailoring the hollow fiber spinning conditions we develop via liquid induced phase separation (LIPS) mechanically stable biodegradable PLLA hollow fibers with very high clean water and medium fluxes (in the microfiltration range) and very low protein retention. Cell culture experiments under static conditions show that cells attach and proliferate very well on our HF whereas high medium perfusion through them suggests that the HF can be used as artificial vasculature for in-vitro tissue engineering scaffolds.

2 Materials and Methods

2.1 PLLA hollow fiber polymer solution

Initially, hollow fibers were fabricated using Poly(L-lactic acid) (PLLA, Mol wt. 1.6×10^5 g/mol, kindly provided by Prof. Dr. D. Grijpma (Biomaterials Science and Technology (BST) group, University of Twente, The Netherlands), of different concentrations: 14, 17 and 20 wt% dissolved in 1,4-dioxane (Merck, 99% purity). These hollow fibers had low porosity. Subsequently to increase porosity and wettability different porogens were added to the polymer solution: 2.5 wt% Poly-vinylpyrrolidone (PVP K-30) (Mol wt. 4×10^4 g/mol), 2.5 wt% Poly-vinylpyrrolidone (PVP K-90) (Mol wt. 3.6×10^5 g/mol) (both Fluka, analytical quality) and 5% Poly (ethylene-glycol) (PEG-400) (Mol wt. ~ 400 g/mol) (MERCK). Since PVP is sparingly soluble in 1, 4 dioxane, these additives were initially dissolved in 10 wt% *N*-Methyl-2-pyrrolidone (NMP) (ACROS 99% purity) and then added to the PLLA polymer solution. In most cases non solvent ethanol (MERCK 99.9% purity) was added in to the polymer solution to decrease the time for phase separation. Details about the selection of the spinning compositions are discussed in the results section. In all cases the polymer dopes were filtered through a 25 μ m metal filter and degassed for at least 1day before spinning.

2.2 Spinning set-up

A special miniaturized spinning system was developed since only small amounts of polymers were available to process. The degassed spinning dope was maintained at 60°C before loaded into the syringe of the spinning setup. The syringe and the spinneret were also maintained at 60°C during spinning, using a tape heater. The syringe was pressurized using nitrogen gas at pressure of 1bar to extrude the dope solution through spinneret, which consisted of outer and inner needles of diameter 0.5mm and 0.2 mm respectively (Figure 1). Ethanol (MERCK

99.9% purity) was used as non-solvent maintained at various temperatures by circulating coolant through the jacketed walls of coagulation bath. Ethanol was used as bore liquid at room temperature at a flow rate of 1ml/min. The prepared fibers were first collected at the bottom of the non-solvent bath and later were soaked in ethanol at 4°C for at least 72 hours to remove residual solvent.

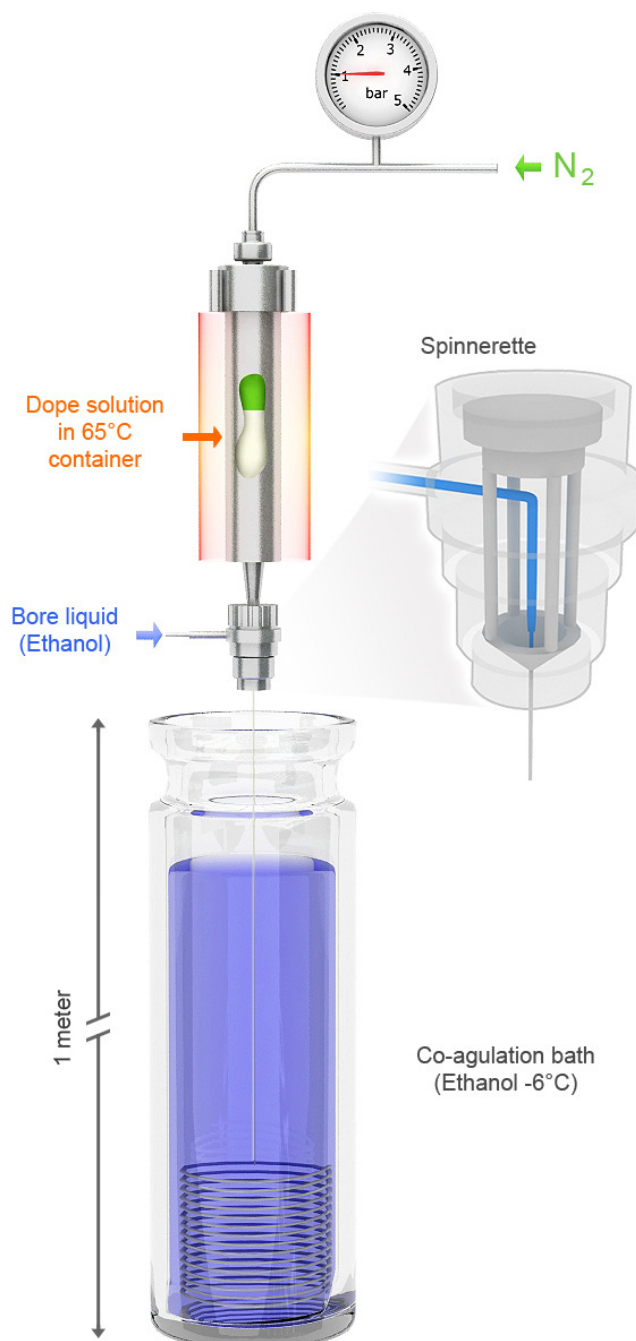


Figure 1. Schematic of miniaturized hollow fiber spinning set-up.

2.3 Membrane treatment

2.3.1 Gas Plasma treatment

To increase the membrane surface porosity, some hollow fibers were treated with oxygen plasma (PlasmaFAB-508, Electrotech) at varying power input (10 – 30 W) and etching time (10 – 30min) with intermediate relaxation or cooling steps. For the plasma treatment, the hollow fibers were hung horizontally in the center of the plasma chamber to expose complete surface of the fiber to the generated plasma.

2.3.2 Sodium hypochlorite treatment

Sodium hypochlorite (NaOCl) treatment was used to remove PVP from the fiber matrix and increase membrane porosity. In fact, the hollow fibers after extensive washing in ethanol were first transferred to running tap water bath for 24 hours and then transferred into the 4000 ppm NaOCl solution for 4 and 24 hours. Subsequently, the fibers were washed with running tap water for 24 hours before storing in ethanol.

2.4 Hollow fiber characterization

2.4.1 Scanning Electron Microscopy (SEM) analysis

SEM images of dry PLLA fibers were obtained using JeoL 5600LV scanning electron microscope at accelerating voltage of 5kV. Fibers dried overnight in vacuum oven at 30°C were directly used for SEM analysis after carefully fractured in liquid nitrogen. All samples were sputtered with gold (~15 to 20 nm-thick, Balzer-Union SCD-040).

2.4.2 Water permeability

For the pure water permeability experiment, de-mineralized water was pressurized through the lumen of the PLLA hollow fiber (inside-out permeation). The experiments were carried out in modules containing single hollow fiber prepared using 6 mm polyethylene tube housing of approximately 10 cm long. The fibers were carefully inserted into the polyethylene tube and sealed with polyurethane glue. In the middle of the housing, a T-junction was placed to collect the flowing permeate. Before measuring the clean water flux, the fibers were first flushed with ethanol to improve their wettability. Subsequently, water was pumped through the modules for at least an hour to remove/exchange the ethanol. The flux (J) through the

membrane was measured at different trans-membrane pressure ranging between 100 – 500mbar at $20 \pm 2^\circ\text{C}$. The flux ($\text{L}/(\text{m}^2\text{h})$) at each pressure was successively measured by collecting permeating water (L) with respect to time (h, at least 60min) and active fiber surface area (m^2). The pure water permeance ($\text{L}/(\text{m}^2\cdot\text{h}\cdot\text{bar})$) was calculated using the slope of flux versus pressure plot. The data presented in this work is an average of 5 hollow fiber modules prepared from different sections of the total fiber spun.

2.4.3 Protein permeability

Protein permeation experiments through PLLA fiber were carried out using model protein Bovine Serum Albumin (BSA) solution of 0.5 g/l (molecular weight ~ 66 kDa) and Fetal Bovine Serum (FBS) (containing a cocktail of albumin 65% and other small chain proteins extensively used as a supplement with cell culture medium). Both proteins were dissolved in phosphate buffer solution (PBS) at pH 7.3 and the filtration experiments was carried out using hollow fiber modules prepared similar to that used for water permeability experiments. The data presented here is an average of 5 different hollow fiber modules tested for each protein type. Trans-membrane pressure of 0.1 bar was applied across the hollow fiber and the collected permeate was analyzed for protein rejection every 30 min for 6 hours of continuous filtration. BSA concentration was analyzed using UV-VIS spectrophotometer (Varian – CARY 300 Scan) at 278 nm. Whereas FBS was analyzed using BCA (bi-cinchoninic acid) assay kit, which is a colorimetric assay read at 562nm using 96 micro-well plate spectrophotometric reader. In all cases the feed and permeate concentration of protein were monitored, too.

2.4.4 Mechanical properties

The mechanical properties of hollow fiber were measured using a tensile testing machine (Zwick, Static Material Prufung unit). The testing of hollow fibers was carried out using an ISO standard specified for tubes/cylinders. A dry 10cm long hollow fiber was clamped vertically between the holders/clamps of the Zwick test machine (Z020) separated by 5cm. 500N load cell was used to apply constant pressure on the hollow fiber elongated at a constant rate of 50mm/min until break point. The data presented here is an average of 5 fibers. The E-modulus of the fiber was estimated using the slope at the initial part of the stress strain curve. The maximum stress and stress at break were noted from the stress strain curve correspondingly.

2.4.5 Cell culturing

Mouse pre-myoblast, C2C12 cells were cultured in proliferation medium containing Dulbecco's Modified Eagle's Medium (D-MEM, Gibco) supplemented with 10% Fetal Bovine Serum (FBS, Cambrex), 100 U/ml penicillin (Gibco) and 100 µg/ml streptomycin (Gibco). Cells were initially plated in T-flask for expansion at 2000 cells/cm² until they reached 70-80% confluence, after which they were trypsinized using 0.05% Trypsin contained in 1mM EDTA. The obtained C2C12 cells were subsequently seeded on to the outer surface of the hollow fiber and were allowed to attach for 6 hours before the static or dynamic culture experiments.

Static culture - Hollow fibers 2 cm long, fabricated of 17% PLLA treated with NaOCl for 24h were first sterilized in excess of 70% ethanol and iso-propanol, after evaporation of the alcohols inside sterile flow-hood, the fibers were washed 3 times with PBS and finally neutralized in proliferation medium. Five such fibers were kept inside the tissue culture plate (non-treated) and seeded with C2C12 cells. These samples were cultured for 0, 3 and 7 days in an incubator with proliferation medium being exchanged every alternate day.

Dynamic culture - Hollow fibers fabricated of 17% PLLA treated with NaOCl for 24h were potted at both ends using poly-urethane inside 6 mm silicon tubing, such that 2 cm long fiber surface in the middle was exposed for cell adhesion and proliferation. The modules prepared were sterilized by pumping 70% ethanol, PBS and proliferation medium correspondingly at low pressure (~0.1bar). The sterilized fiber modules were seeded with C2C12 cells and cultured in a recirculation perfusion bioreactor (see details later) for 0, 3 and 7 days. Trans-membrane pressure of ~0.1bar was maintained across the cell seeded fiber module in the bioreactor system with an average cross flow velocity of 1ml/min.

For visualization of cell adhesion and proliferation using light microscopy, 4000 cells/cm² were cultured in both static and dynamic culture. For the DNA analysis, fibers were placed in different wells and 2×10^6 C2C12 cells / fiber were seeded. Quantification of total DNA concentration per sample was measured according to the manufacturer's protocol (CyQuant Cell Proliferation Assay Kit, Invitrogen/Molecular probes) using a fluorescent plate reader (Perkin Elmer).

3 Results and discussion

3.1 Preparation of PLLA hollow fiber

Initially various organic solvents were screened for the preparation of PLLA fibers. Especially, the morphology and mechanical stability of the fiber were evaluated. Table 1 presents the best results obtained for 3 different solvents with corresponding polymer concentrations and mixing temperature to extrude hollow fiber. In all these cases ethanol was used as non-solvent at 4°C, as has been reported for fabrication of PLLA porous flat membranes [9]. Only the PLLA fibers prepared in 1,4 dioxane were mechanically stable and could be used for further tests (SEM, permeation experiments etc). Despite this, these fibers were also rather dense with thin skin layer and closed pores.

Table 1. Screening of PLLA spinning solvents.

Spinning dope		Mixing Temperature (C)	Hollow fiber morphology	Remarks
Components	Concentration (wt %)			
PLLA : NMP	12:88	80	Dense skin with closed pores	Sparingly soluble + low mechanical stability
PLLA : CHCl ₃	18:82	52	Dense skin with closed pores	High viscosity+ Low mechanical stability
PLLA : Dioxane	24:76	75	Dense skin with closed pores	Gelation at RT

Earlier studies (some of them performed in our group) showed that PVP (K15, K30, K90) [10-13] and PEG (200 and 400 g/mol) [14] can increase the porosity and pore interconnectivity of membranes. To identify the optimum cocktail of porogens for fabricating highly porous and mechanically stable fibers we also performed extensive screening. Hence, we fabricated HF with 14 wt% PLLA, different concentrations of PVP (2.5, 5, 7.5 wt %) of various molecular weights (K15, K30, K90) and PEG (molecular weight 200 and 400g/mol) of different concentrations (2.5, 5 and 10 wt%). The best result concerning mechanical stability was obtained for the fibers fabricated with PVP (2.5 wt% K30 and 2.5 wt% K90) and PEG (5 wt %) dissolved in NMP (10 wt %) in the dope solution. Hence results with these porogens in the dope solution of different PLLA concentrations and spinning parameters are presented further in this work.

Furthermore, to minimize the formation of dense skin layer of the hollow fiber we also investigated the effect of the non solvent temperature. Besides 4°C, we also spun fibers at 0, -4, -6, -10°C. The most promising fibers with open surface were obtained with non-solvent bath temperature of -6°C.

In the following sections, the spinning tests were performed using PLLA of various polymer concentration, with various percentages of non solvent (ethanol) in the polymer dope with 2.5 wt% K30 PVP and 2.5 wt% K90 PVP, PEG (5 wt %) dissolved in NMP (10 wt %) as porogens. In all cases the temperature of non solvent (ethanol) was constant at -6°C. Table 2 presents the polymer dopes investigated.

Table 2. PLLA spinning dopes used in this study to fabricate hollow fiber at -6°C.

Dope solution code	PLLA wt%	Additives, wt%					Dioxane wt%
		PVP K30	PVP K90	PEG	NMP	Ethanol	
D1	14	2.5	2.5	5	10	-	66
D2	14	2.5	2.5	5	10	1	65
D3	17	2.5	2.5	5	10	1	62
D4	20	2.5	2.5	5	10	1	59

3.1.1 Effect of air gap and non-solvent in dope solution

Figure 2 shows the effect of the air gap on membrane morphology for fiber spun with dope solution D1 (14 wt% PLLA) and additives (PVP and PEG). For air gap of 1 and 2 cm the fibers had outer skin and low porosity. An increased air gap results in a longer residence time in air, whose magnitude can be roughly estimated using the average velocity of the polymer solution as it exits the spinneret and the take-up velocity [15]. Although a spongy porous matrix was formed (see cross sectional SEM images in Figure 2) the evaporation of the volatile dioxane and the delayed demixing at the surface causes skin formation. Figure 2 also shows the effect of adding 1% non-solvent ethanol to the 14 wt% PLLA dope solution (D2). With this the polymer solution approaches the binodal demixing and nucleus growth is accelerated [13, 16]. Thus slight change in the solvent composition results in faster demixing and a more open porous structure. In fact, rapid demixing is desired also due to the short non-solvent bath in miniaturized setup.

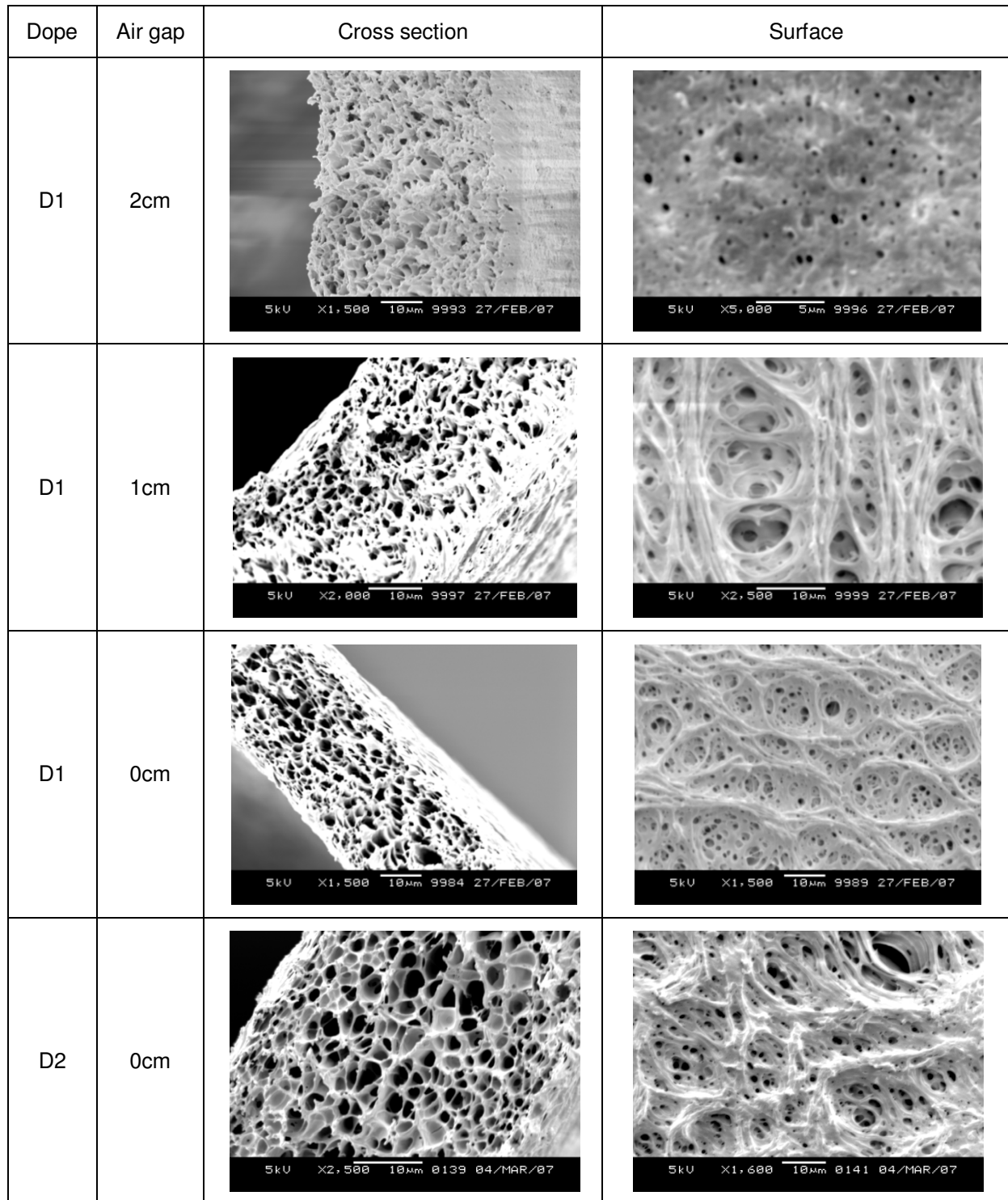


Figure 2. Effect of air gap and non solvent in the dope solution on PLLA hollow fiber morphology.

3.1.2 Effect of polymer concentration in dope solution

Different PLLA concentrations along with additives as listed in Table 2 were tested to prepare optimum fiber with high porosity and mechanically stable structure. Figure 3 shows SEM images of fiber spun with dope solution D2, D3 and D4.

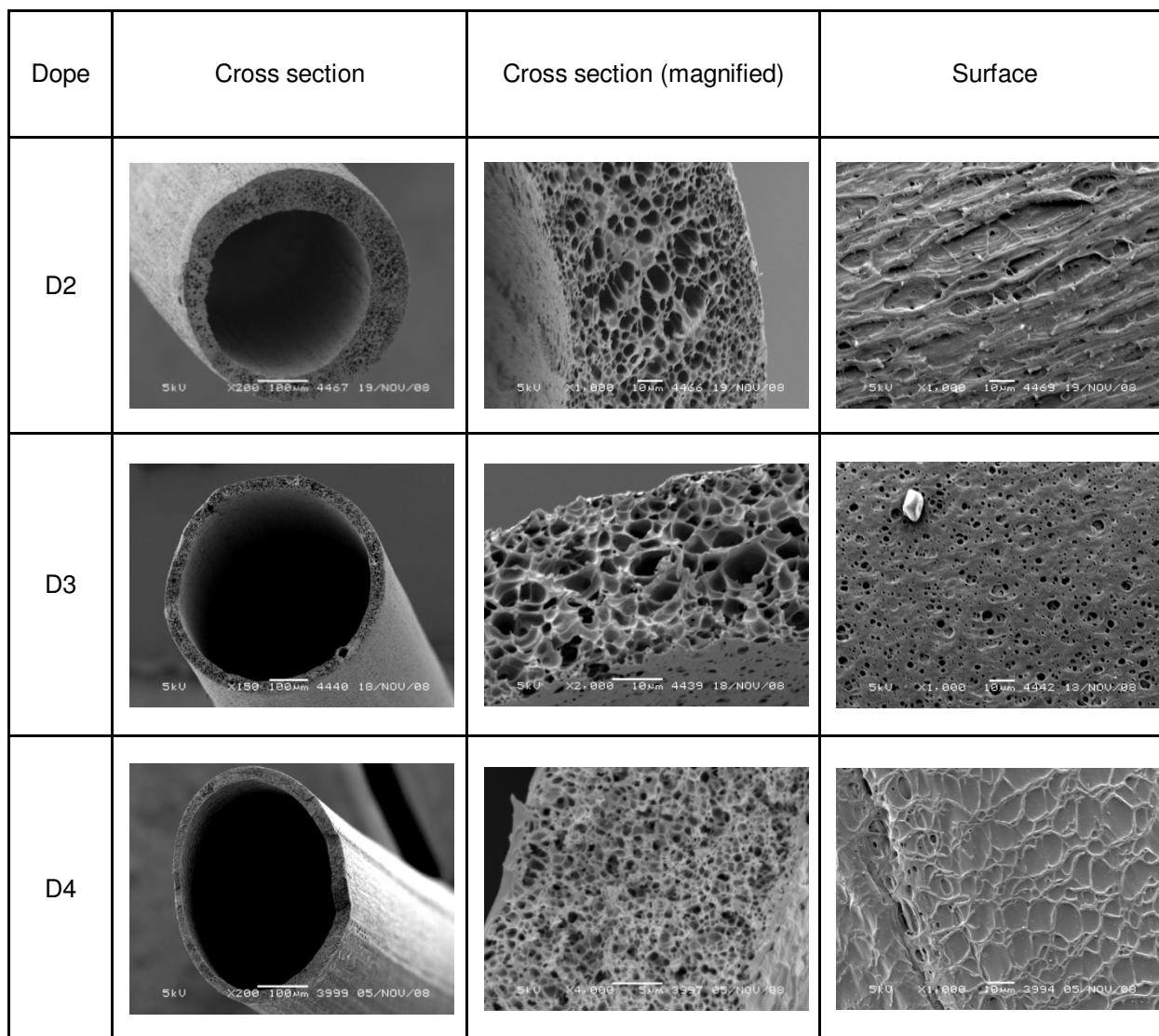


Figure 3. Effect of PLLA polymer concentration in the dope solution on PLLA hollow fiber morphology.

The cross sections of the fibers spun with D2 and D3 show a well-distributed porous structure, but the fibers have dense outer skin. D4 fibers have poor interconnectivity and a dense skin layer. When compared for mechanical strength, the order is directly proportional to increasing polymer concentration i.e. the D4 fibers are the most mechanically stable, but with

closed pores across the wall of the membrane. This decrease in porosity is expected due to the higher polymer concentration. The fibers spun with dope solution D3 seem to be the most optimal concerning to wall and surface porosity (pore size range 0.5 - 5 μ m) and mechanical stability. Hence, further optimization was carried out on fiber spun with dope solution D3.

3.2 Hollow Fiber post treatment

3.2.1 Plasma treatment

Oxygen plasma etching was carried out to remove the outer skin of the hollow fiber. Plasma treatment causes an increase in both contact angle and roughness, altering the surface morphology and insertion of polar groups, which consequently, enhancing the hydrophilicity of the polymer [17]. Optimization of the etching conditions was performed to evaluate the etching rates and etching time. SEM pictures of a few positive results are shown in Figure 4. Low intensity of 10W does not open the fiber skin even after exposure for 3 times of 10 min each. Intensity of 30W etching opens the fiber skin but the fibers melt due to heating (see Figure 4, 3 times 10 min exposure at 30W). Although the surface opens, the sub-layer becomes denser due to polymer melting. Most of the etched fibers are extremely fragile to handle. Based on these results, the plasma treatment does not offer promising results concerning fiber structure optimization. Hence plasma treated HF were not considered for further characterization.

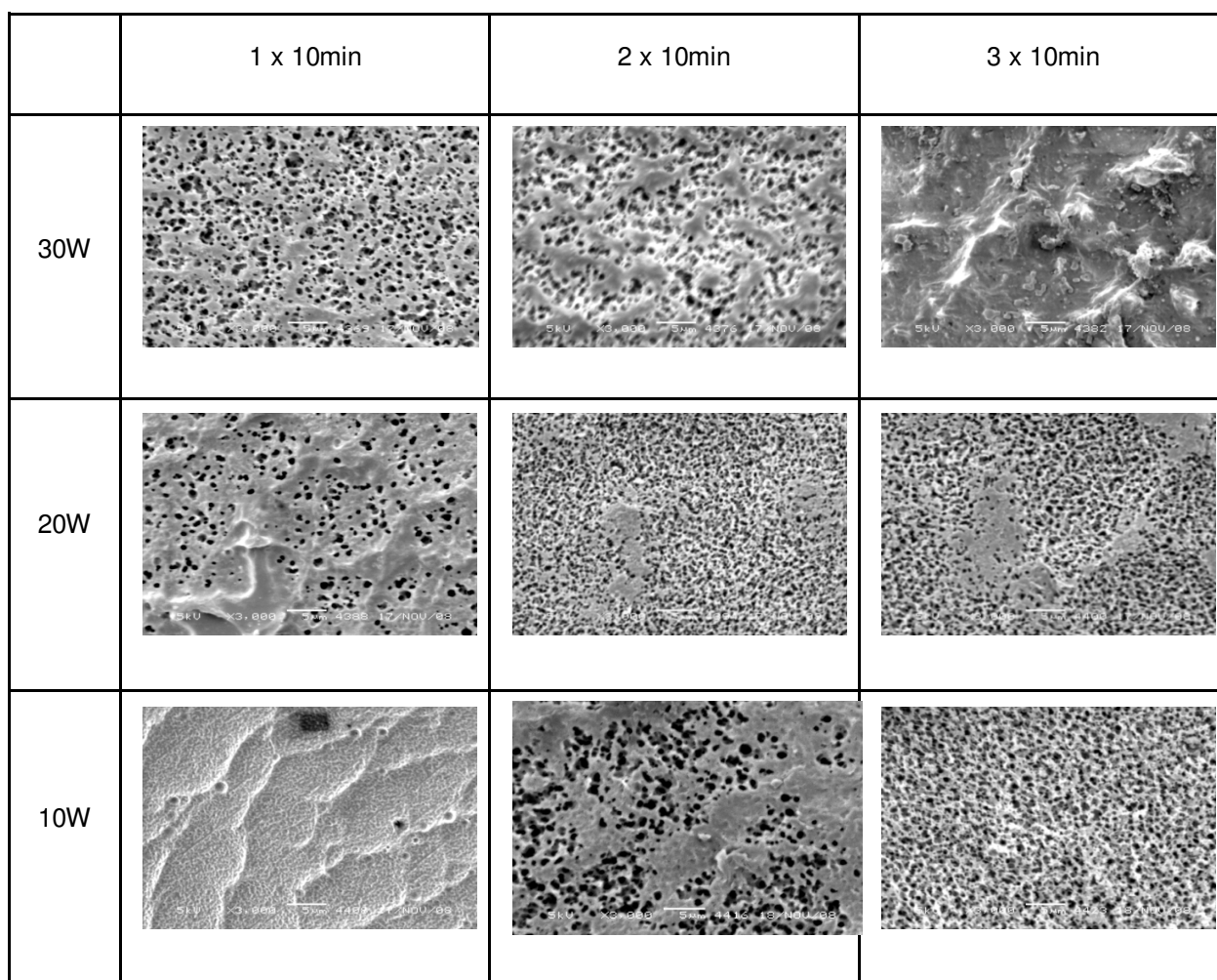


Figure 4. SEM images of PLLA hollow fiber (D3, 17% PLLA dope solution) after oxygen plasma treatment.

3.2.2 Sodium hypochlorite treatment

Another post treatment to increase membrane porosity and pore-interconnectivity is removal of PVP using NaOCl. In preparing a porous membrane PVP is not mixed with polymer on the molecular level (heterogeneous blend), but it will be located at the surface of the pore wall [10]. The removal of PVP can be achieved with 4000ppm NaOCl treatment. Therefore the fibers fabricated with D3 were treated by immersing in the NaOCl bath for 4 and 24 hours. Figure 5 shows that the fibers treated for 24 hours with NaOCl are very open and those fibers are further characterized in the following paragraphs (permeance and mechanical testing and cell culture).

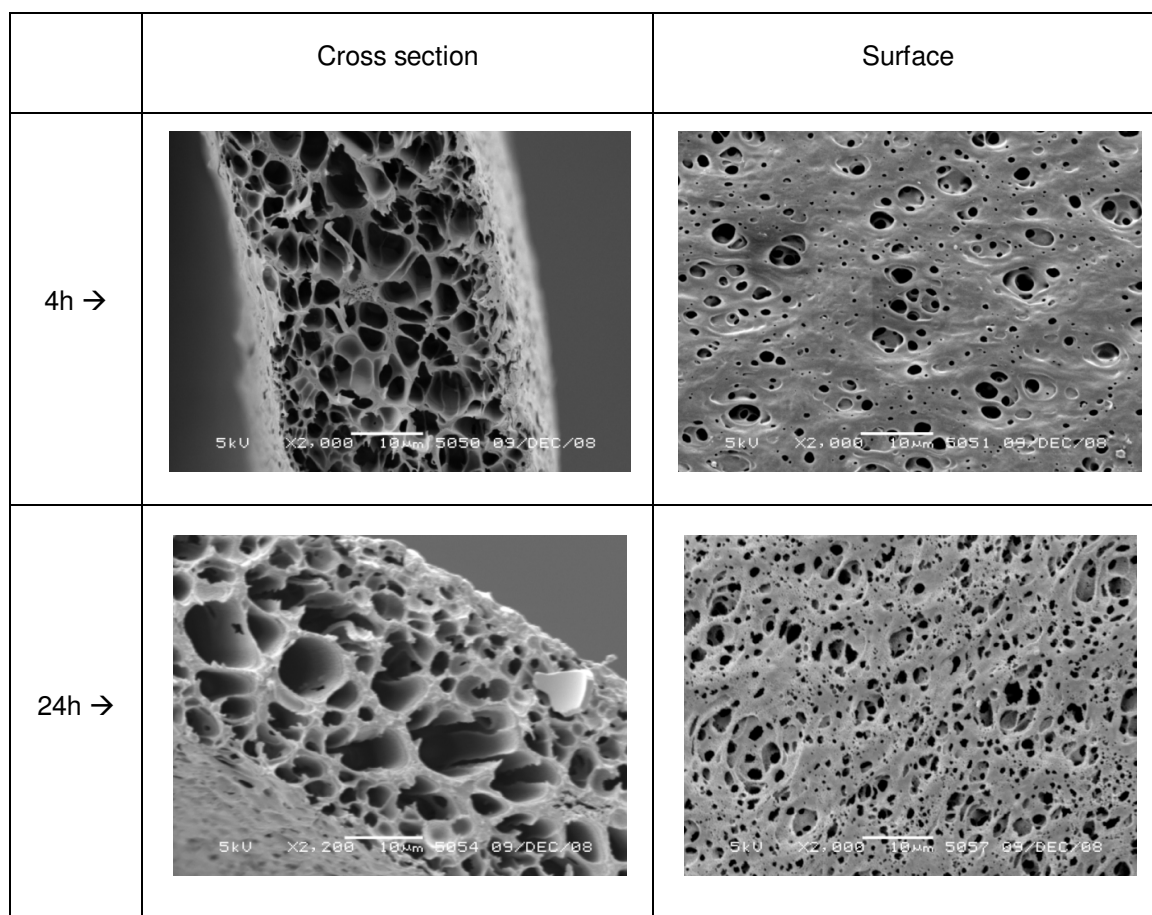


Figure 5. SEM images of surface and cross section of PLLA hollow fiber (D3, 17% PLLA dope solution) treated with sodium hypochlorite (4000ppm) for 4h and 24h.

According to earlier studies performed in our laboratory for PEI hollow fibers with 25 wt% PVP (K-30) [10] and PES fibers with 33 wt% PVP (K90 and K30) in the membrane [18], only small amounts of PVP remain in the membrane after NaOCl treatment for 24h (<7 wt% for the PEI and < 2 wt% for PES fibers). Since the amount of PVP in our PLLA membrane is 18.5 wt% (5g PVP / 27 g total polymer), we anticipate having only traces of PVP left in the PLLA fibers after NaOCl treatment. These traces may increase the membrane hydrophilicity and permeance, and positively influence the fiber cytocompatibility [19-21].

3.3 Mechanical properties

Mechanical strength of hollow fibers is important as all the forces encountered act on the porous walls of the fiber. The stress versus strain curve was measured for the PLLA fiber prepared using dope D3 (17 wt% PLLA in dope solution, 24h NaOCl treated). Force per unit area (stress) was measured when the hollow fibers were subjected to elongation at constant rate of 50mm/min. For this fiber, the E-modulus is 335 ± 15 MPa (obtained from slope of stress-strain curve) and it is higher compared to PLLA [8], PLGA and PLGA-PVA [22] hollow fibers reported in other studies probably due to the high molecular weight of PLLA used in our study and the obtained spongy porous structure without macrovoids. Our fiber has elongation at break of 75 – 85% (see Figure 6).

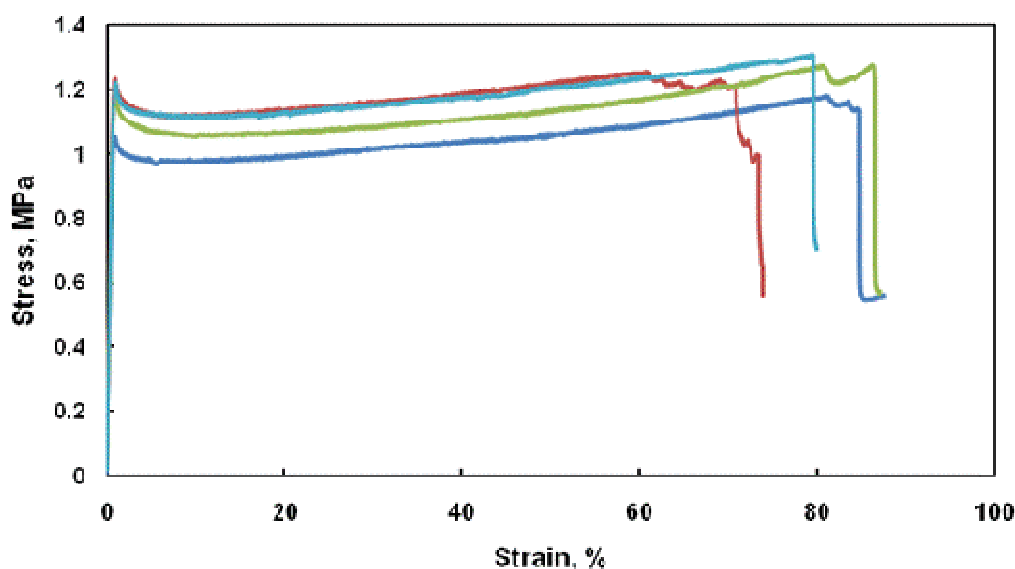


Figure 6. Stress strain curves of the PLLA fibers. The different lines represent different fiber samples.

3.4 Hollow fiber permeability

Pure water permeability experiments were carried out for the fiber prepared by D3 (17 wt% PLLA, treated with NaOCl for 24h) at room temperature in a dead-end filtration setup. Figure 7a shows that the flux at various trans-membrane pressures (0.1 – 0.5 bar), is linear with no compaction (several cycle of increasing and decreasing pressure flux were tested). The clean water permeance (slope in Figure 7a) is $2094 \text{ L}/(\text{m}^2 \cdot \text{h} \cdot \text{bar})$, which indicates that the fiber is of

a microfiltration type. The maximum allowable pressure in a bioreactor system for tissue engineering application mimicking the physiological condition for cell culture is ~ 0.15 bar corresponding to human systolic blood pressure. Our fiber performs very well at these low trans-membrane pressures.

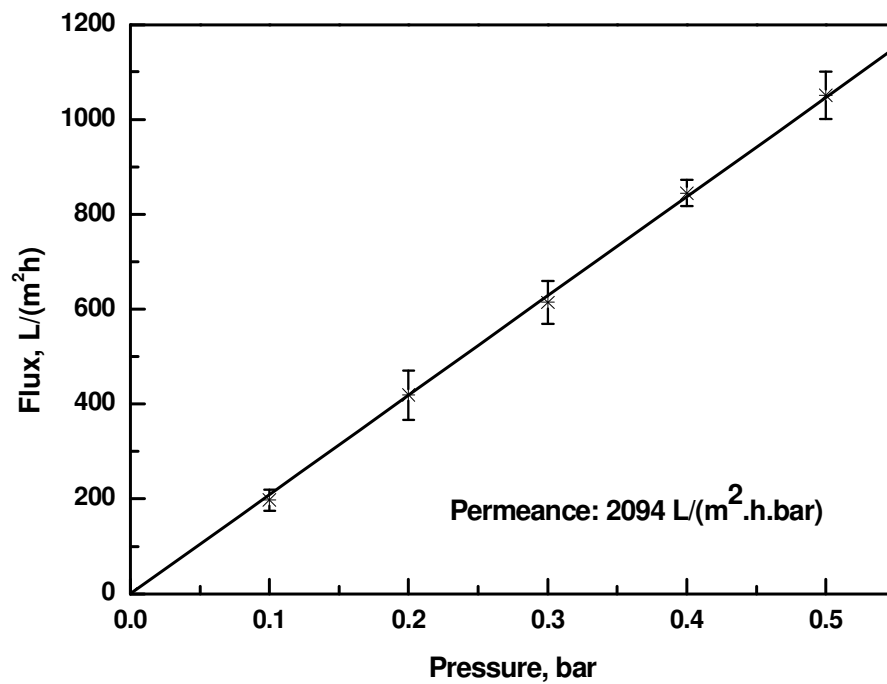


Figure 7(a) Clean water flux through PLLA hollow fiber (D3, 17% PLLA dope solution) with respect to applied trans-membrane pressure.

For mimicking vasculature in tissue engineering application, the fiber should deliver culture medium containing Fetal Bovine Serum (FBS) to the cells. FBS is a cocktail of 65% albumin and other small chain proteins. Hence the permeation of model protein, Bovine Serum Albumin (BSA, molecular weight ~ 66 kDa) through the lumen of the fiber was tested at 0.1 bar trans-membrane pressure. Figure 7b shows that more than 90% of BSA permeates through the membrane (feed concentration - 0.5g/l) and at permeance of 1963 L/(m².h.bar) over a period of 6 hours.

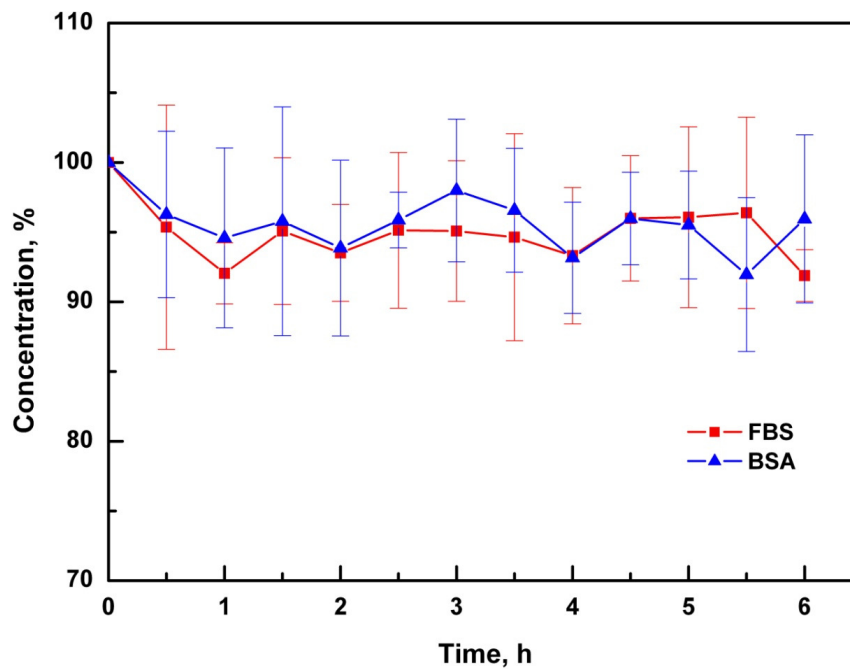


Figure 7(b) Permeation of BSA and FBS (dissolved in PBS at pH 7) through PLLA hollow fiber (D3, 17% PLLA dope solution) with respect to initial feed concentration, at 0.1bar trans-membrane pressure.

For the permeation experiments, we could not use D-MEM culture medium due to the presence there of phenol red which causes problems during BCA analysis of the proteins. Instead, we used a solution of 10% FBS dissolved in PBS of pH 7.3 (comparable to normal culture medium composition). Figure 7b shows the permeation results obtained for 5 different fiber modules tested. High permeability of 1939 L/m².h.bar (> 90% of pure water flux) and less than 10% retention of FBS molecules over a period of 6 hours indicates the suitability of produced PLLA fiber for delivering of the culture medium to the cells in a perfusion bioreactor system.

3.5 Cell culture

Static culture. We performed static cell culture experiments using fibers prepared from D3 (17% PLLA in dope solution, treated for 24h with NaOCl) that have very high medium permeance and mechanical stability. Figure 8a shows light microscopy images of C2C12 cells (stained with methylene blue) cultured for 0 (seeding day), 3 and 7 days. The cells attach and proliferate well on HF surface (as observed visually) showing high affinity of the cells to the material. In addition, these results suggest that no traces of solvents (dioxane, NMP and ethanol) remain within the porous HF membrane after the membrane preparation. Figure 8b presents the DNA per cm^2 of PLLA fiber. As expected, the DNA (and the corresponding cell number) increases in time due to cell proliferation on our fibers.

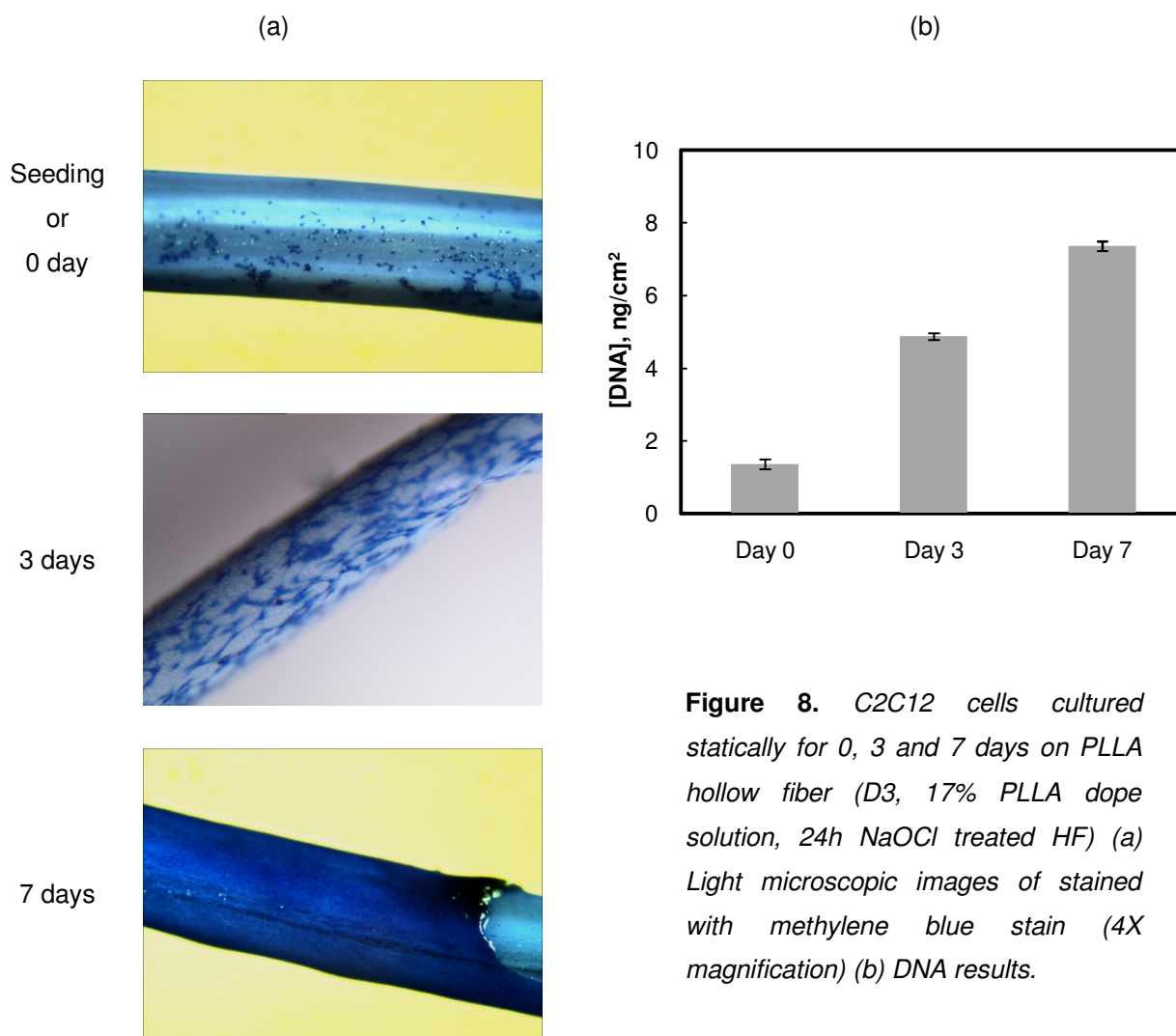


Figure 8. C2C12 cells cultured statically for 0, 3 and 7 days on PLLA hollow fiber (D3, 17% PLLA dope solution, 24h NaOCl treated HF) (a) Light microscopic images of stained with methylene blue stain (4X magnification) (b) DNA results.

Dynamic culture. Dynamic cell culturing on D3 fiber surface (17% PLLA, treated for 24h with NaOCl) was tested in recirculation perfusion bioreactor system (Figure 9) which was built inside a sterile incubator. Statically seeded hollow fiber module was placed inside the glass bioreactor and cultured by perfusing medium through the lumen of the fiber. Steady trans-membrane pressure of 0.1bar (flow rate - 1ml/min) was maintained to deliver nutrients to the proliferating cells on the outer surface of the fiber.

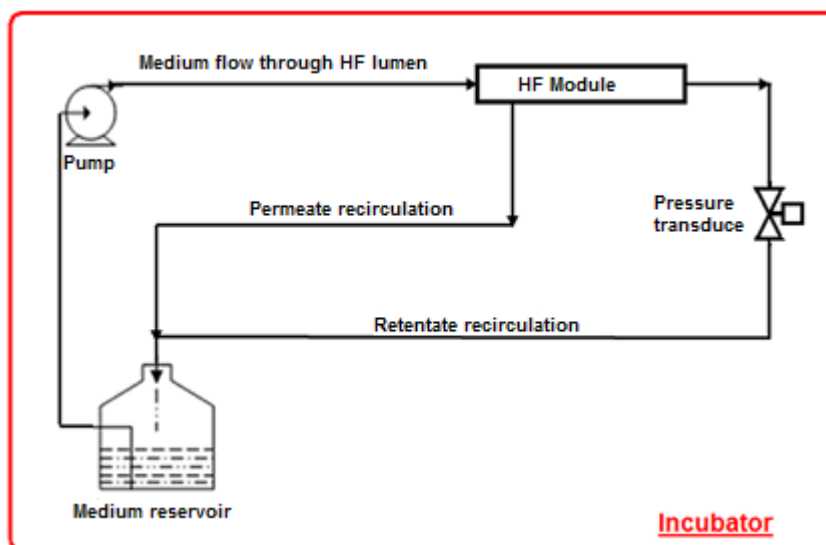


Figure 9. (a) Schematic illustration of re-circulating hollow fiber perfusion bioreactor system

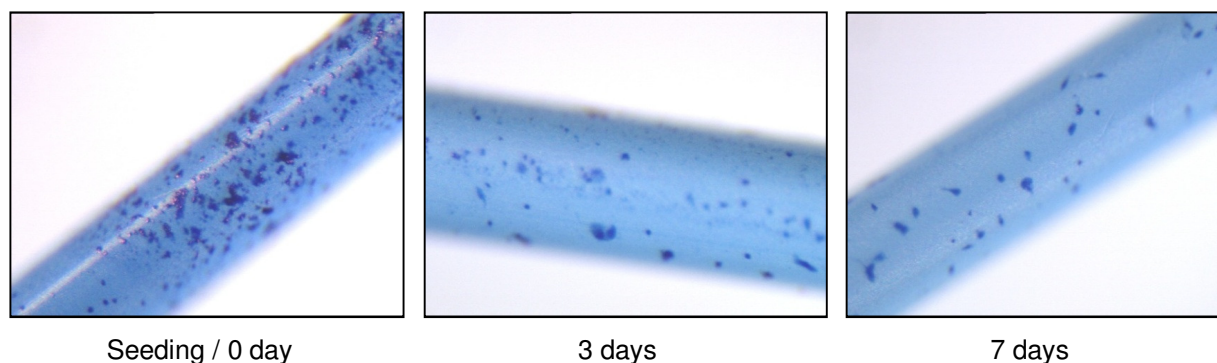


Figure 10. Light microscopic images of C2C12 cells cultured dynamically in a perfusion bioreactor for 0, 3 and 7 days on PLLA hollow fiber (D3, 17% PLLA dope solution, 24h NaOCl treated HF), stained with methylene blue stain, seeding density – 4000cells/cm² (4X magnification)

Figure 10 shows light microscopic images of dynamic cultured, fiber-cell module stained with methylene blue after 0 (seeding), 3 and 7 days culturing period. In contrast to the static culture very few cells adhere on the fiber surface due to the flow of the medium. The DNA results for these fibers were also very low (below the detection limit of our analysis). Since the cell attach and proliferate well under static conditions (see earlier) this low cell adhesion on the fiber under dynamic conditions can only be due to de-attachment of the cells due to the medium flow. This phenomenon may be advantageous during dynamic cell culture as the fiber permeance would remain stable with low pressure drop and low fouling. Nonetheless when these fibers are integrated into the scaffold, the flow conditions need to be adapted carefully to keep the fiber pores open without causing de-attachment of the cells in the surrounding tissue scaffold.

4 Conclusion - Outlook

In this work, PLLA microfiltration hollow fibers with interconnected porous structure have been developed. The high clean water, BSA and FBS protein permeation through the fiber indicates its suitability for delivering medium to the cells in perfusion tissue engineering bioreactor systems. The static culture studies onto our fibers show that the cells attach and proliferate there well showing that there are no solvent / non-solvent extractable from the fiber to influence the cell attachment and proliferation. In dynamic culture, the cells de-attach from the fiber surface probably due to the medium flow but this could be favourable for avoiding fiber fouling during bioreactor studies. Our future work will be focussed of the incorporation of the developed PLLA fiber into tissue engineering scaffolds and the optimization of tissue culture bioreactor conditions.

5 Acknowledgements

The authors would like to acknowledge the financial support from Technology Foundation STW (Project number – TKG. 6716). We also thank Prof. Dr. D. Grijpma (Biomaterials Science and Technology (BST) group, University of Twente, The Netherlands) for kindly providing the PLLA polymer and Prof. Dr. C.A. van Blitterswijk (Tissue Regeneration (TR) group University of Twente, The Netherlands) for allowing to perform cell culture experiments in his lab. Thanks are also due to S. Schuller and J.B. Bennink for assistance with mechanical testing equipment and set-up artwork respectively.

Abbreviations

3D	-	3 dimensional
BCA	-	Bi-cinchoninic acid
BSA	-	Bovine Serum Albumin
C2C12	-	Mouse pre-myoblast cells
D-MEM	-	Dulbecco's Modified Eagle's Medium
EDTA	-	Ethylene-di-amine-tetra-acetic acid
FBS	-	Fetal Bovine Serum
LIPS	-	Liquid induced phase separation
NaOCl	-	Sodium hypochlorite
NMP	-	N-Methyl-2-pyrrolidone
PBS	-	Phosphate buffer solution (pH=7.3)
PEG	-	Poly (ethylene-glycol)
PLGA	-	Poly (lactic-co-glycolic acid)
PLLA	-	Poly (l-lactic acid) / Poly (l-lactide)
ppm	-	Parts per million
PVA	-	Poly (vinyl alcohol)
PVP	-	Poly-vinyl-pyrrolidone
SEM	-	Scanning electron microscope

References

- [1] R.S. Langer, J.P. Vacanti, Tissue Engineering: The Challenges Ahead., Scientific American, 280 (1999) 86-90.
- [2] R.S. Langer, Perspectives and Challenges in Tissue Engineering and Regenerative Medicine, Advanced Materials, 21 (2009) 3235-3236.
- [3] H.K. Awwad, M. El Naggar, N. Mocktar, M. Barsoum, Intercapillary distance measurement as an indicator of hypoxia in carcinoma of the cervix uteri, International Journal of Radiation Oncology Biology Physics, 12 (1986) 1329-1333.
- [4] M.J. Ellis, J.B. Chaudhuri, Poly(lactic-co-glycolic acid) hollow fibre membranes for use as a tissue engineering scaffold, Biotechnology and Bioengineering, 96 (2007) 177-187.
- [5] M.J.D. Eenink, J. Feijen, J. Olijslager, J.H.M. Albers, J.C. Rieke, P.J. Greidanus, Biodegradable hollow fibres for the controlled release of hormones, Journal of Controlled Release, 6 (1987) 225-247.
- [6] J.M. Schakenraad, J.A. Oosterbaan, P. Nieuwenhuis, I. Molenaar, J. Olijslager, W. Potman, M.J.D. Eenink, J. Feijen, Biodegradable hollow fiber for the controlled release of drugs, Biomaterials, 9 (1988) 116-120.
- [7] P. Van de Witte, H. Esselbrugge, A.M.P. Peters, P.J. Dijkstra, J. Feijen, R.J.J. Groenewegen, J. Smid, J. Olijslager, J.M. Schakenraad, M.J.D. Eenink, A.P. Sam, Formation of porous membranes for drug delivery systems, Journal of Controlled Release, 24 (1993) 61-78.
- [8] A. Moriya, T. Maruyama, Y. Ohmukai, T. Sotani, H. Matsuyama, Preparation of Poly(lactic acid) Hollow Fiber Membrane via Phase Separation Methods, Journal of Membrane Science, 342 (2009) 307-312.
- [9] B.J. Papenburg, L. Vogelaar, L.A.M. Bolhuis-Versteeg, R.G.H. Lammertink, D. Stamatialis, M. Wessling, One-step fabrication of porous micropatterned scaffolds to control cell behavior, Biomaterials, 28 (2007) 1998-2009.
- [10] H.D.W. Roesink, M.A.M. Beerlage, W. Potman, T. van den Boomgaard, M.H.V. Mulder, C.A. Smolders, Characterization of new membrane materials by means of fouling experiments Adsorption of bsa on polyetherimide-polyvinylpyrrolidone membranes, Colloids and Surfaces, 55 (1991) 231-243.
- [11] X. Zhen-Liang, C. Tai-Shung, H. Yu, Effect of polyvinylpyrrolidone molecular weights on morphology, oil/water separation, mechanical and thermal properties of polyetherimide/polyvinylpyrrolidone hollow fiber membranes, Journal of Applied Polymer Science, 74 (1999) 2220-2233.

- [12] K. Jong Seok, L. Young Moo, Effects of molecular weight of polyvinylpyrrolidone on precipitation kinetics during the formation of asymmetric polyacrylonitrile membrane, *Journal of Applied Polymer Science*, 85 (2002) 57-68.
- [13] C.A. Smolders, A.J. Reuvers, R.M. Boom, I.M. Wienk, Microstructures in Phase-inversion membranes. Part 1. Formation of macrovoids, *Journal of Membrane Science*, 73 (1992) 259-275.
- [14] E. Piorkowska, Z. Kulinski, A. Galeski, R. Masirek, Plasticization of semicrystalline poly(L-lactide) with poly(ethylene glycol), *Polymer*, 47 (2006) 7178-7188.
- [15] K.C. Khulbe, C.Y. Feng, T. Matsuura, D.C. Mosqueada-Jimenez, M. Rafat, D. Kingston, R.M. Narbaitz, M. Khayet, Characterization of surface-modified hollow fiber polyethersulfone membranes prepared at different air gaps, *Journal of Applied Polymer Science*, 104 (2007) 710-721.
- [16] N. Peng, T.S. Chung, K.Y. Wang, Macrovoid evolution and critical factors to form macrovoid-free hollow fiber membranes, *Journal of Membrane Science*, (1-2) (2008) 9.
- [17] B.M.P. Ferreira, L.M.P. Pinheiro, P.A.P. Nascente, M.J. Ferreira, E.A.R. Duek, Plasma surface treatments of poly(L-lactic acid) (PLLA) and poly(hydroxybutyrate-co-hydroxyvalerate) (PHBV), *Materials Science and Engineering C*, 29 (2009) 806-813.
- [18] I. Wienk, Ultrafiltration membranes from a polymer blend PhD thesis, Chapter 4 (1993).
- [19] J. Barzin, S. Siavash Madaeni, H. Mirzadeh, Effect of preparation conditions on morphology and performance of hemodialysis membranes prepared from polyether sulphone and polyvinylpyrrolidone, *Iranian Polymer Journal (English Edition)*, 14 (2005) 353-360.
- [20] J. Xi, L. Kong, Y. Gao, Y. Gong, N. Zhao, X. Zhang, Properties of poly(3-hydroxybutyrate-co-3-hydroxyhexanoate) films modified with polyvinylpyrrolidone and behavior of MC3T3-E1 osteoblasts cultured on the blended films, *Journal of Biomaterials Science, Polymer Edition*, 16 (2005) 1395-1408.
- [21] F. Xu, F.Z. Cui, Y.P. Jiao, Q.Y. Meng, X.P. Wang, X.Y. Cui, Improvement of cytocompatibility of electrospinning PLLA microfibers by blending PVP, *Journal of Materials Science: Materials in Medicine*, 20 (2009) 1331-1338.
- [22] G. Meneghello, D.J. Parker, B.J. Ainsworth, S.P. Perera, J.B. Chaudhuri, M.J. Ellis, P.A. De Bank, Fabrication and characterization of poly(lactic-co-glycolic acid)/polyvinyl alcohol blended hollow fibre membranes for tissue engineering applications, *Journal of Membrane Science*, 344 (2009) 55-61.

Chapter 3

Integration of hollow fiber membranes with 3D scaffolds improves nutrient supply in-vitro

N.M.S. Bettahalli¹, M. Wessling^{1,2}, D.F. Stamatialis^{1,*}

MIRA Institute for Biomedical Technology and Technical Medicine, University of Twente

¹ Membrane Technology Group, Faculty of Science and Technology, PO Box 217, 7500 AE Enschede, The Netherlands.

² RWTH Aachen University, Chemische Verfahren Technik (CVT), 52064 Aachen, Germany

*A great part of courage is the courage of having done the thing before.
(Ralph Waldo Emerson)*

Abstract

Sufficient nutrient and oxygen transport is a potent modulator of cell proliferation in in-vitro tissue engineered constructs. The lack of oxygen and culture medium can create a potentially lethal environment and limit cellular respiration and growth. Diffusion through scaffold and multi-cellular tissue typically limits transport in-vitro, leading to hypoxic regions and limiting the viable tissue thickness. For the in vitro generation of clinically relevant tissue-engineered grafts, these divergent actions of hypoxia and nutrient diffusion should be addressed. Approaches to overcome the transport limitations include culture with bioreactors, scaffolds with artificial microvasculature, oxygen carriers, pre-vascularization etc.

This study focuses on the development and utilization of new perfusion culture system to provide adequate nutrient delivery to the cells within 3D scaffolds. We propose perfusion of oxygenated culture medium through porous hollow fiber (HF) integrated within 3D free form fabricated (FFF) scaffold. As a model system, we use mouse pre-myoblast (C2C12) cells cultured on scaffolds of Poly (ethylene-glycol-terephthalate) - poly (butylene- terephthalate) block co-polymer (300PEGT55PBT45) integrated with porous hollow fiber membranes. Various parameters such as fiber transport properties, fiber spacing within scaffold, medium flow conditions are optimized. Our results show that four hollow fiber membranes integrated with the scaffold improve significantly the cell density and cell distribution. In fact, our study provides a basis for development of new hollow fiber perfusion culture methodology to overcome the limitations of nutrient diffusion in 3D cell-scaffold system for in-vitro tissue engineering.

Adapted from NMS Bettahalli et.al, Integration of hollow fiber membranes with 3D scaffolds improves nutrient supply in-vitro, Submitted.

1 Introduction

Implantation of a tissue engineered construct based on scaffolds integrated with biological cells or molecules may be a potential treatment for tissue defects. However the creation of constructs of clinically relevant dimensions, homogenously filled with corresponding tissue still poses a challenge. This new paradigm requires scaffolds that balance between temporary mechanical support with sufficient mass transport to aid biological delivery and uniform tissue growth.

High-density cell cultures are often limited by inadequate supply of nutrients [1]. More specifically, the transplanted cells compete themselves for oxygen and nutrient supply limiting tissue formation thicker than 200 μ m [2, 3]. Investigators have tried to overcome the diffusion limitations within tissue-engineered constructs by using convective bioreactor culture [4-7]. A spinner flask or rotating flask bioreactor can provide control over the hydrodynamics around the tissue construct, and hence external diffusion limitations can be minimized. Despite this, exponential decrease in cell proliferation and oxygen distribution from periphery to the center of scaffold cultured in spinner flask has been reported earlier for engineered cartilage [7, 8] and cardiac tissue [9]. Although perfusion bioreactor can offer greater control of mass transfer than other convective systems, there still remains the potential for the flow to follow a preferential path through the construct (particularly for scaffold with wide pore size distribution or non-uniform tissue development) creating regions with nutrient deficiency. The above techniques may also induce shear stress due to fluid flow across the scaffolds.

The need for a vasculature to deliver nutrients and oxygen and to remove waste materials is particularly important for 3D thick tissue constructs. Smart scaffold design [10, 11] and mechanical loading of constructs [12-14] have proven to be effective tools to increase histological and biochemical properties of tissue engineered constructs, partly by decreasing the internal diffusion constraints. Despite the fact that mass transfer is increased within the dynamic systems, considerable gradients are still present inside the obtained tissue engineered constructs.

In this work we present the proof of concept of improving nutrient transport into a scaffold by using of hollow fiber membranes. In our concept, the fibers are incorporated into the scaffold and act as artificial capillaries providing nutrients and oxygen to the cells during cell culture

in vitro. To demonstrate our concept, we selected a scaffold system prepared by free form fabrication (FFF) of poly (ethylene glycol terephthalate) (PEGT) and poly (butylene terephthalate) (PBT) polymer, for which literature reports showed limited nutrient and oxygen supply to the cells in its core [8]. In our study, we give particular emphasis on:

- ✓ The selection of the best hollow fiber for this application (the fiber with good biocompatibility, high medium delivery to the cells and low fouling),
- ✓ The optimal integration of the fibers into the scaffold and the numbers of fibers used
- ✓ The optimal cell culture conditions in vitro. For this we compare static and dynamic cell culture conditions in a bioreactor. For the dynamic studies we compare three different cases: medium flow through the scaffold (as typically done in the dynamic experiments), medium flow via the lumen of integrated hollow fibers alone and dual flow (combining the two flows through the scaffold and via the hollow fibers).

2 Materials and Methods

2.1 FFF Scaffold with integrated HF module

FFF scaffold fabrication

Three dimensional FFF scaffold (indicated as 3DF) were fabricated using biodegradable Poly (ethylene glycol terephthalate) - poly(butylene terephthalate) (PEGT/PBT) block co-polymers, kindly provided by Prof. Dr. C.A. van Blitterswijk, Tissue Regeneration group, University of Twente, The Netherlands. The co-polymer chemical composition is represented by the notation aPEGTbPBTc, where a is the molecular weight of the starting poly(ethylene glycol) PEG segments used in the polymerization process, while b and c refer to the weight ratio between PEGT and PBT blocks, respectively. For this study, 300PEGT55PBT45 co-polymer was used due to their high mechanical stability, low swelling, good cell adhesion and suitability for tissue formation [15-18].

3DF scaffolds were produced based on 3D fiber deposition technique using Bioplotter device (Envisiontec GmbH, Germany), which is a XYZ plotter scaffold construction device [19-23]. To extrude highly visco-elastic fibers, the bioplotter underwent few modifications as reported

by Moroni et al.[24-26]. Briefly, the granules of PEGT/PBT polymer was fed in to the stainless steel syringe and heated to 190°C using the thermostat heating unit attached to the bioplotter mobile arm. Inert nitrogen gas pressure of 4 bars was applied to the top of the syringe to extrude molten polymer through the nozzle attached at the bottom. The nozzles used to extrude the polymer were stainless steel luer lock hypodermic needles with internal diameter (ID) of 400µm shortened to a length of approximately 15 mm. The desired scaffold design was loaded to the CAM program (PrimCAM, Switzerland) and the polymer extruded through the nozzle was deposited layer by layer on a stagnant stage (Figure 1). The deposition speed was set to ~ 200 mm/min with fiber spacing of 1mm and layer thickness of 250µm. The 0-90 fiber deposition scaffold architecture was chosen, where fibers were deposited with 90° orientation steps between successive layers. The

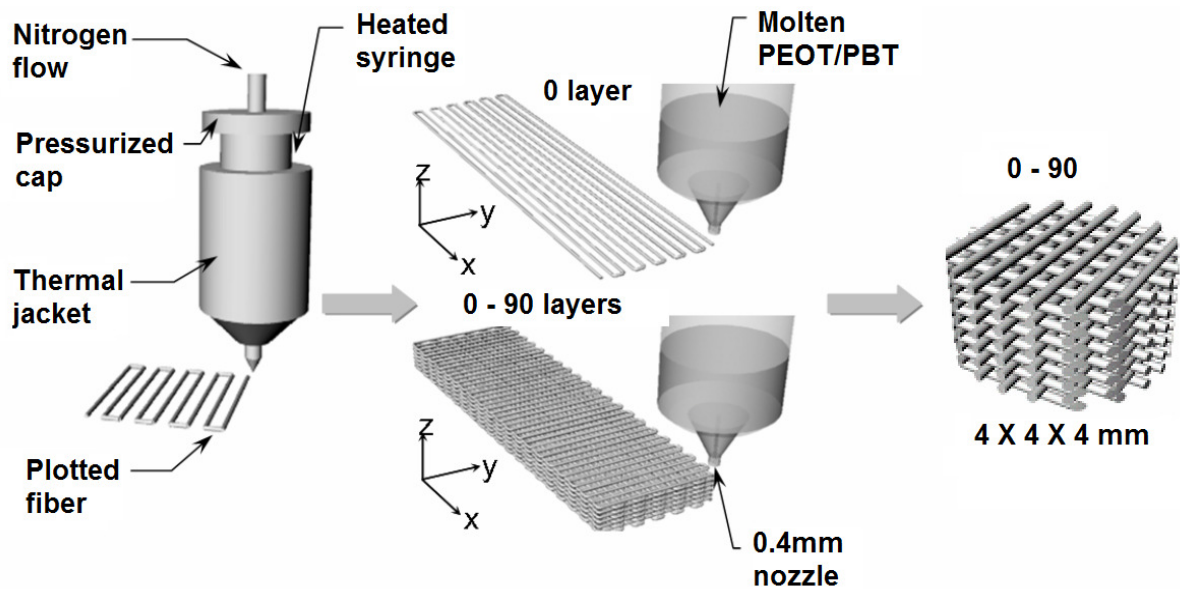


Figure 1. Schematic of a Bioplotter device and 3DF scaffold fabrication process with 0-90 scaffolds architecture in alternate layers are presented. Scheme adapted from [42]

Cubical samples of 4mm³ (4X4X4 mm) were punched out from large fabricated scaffold block for further experiments. These scaffolds were further treated with gas plasma, by placing inside the plasma chamber or radiofrequency glow discharge chamber. A vacuum was applied to the chamber (0.01 mbar), which was then four times flushed with argon (purity ≥ 99.999%). The scaffolds were treated under argon plasma (0.1–0.2mbar) for 10 min. After cooling the scaffolds were turned around and again treated for 10 min as explained above.

Hollow fiber membranes

As we mentioned earlier, the hollow fibers for our concept should have good biocompatibility, high medium delivery to the cells and low fouling. Therefore, we selected three commercial porous hollow fibers made of biocompatible materials: (i) modified polypropylene (Membrana GmbH), (ii) modified poly (ether-sulfone) (Gambro GmbH), and (iii) modified polysulfone (Asahi Kasei Medical Co. Ltd.) which are currently used in plasmapheresis (separation of blood cells from plasma). These membranes are designed to work well (low fouling, high plasma transport) during plasmapheresis treatment of 3-4 hours, however to the best of our knowledge for these fibers there are no reported performance data with cell culture medium (flux or fouling behavior) especially for long time (up to 14 days as required in this work). To select the best membrane for our concept, we performed such studies as well as clean water permeation studies (to evaluate the fiber porosity) and scanning electron microscopy (SEM).

2.1.1 3D scaffold hollow fiber integration - module assembly and treatment

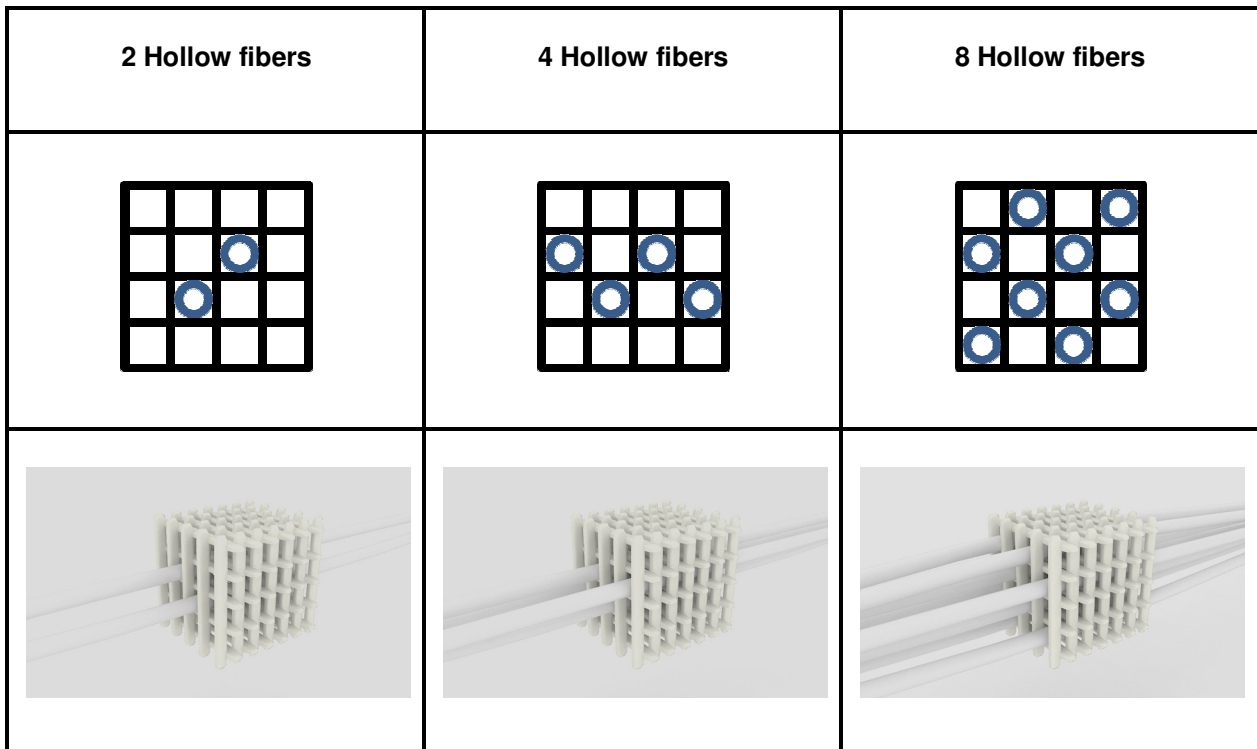


Figure 2. 2D and 3D illustration of hollow fiber integration architecture within 4mm³ free form fabricated scaffold

The scaffold integrated with hollow fibers (indicated as 3DF-HF) modules was prepared manually by inserting the hollow fibers through the porous scaffold structure. The number of HF and the position within the scaffold was predefined to achieve symmetry as shown in Figure 2. Both ends of the hollow fibers were embedded in polyurethane glue within 6mm polyethylene tubing, such that 2cm of HF would be available for perfusion (Figure 3). The 3DF-HF modules were first sterilized by pumping 70% ethanol through the hollow fiber at low pressure (0.1bar) in sterile environment. Further they were conditioned by pumping PBS and proliferation medium correspondingly.

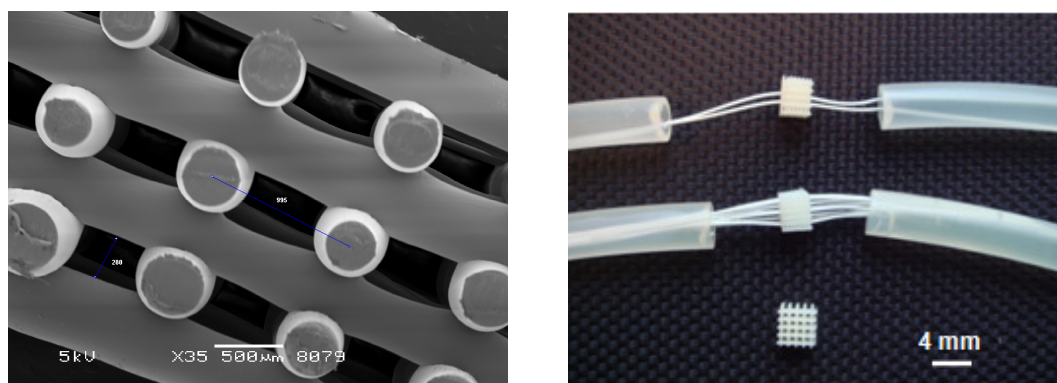


Figure 3. SEM image of 3DF scaffold fabricated using bioplotter and photographic image of 3DF-HF integrated scaffold module with 2 and 8 HF with HF ends embedded in polyurethane glue inside 6mm polyethylene tube

2.2 Characterization

2.2.1 Scanning electron microscopy (SEM)

SEM images of 3DF scaffold and HF were obtained using JEOL 5600LV scanning electron microscope at accelerating voltage of 5kV. Samples were dried in vacuum oven at 30°C overnight and then used for surface scan, whereas samples for cross sectional observation were carefully fractured in liquid nitrogen. All the samples were sputtered with gold (~15 to 20 nm-thick, Balzer-Union SCD-040).

2.2.2 HF permeability

Water permeability

Pure water permeability of the HF was determined by pressurizing ultrapure water (18.2 M Ω cm, MilliQ) through the lumen of the HF (inside-out permeation). The experiments were carried out in modules containing two hollow fibers each prepared using 6 mm polyethylene tube housing of approximately 8 cm long. The fibers were carefully inserted into the polyethylene tube and sealed with polyurethane glue. In the middle of the housing, a T-junction was placed to collect the flowing permeate. Before measuring the clean water transport, the fibers were pre wetted by pumping water through the modules for at least 30 min. The flux (J) through the membrane was measured at different trans-membrane pressure ranging between 0.1 – 0.3 bar at $20 \pm 2^\circ\text{C}$. The flux (Kg/m²h) at each pressure was successively measured by collecting the permeating water (Kg) for at least 60 min. The pure water permeance (Kg/m²hbar) was calculated using the slope of flux versus pressure plot. The data presented in this work is an average of five different hollow fiber modules.

Medium permeability

The proliferation medium permeability experiments was performed in sterile cross flow setup by pumping Dulbecco's Modified Eagle's Medium (D-MEM, Gibco) supplemented with 10% Fetal Bovine Serum (FBS, Cambrex), 100 U/ml penicillin (Gibco) and 100 $\mu\text{g/ml}$ streptomycin (Gibco) through the lumen of the HF. The maximum allowable pressure in a bioreactor system for tissue engineering application mimicking the physiological condition for cell culture is in between 0.1 to 0.15 bar corresponding to human diastolic and systolic blood pressure. In this study, we choose to perform medium permeation experiments at 0.1 bar trans-membrane pressure (the lower margin of the physiological conditions) at $20 \pm 2^\circ\text{C}$. During the experiment the medium reservoir (feed) was stirred and pumped to the membrane module using a peristaltic pump with recirculation. The collected permeating medium and unfiltered medium was also used to statically culture mouse pre-myoblast (C2C12) cells in T-flask for comparison of cell proliferation rate.

Static cell culture on hollow fiber

Fibers of 2 cm long were first sterilized in excess of 70% ethanol and iso-propanol, after evaporation of the alcohols inside sterile flow-hood, the fibers were washed 3 times with PBS and finally neutralized in proliferation medium. Five such fibers were kept inside the tissue culture plate (non-treated) and seeded with C2C12 cells. These samples were cultured for 3 and 7 days in an incubator with proliferation medium being exchanged every alternate day.

Dynamic cell culture on hollow fiber

Hollow fibers to be tested for dynamic perfusion cell culture were potted at both ends using poly-urethane inside 6 mm silicon tubing, such that 2 cm long fiber surface in the middle was exposed for cell adhesion and proliferation. The hollow fiber modules were sterilized by pumping 70% ethanol and then conditioned by pumping PBS and proliferation medium correspondingly at low pressure (~0.1 bar). The sterilized fiber modules were seeded with C2C12 cells and cultured in a recirculation perfusion bioreactor for 3 and 7 days (see details later). Trans-membrane pressure of 0.1 bar was maintained across the cell seeded fiber module with an average cross flow velocity of 1ml/min. The fibers cultured statically or dynamically were analyzed for cell adhesion and proliferation using a light microscope. For this, the cells were stained with methylene blue stain.

2.3 Cell seeding

Mouse pre-myoblast, C2C12 cells were cultured in proliferation medium containing Dulbecco's Modified Eagle's Medium (D-MEM, Gibco) supplemented with 10% Fetal Bovine Serum (FBS, Cambrex), 100 U/ml penicillin (Gibco) and 100 µg/ml streptomycin (Gibco). Cells were initially plated in T-flask for expansion at 2000 cells/cm² until they reached 70-80% confluence, after which they were trypsinized using 0.05% Trypsin contained in 1mM EDTA. The obtained C2C12 cells were aggregated and re-suspended in 50µl medium subsequently seeded on to the scaffold module at 3×10^6 cells in special seeding box which accommodates the 3DF-HF modules. The cells were allowed to attach for 3 days with medium refreshed every day in seeding box before performing the static or dynamic culture experiments.

2.4 Cell culturing

2.4.1 Static culture

3DF-HF scaffold modules seeded with cells were statically cultured in non-treated petri-dish. The samples were cultured for 3, 7 and 14 days in a sterile incubator with 25ml of proliferation medium refreshed every alternate day. The resulting samples were analysed using SEM and light microscopy for spatial distribution and were quantified by total DNA assay.

2.4.2 Dynamic culture

The dynamic cell culture within glass bioreactor was performed using a perfusion system consisting of a medium reservoir (Schott AG), FDA approved platinum cured silicon tubing (Masterflex), a multi-channel precision flow peristaltic pump (Watson-Marlow), click connectors and a pressure sensor (see Figure 4a). The whole perfusion bioreactor system was built within temperature, humidity and CO₂ controlled sterile incubator. Reservoir containing 100ml of proliferation medium was re-circulated to feed cells for 84 hours before refreshing. The medium pumped from the reservoir was oxygenated before entering the bioreactor by using long (~1.5m) gas permeable silicon tubing. A peristaltic pump with different tube diameter for controlled medium volumetric flow rate was used. Pressure sensor was used to regulate the input trans-membrane pressure of the medium across the HF. All the various parts of bioreactor were sterilized by autoclaving before each experiment.

Fresh medium was perfused in single-pass and the stream leaving the bioreactor was collected as waste until approaching the steady state. When the system reached the steady state, the stream leaving the bioreactor was recycled. Media samples were collected from the outlet stream to evaluate the glucose depletion and lactate formation using Vitros-DT60 diagnostic slides (Ortho-Clinical Diagnostics).

The glass bioreactor itself consists of scaffold-fiber module housed in a glass tube reactor of 1cm diameter and 5cm long with two side ports for medium flow and recirculation (Figure 4b). The module with scaffold seeded with cells was held freely in the center of the glass reactor by using screw cap and silicon sealant rings mounted on the 6mm tubing at both ends of the scaffold module (Figure 4b).

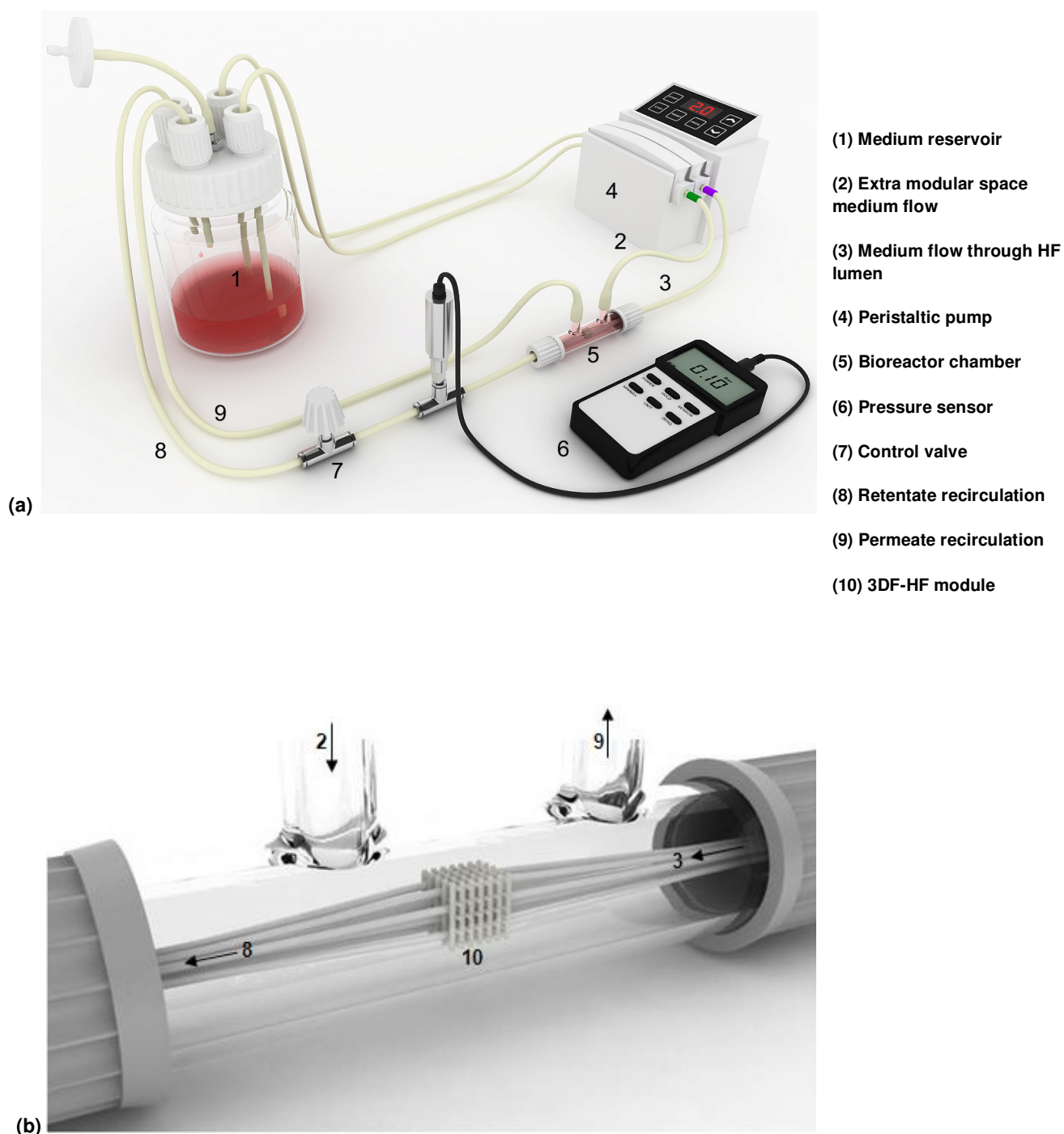


Figure 4. Schematic of dynamic perfusion cell culture system illustrating (a) perfusion bioreactor setup with various components and (b) 3DF-HF integrated module mounted within glass bioreactor with side ports

In this study, we studied three different cases of medium flow:

- **Medium flow through the scaffold (FTS):** the medium was pumped through the scaffold (as done in conventional dynamic experiments). An average flow rate of approximately 0.26ml/min was maintained.
- **Medium flow through HF lumen:** the medium was pumped only through the lumen of the HF. The trans-membrane pressure across the HF was monitored and kept constant at 100 mbar corresponding to human diastolic blood pressure, with an average cross flow velocity of approximately 1ml/min. The permeating medium through the hollow fiber refreshes the medium in the bioreactor and exits through the side ports to the reservoir.
- **Dual flow through the scaffold and the HF lumen (FTS+HF):** the medium was pumped simultaneously through the scaffold (FTS) and through the HF lumen in counter current direction using the flow rates described earlier (it is combination of cases 1 + 2). The flow rates were maintained using single peristaltic pump with different tube diameter. The same proliferation medium reservoir was used for both flows in the bioreactor.

2.5 Scaffold-cell sample analysis

2.5.1 Critical point dried sample for SEM

For the SEM analysis, cell cultured scaffold samples were washed with PBS to remove culture medium prior to fixation by incubating for at least 1hr with freshly prepared 4% Para-formaldehyde (Merck). Further the samples were dehydrated in 50%, 70%, 80%, 90%, 98% and 100% ethanol for at least 4 hr each step. Dehydration in 100% ethanol was performed for two additional times to remove all the water. Dehydrated samples were dried using liquid carbon-di-oxide using Blazers CPD 030 Critical Point Drier. SEM images were taken as described above.

2.5.2 Embedding and staining for light microscopy

Cell-scaffold samples were fixed for 6 hours in 10% neutral buffered formalin and dehydrated (as explained above for critical point drying) before embedding in 2 component Glycol

Methacrylate Acrylic resin (GMA) (Merck) mixed according to the protocol for cross linking (provided by Merck). Transverse microtome sections were made to yield 5 μ m thick sections which were placed on silanized slides and dried on hot plate before staining with Hematoxylin and Eosin (H&E) (Sigma-Aldrich) according to the protocol. The resulting stained samples were stored dry until further use for light microscopic analysis to visualize cells/cell nuclei. The slides were examined under light microscope (Nikon Eclipse E400) and representative images captured using a digital camera (Sony Corporation, Japan) and Matrix Vision software (Matrix Vision GmbH, Germany).

2.5.3 Cell proliferation assay

The concentration of DNA per scaffold sample (at different culture time of 0, 3, 7 and 14 days) was used as an indication for cell proliferation. The samples to be assayed were washed with PBS and stored at -85°C for at least 1 day. The samples before performing the DNA assay were allowed to attain room temperature and sliced to small pieces such that they could be immersed in small quantity (1ml) of cell lysis buffer. Quantification of total DNA concentration per sample was measured according to the manufacturer's protocol (CyQuant Cell Proliferation Assay Kit, Invitrogen/Molecular probes) using a fluorescent plate reader (Perkin Elmer).

3 Results and discussion

3.1 Fabrication and characterisation of 3DF scaffold

It has been demonstrated that the effective diffusion within porous scaffolds is proportional to the porosity and inversely proportional to the square of the geometrical tortuosity of the path that the substrate encounter through the pores [27]. Hence to minimize the tortuosity, the scaffold was fabricated based on fiber deposition technique to produce interconnected straight pores. 300PEGT55PBT45 copolymer was chosen over wide range of different copolymer composition due to its balanced hydrophobic nature and low swelling property (approximately 2% as reported by Woodfield et. al. [22]). 3DF scaffold of 4mm³ used for all cell culture experiments in this study were punched out of large (30X30X4mm³) block fabricated with high degree of reproducibility by accurately controlling the deposition

parameters like fiber spacing, temperature, syringe pressure, velocity etc. Uniform scaffold made of straight smooth fibers of approximately 400 μ m in diameter resulted with 61-65% porosity having average interconnected pore size in the x-y plane was approximately 600 μ m and 250 μ m in z plane. The SEM image in Figure 3 confirms that 3D deposited scaffold fabricated consists of 100% interconnected pores with continuous straight channels.

3.2 Hollow fiber selection

3.2.1 Scanning electron microscope

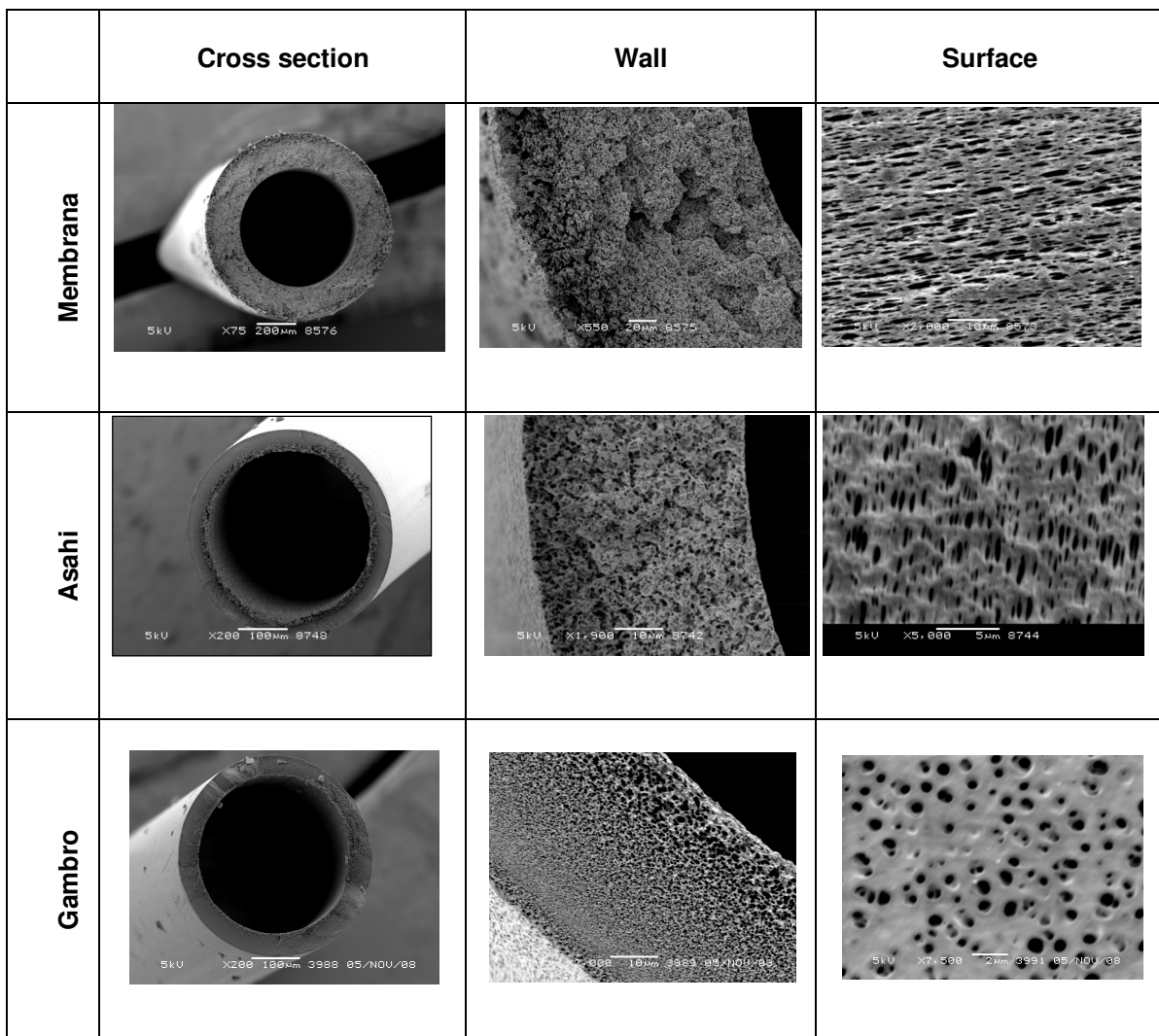
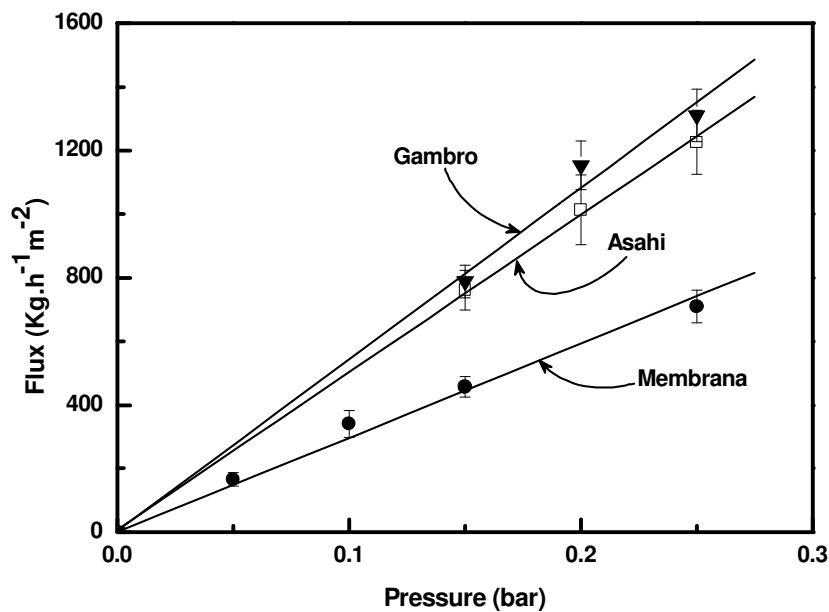


Figure 5. SEM images of biocompatible hollow fibers screened

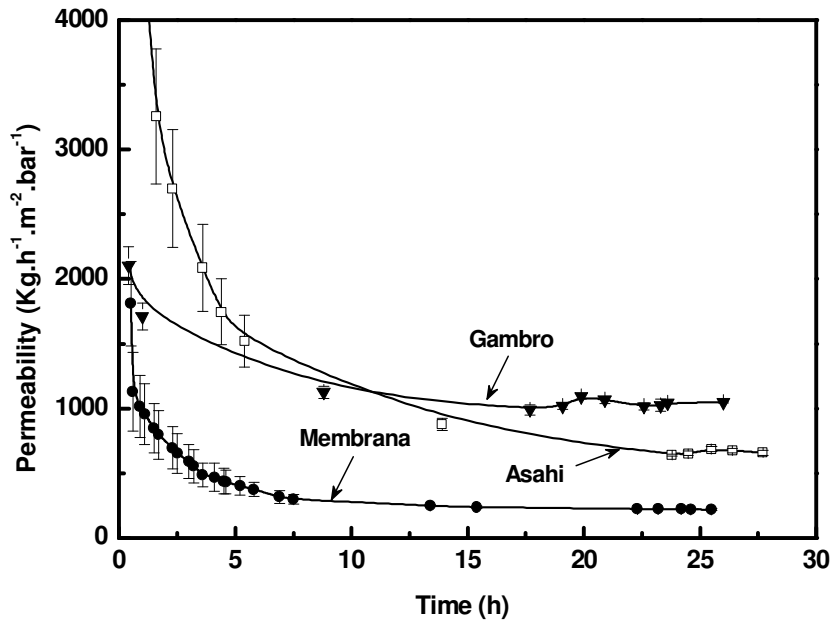
Figure 5 shows the SEM images of all the hollow fibers studied. The fiber surface images show that the pores on the outer surface of the hollow fiber are between 0.5 to 3 μm so the fiber wall acts as a barrier and inhibits cell infiltration into the pores of the hollow fiber.

3.2.2 Clean water and medium permeation

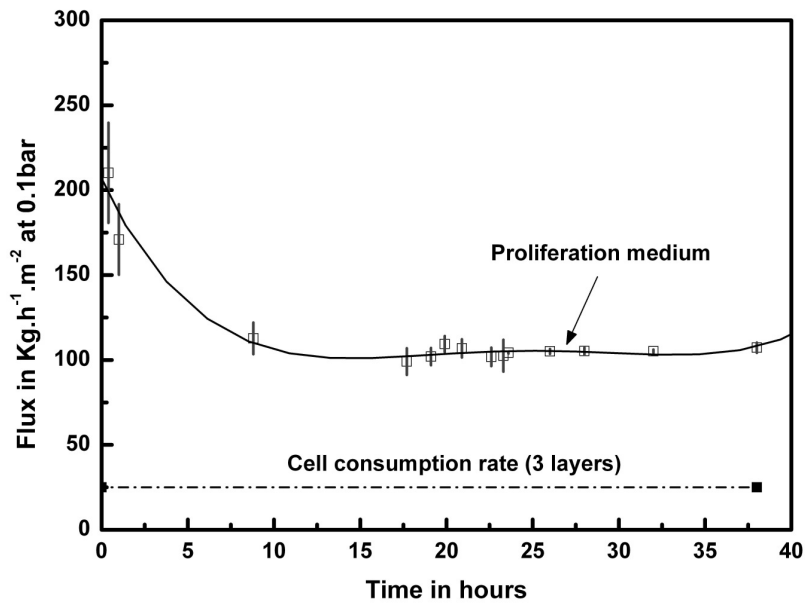
Clean water flux through the fiber gives an indication of HF porosity, pore connectivity and tortuosity. Figure 6a shows that the clean water flux at various trans-membrane pressures (0.1 – 0.25 bar) is linear with no compaction (several cycle of increasing and decreasing pressure flux were tested). Table 1 shows the water permeance (slope of Figure 6a) of the HF tested. For the Gambro and Asahi fibers, it is approximately 5000 $\text{Kg} / \text{m}^2 \text{ h bar}$ and it is much higher than that of Membrana fibers (3010 $\text{Kg} / \text{m}^2 \text{ h bar}$).



(a)



(b)



(c)

Figure 6. Plot of different biocompatible hollow fiber tested for (a) Clean water flux (b) proliferation medium permeability and (c) Flux of proliferation medium at trans-membrane pressure of 0.1bar in-comparison with cell consumption rate

Figure 6b shows that the medium permeance of all HF membranes decreases in time and reaches a plateau (steady state) due to deposition of medium proteins in the membrane pores. For all membranes, despite their design and credential (used in plasmapheresis applications), the transport of medium decreases in time due to membrane fouling but nonetheless, their pores do not seem to block completely and medium transport can be maintained at lower levels after a steady state is reached. Table 1 shows the individual medium permeance of the HF tested after attaining steady state flux. Based on these results, the Gambro fibers were chosen for all cell culture experiments due to the fact that they attain the plateau of constant medium permeation faster (10 hours) and have the highest medium steady state permeance of 1040 Kg / m² h bar. Figure 6c shows the actual medium flux through the Gambro fiber at trans-membrane pressure of 0.1 bar (this flux stays constant at this level for more than 15 days - results not shown) and the calculated medium glucose consumption by 3 layers of cells cultured in confluence over the surface of the hollow fiber (corresponding to the theoretical data for glucose consumption by the cells [28, 29]). Our results suggest that the medium flux through the Gambro fiber would be sufficient for multi layer tissue culture of approximately 12 layers of cells in confluence per unit active hollow fiber surface area.

Hollow fiber type	Material	Water permeance Kg / m ² h bar	Medium permeance Kg / m ² h bar (at steady state)
Membrana	Polypropylene (PP)	3010	300
Asahi	Modified Polysulfone (PS)	4990	662
Gambro	Modified Poly(ether sulfone) (PES)	5410	1040

Table 1. Screening of biocompatible hollow fibers based on water and medium permeability

Furthermore, the medium permeated through the Gambro HF at steady state was tested for C2C12 cells culture in T-flask and the results were compared to cell culture with proliferation medium and DMEM (without FBS) (as control) to check whether there is any difference in proliferation rate due to HF permeation. Figure 7 shows the light microscopic images of C2C12 cells and the numbers of cells obtained in culture after 1 and 5 days with the respective media refreshed every alternate day. These results show that the proliferation of cells cultured with medium after HF filtration and standard proliferation medium is identical, proving that the Gambro fiber indeed delivers to the cells all valuable medium components.

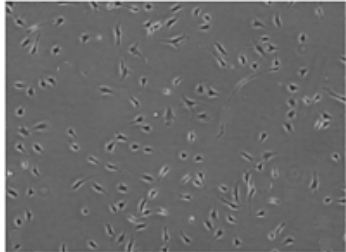
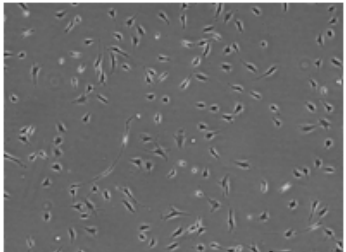
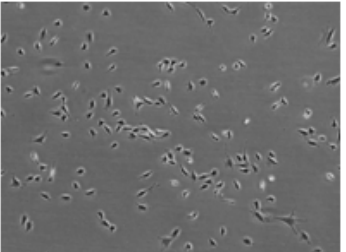
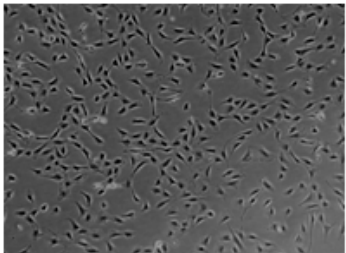
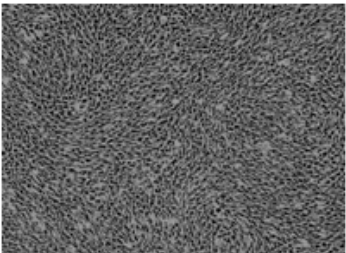
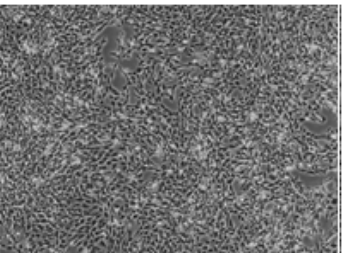
	Medium (DMEM)	Proliferation medium (DMEM + 10% FBS)	Proliferation medium permeated through HF
1 day	 (~ 1700 cells/cm ²)	 (~ 1700 cells/cm ²)	 (~ 1700 cells/cm ²)
5 days	 (~ 4100 cells/cm ²)	 (~ 18900 cells/cm ²)	 (~ 18400 cells/cm ²)

Figure 7. Light microscopic image of C2C12 cells cultured for 1 and 5 days with DMEM, proliferation medium and HF permeated medium (Gambro) (seeding density – 2000cells/cm²)

3.2.3 HF biocompatibility

Figure 8 shows light microscopy images of C2C12 cells (stained with methylene blue) cultured statically on the Gambro fibers for 3 and 7 days in non treated culture plate with medium refreshed every alternate day. The cells attach and proliferate well on the fiber surface. Cell attachment and ECM production indicates that the cells are alive on the fiber

surface which in-turn confirms the good biocompatibility of the hollow fiber. Figure 8 also shows images of dynamically cultured C2C12 cells in perfusion bioreactor. Very few cells observed on the fiber surface indicate that the permeating medium restricts adhesion of proliferating cells on the fiber surface. The low cell adhesion on the fiber surface under dynamic conditions is advantageous as permeability of the fiber during cell culture would remain stable with low pressure drop and low fouling. This indicates that the fiber would be suitable for supplying nutrient for long term tissue culturing in-vitro (see next section).

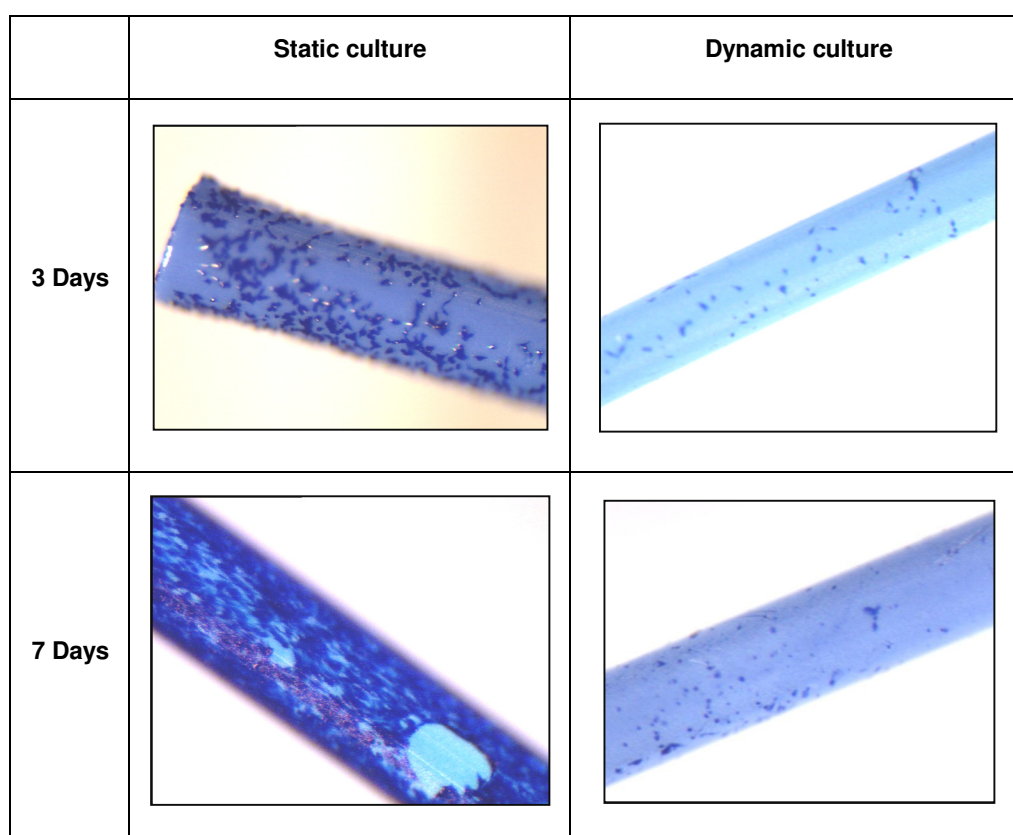


Figure 8. Light microscopic images of C2C12 cells cultured statically and dynamically for 3 and 7 days on Gambro fibers and stained with methylene blue stain, seeding density – 4000cells/cm² (4X magnification)

3.3 Bioreactor experiments

Perfusion bioreactor cell culture experiments were carried out on 3DF-HF scaffold containing 2, 4 and 8 hollow fibers with symmetric distribution along the horizontal axis within the scaffold (see Figure 2). For all bioreactor experiments the medium used in the reservoir was pre-conditioned by allowing medium gas exchange by pumping through gas permeable platinum cured silicon tubes built within temperature, CO₂ and humidity controlled incubator for at least 12 hours. During culturing, the medium was maintained with minimum glucose at $17\pm 0.5\text{mM}$ and maximum lactate at $6.5\pm 0.7\text{mM}$ concentration before refreshing in the reservoir for both static and dynamic culture (compared to fresh medium concentration of $25.1\pm 0.4\text{mM}$ and $0.9\pm 0.3\text{mM}$ respectively) to avoid the risk of re-circulating toxic waste to the proliferating cells.

Comparison of flow cases

The 3 different cases of medium flow through the bioreactor were assessed by carrying out cell culture experiments on 3DF-HF module with 2 hollow fibers. Medium flow through the scaffold (FTS), flow through the HF alone and dual flow (FTS and through the HF combined) were tested. For comparison cell seeded 3DF-HF scaffolds were also cultured statically in petri-dish as control.

Figure 9 shows the SEM images confirming histological observations that the cells attach well on the 3DF-HF scaffolds cultured for 7 days under static and dynamic conditions. The images show the cells and ECM deposited on the surface and approximately 1.5mm depth inside the scaffold. Figure 10 depicts the total cell number per scaffold (calculated based on DNA assay) cultured for 0 (seeding), 3, 7 and 14 days in corresponding culture conditions. Although the cell number for static culture increases (see Figure 10) in time, the cells tend to proliferate only on the outer surface. As figure 9a and 9b show the scaffold surface is completely covered with cells and ECM but the scaffold interior has almost no cells. This observation is in accordance with literature studies where a drastic decrease in cell number and oxygen concentration was reported in the interior of the scaffold under static culture conditions [2, 30].

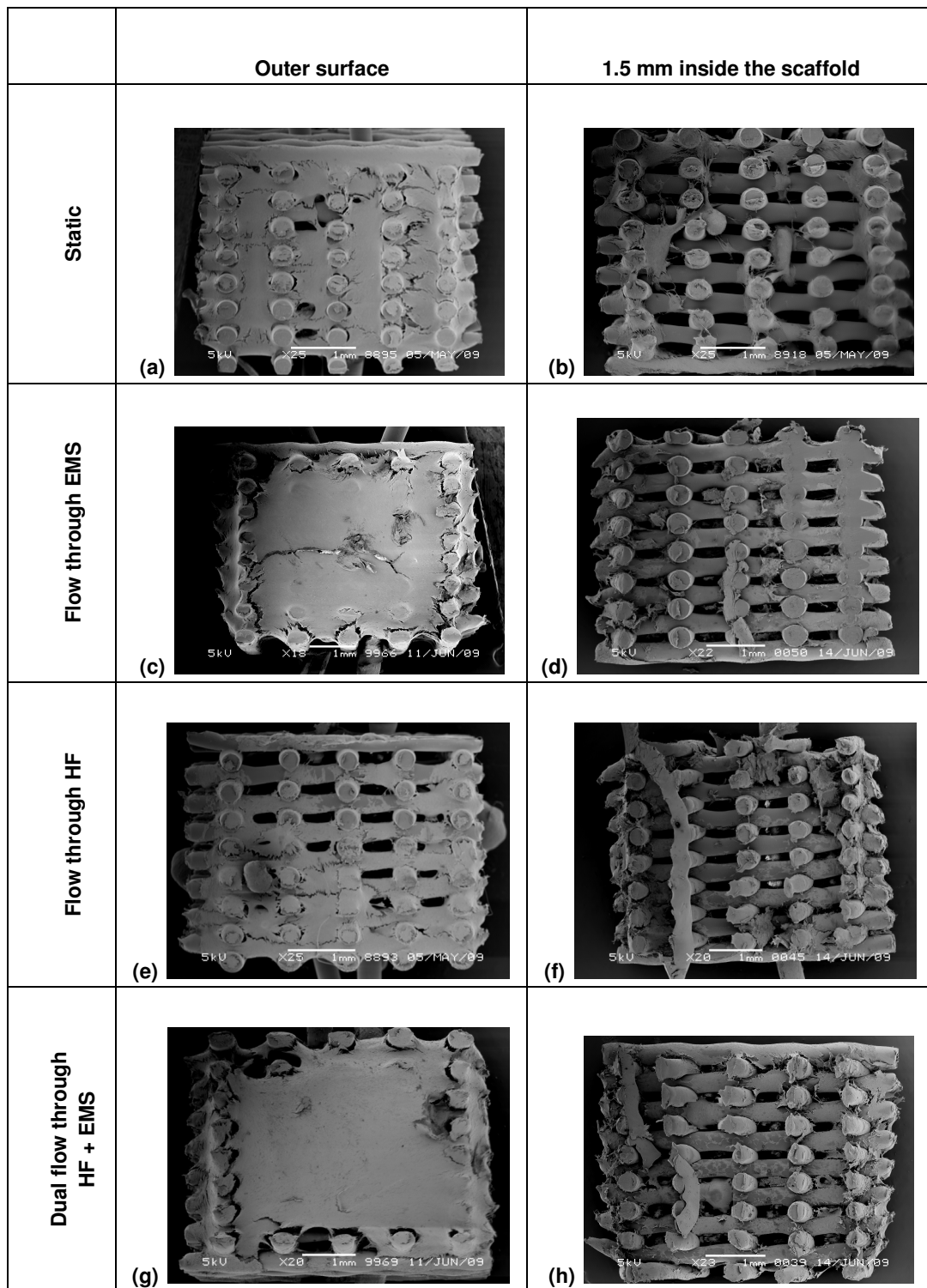


Figure 9. SEM images of cell cultured for 7 days on 3DF scaffold integrated with 2 hollow fibers in static and dynamic culture conditions (with different bioreactor flow conditions)

In the case of flow through the scaffold (FTS), it seems that the medium is only refreshed well around the scaffold and the results are similar to static culture experiment in bioreactor (Figure 9c and 9d show similar cell and ECM deposition as that of static culture). It seems that in this case, although the medium is refreshed constantly at 0.26ml/min, the ECM on the surface acts as a barrier for nutrient transport into the centre of the scaffold. Hence similar cell numbers compared to static culture are obtained for this case, too (see Figure 10).

In the case of perfusion via the HF lumen only (Figure 9e and 9f), the cell number in the interior of the scaffold is slightly higher and higher ECM deposition occurs close to the fibers. The ECM deposition on the scaffold surface is low compared to statically cultured scaffolds probably due to the insufficient refreshing of medium there by the fibers. This decrease is also reflected in cell number results which are about 50% lower than those of the static culture after 7 days culturing (see Figure 10). Although the overall cell density is low, these results are rather encouraging concerning increase of cell number inside the scaffold. Figure 9g and 9h depict the ECM deposited by the cells when medium perfusion occurs through the scaffold (FTS) and the HF. The images show that the outer surface of the scaffold is entirely covered by ECM, while the scaffold interior contains ECM deposited with a gradient from periphery to centre of the scaffold. The cell numbers for this dual flow (FTS+HF) (Figure 10) is slightly higher with large standard deviation compared to static culture. In conclusion, our results suggest that dual flow cell culture with 2 HF improves slightly the cell proliferation inside the scaffold however more fibers should be integrated to obtain good cell distribution in the scaffold. This is investigated in the next section.

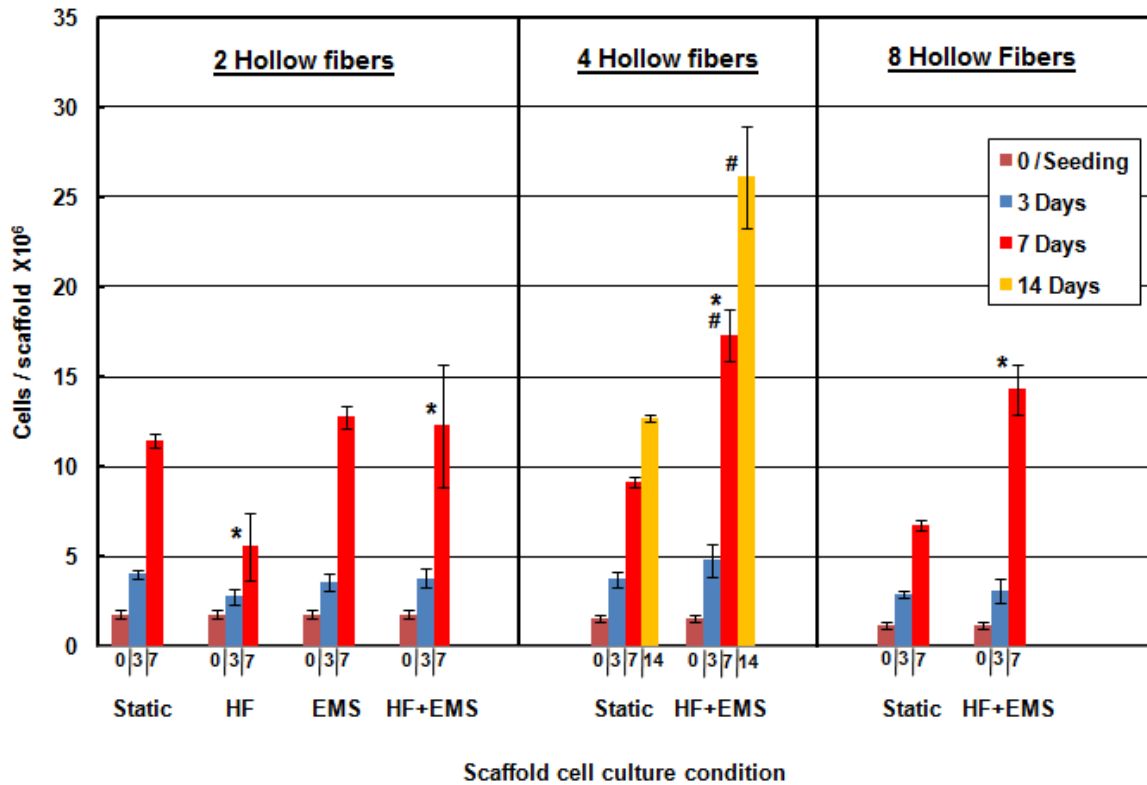


Figure 10. C2C12 cell proliferation within 3DF-HF scaffold module with 2, 4 and 8 hollow fiber integrated module cultured statically and dynamically for 0, 3, 7 and 14 days. [* = significant difference against 7 days culture, # = Significant difference against 7 days versus 14 days ($p < 0.05$), error-bars indicate standard deviation]

3.3.1 Optimization concerning number of integrated HF

Since the integration of only 2 hollow fibers was not sufficient to improve significantly cell proliferation and achieve better cell distribution into the scaffold, we investigated the integration of 4 and 8 hollow fibers, too.

Integration of 4 HF

The total cell number for scaffold integrated with 4 HF cultured in dual flow (FTS+HF) bioreactor increases almost exponentially compared to scaffold with 2 HF (Figure 10). The SEM images of the scaffold integrated with 4 HF and cultured for 7 and 14 days in dual flow bioreactor are also consistent with the cell number results showing high amount of ECM deposition on the surface and in the interior of the scaffold (Figure 11). Furthermore for cell culture of 14 days, the almost exponential increase of cell number in the scaffold and the very

high ECM deposition in between the pores of the scaffold confirm the ability of the fibers to achieve sufficient long term perfusion (Figures 10 and 11).

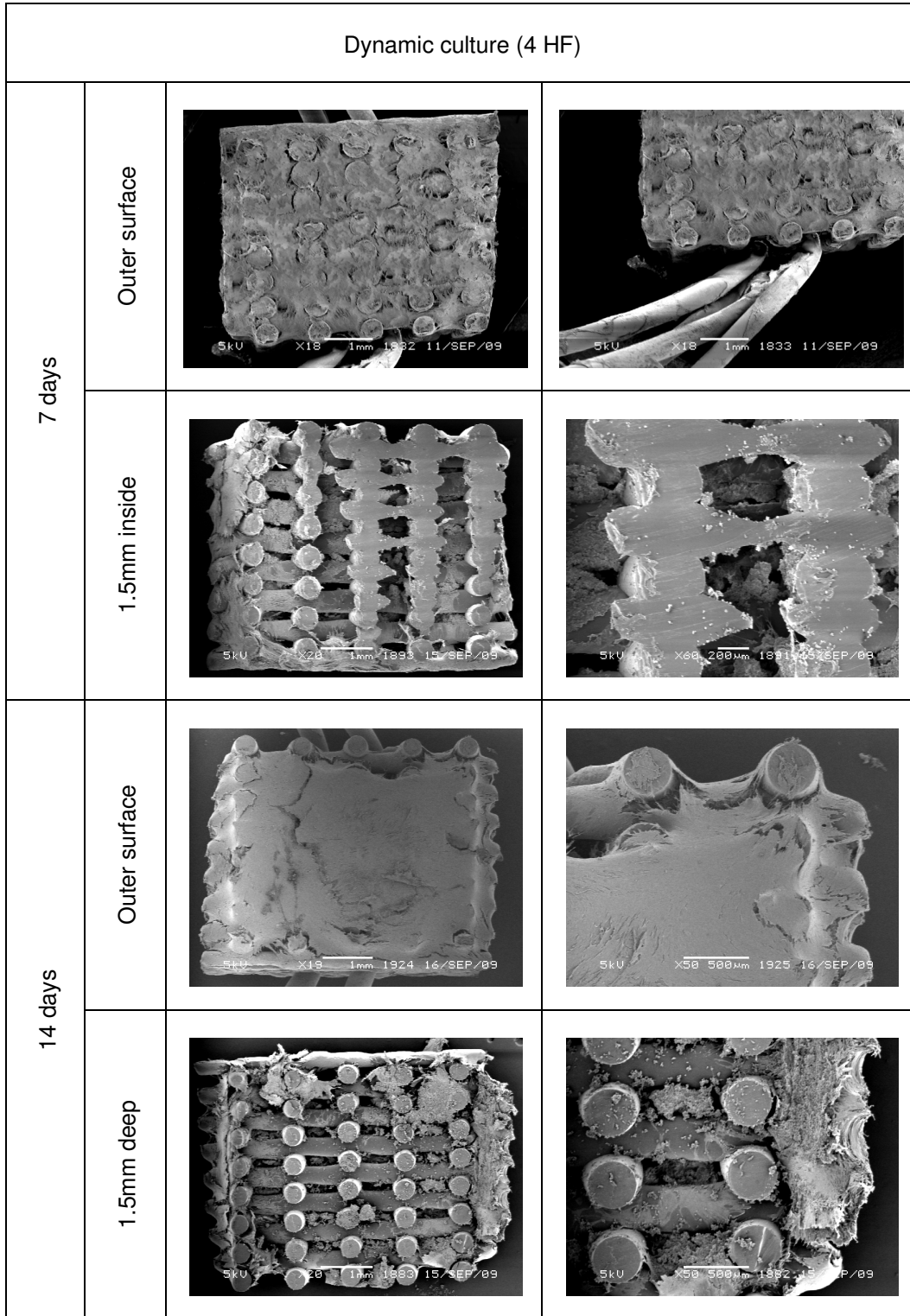


Figure 11. SEM images of C2C12 cells cultured for 7 and 14 days on 3DF scaffold integrated with 4 hollow fibers in dual perfusion bioreactor system with medium flow through EMS and HF lumen

The cell distribution within the scaffold with 4 HF cultured for 7 days statically and dynamically was further analysed by sectioning the embedded sample at different depths and staining the cells. Figure 12 and 13 show light microscopic images of 5-8 μ m thin microtome sections of GMA embedded the H&E stained scaffolds. Figure 12 shows the microscopic image of statically cultured samples with 4 HF integrated within scaffold and cultured for 7 days with medium refreshed every alternate day. The images clearly show that the cells (indicated as C) stained purple are mostly located in confluence at the outer surface (see images at 0.2mm deep section). The images at 1, 1.5 and 2 mm depth show cells (C) clustered at the periphery of the scaffold forming a barrier for medium diffusion. The images at the center of the scaffold have no cells and the empty space of the porous scaffold (S) is filled with GMA embedding material (indicated as G). This result illustrates again the limited nutrient diffusion to the interior of the scaffold (due to ECM produced by the cells at the periphery which acts as barrier) and subsequent cell death at the interior of the scaffold due to necrosis under static culture conditions.

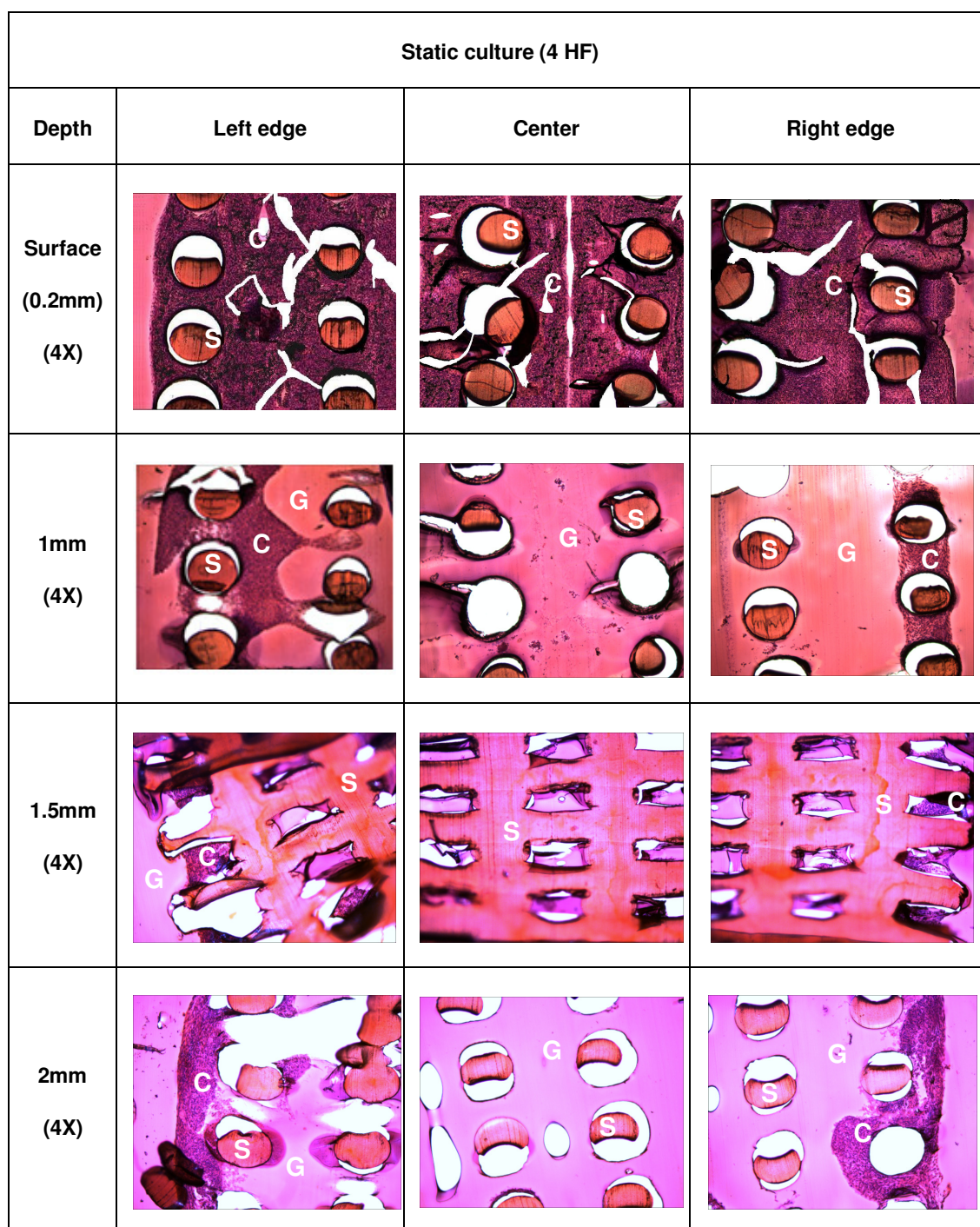


Figure 12. Light microscopic images of H&E stained microtome sections of scaffold embedded in GMA, of cell cultured statically for 7 days on 3DF-HF module integrated with 4 hollow fibers [G → GMA embedding resin, S → Scaffold polymer and C → Cells]

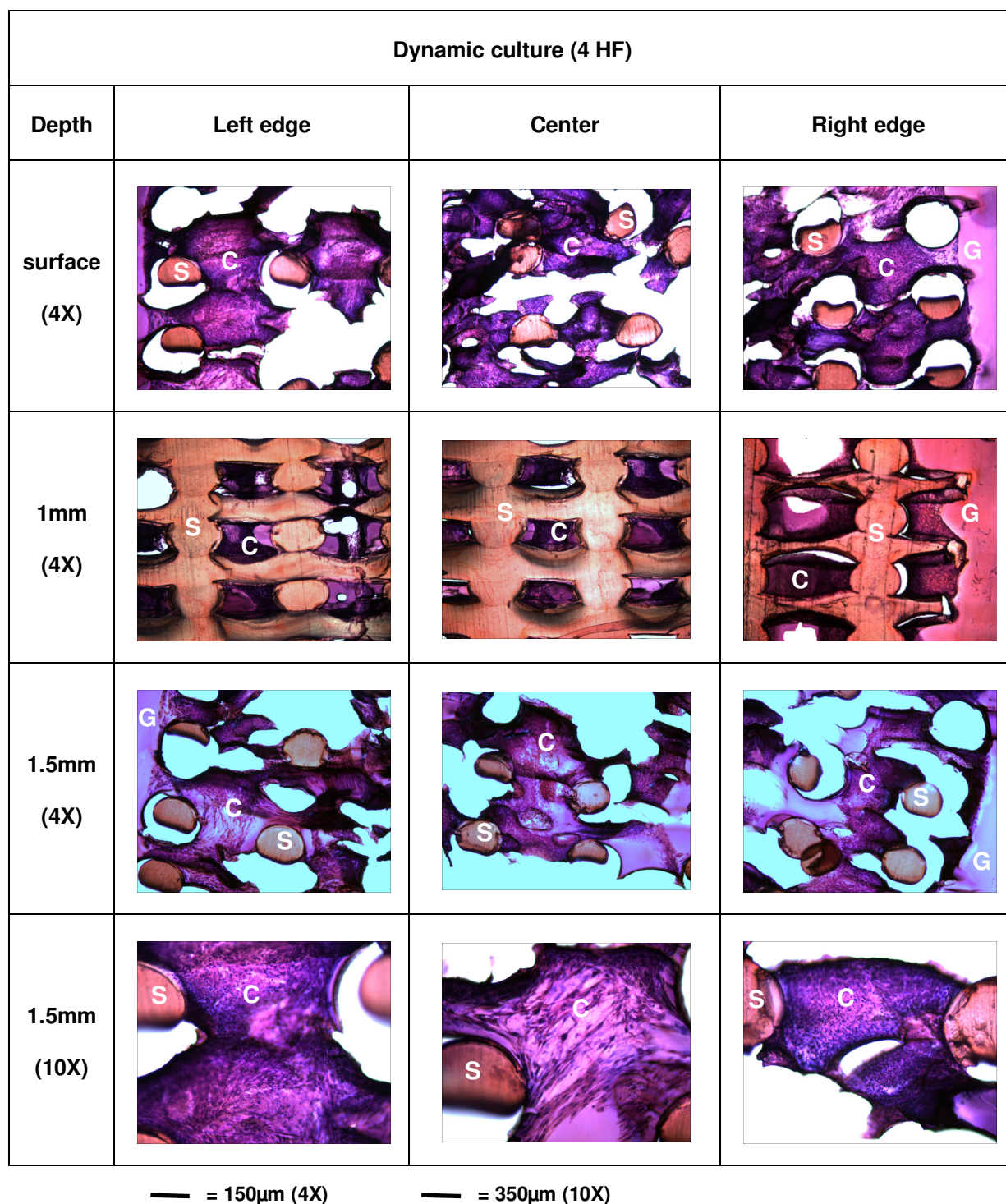


Figure 13. Light microscopic images H&E stained microtome sections of scaffold embedded in GMA, of dynamically cultured for 7 days on 3DF-HF module integrated with 4 hollow fibers in dual perfusion bioreactor system with medium flow through EMS and HF lumen [G \rightarrow GMA embedding resin, S \rightarrow Scaffold polymer and C \rightarrow Cells]

Figure 13 presents the cell distribution within the scaffold integrated with 4HF and cultured in dual flow perfusion bioreactor system for 7 days. For these scaffolds, high cell density is observed at the periphery as well as in the interior of the scaffold and the scaffold pores are completely filled with cells and ECM. In fact, the cell number there is so high that only very little amount of GMA embedding material could infiltrate into the pores and therefore some of the images have cracks and holes. The high magnification (10X) images at depth of 1.5mm from the scaffold surface show that the cells stretch in between the porous space of adjacent scaffold fibers, which indicates that they are live cells (Figure 13).

Integration of 8 HF

Figure 10 shows that the cell proliferation for dynamic cell culture of 7 days using dual flow (FTS+HF) for scaffolds with 8 hollow fiber cell is significantly higher compared to static culture but significantly lower when compared to dynamic experiment with 4 HF. This difference in cell proliferation may be due to decrease of scaffold porosity due to space occupied by the 8 hollow fibers. (In fact the porosity of the scaffold decreases by 25% due to the presence of the 8 HF). The seeding efficiency or the initial number of cells seeded on the scaffold also decreases with increasing number of hollow fibers due to fact that the hollow fibers themselves block the free straight - through pores of the 3DF scaffold. Obviously, integration of 8 fibers to the specific scaffold is detrimental for achieving our goals and should be avoided.

4 Conclusion – Outlook

Our results demonstrated the proof of concept of using polymeric hollow fibers as artificial capillaries to supplement proliferation medium for long term (up to 14 days) at physiological trans-membrane pressure (0.1bar) for in-vitro 3D tissue culture. For the specific type and size of scaffold, integration of four HF and dual flow perfusion (through the scaffold and via the fiber) is the optimal configuration to achieve high cell proliferation and homogenous cell distribution within the scaffold. The proof of concept of our approach was shown using combination of techniques. The SEM analysis showed clearly that only integration of fibers achieves homogenous cell distribution. The H&E staining confirmed the cell distribution visualized by SEM at the surface and inside the scaffold and showed in more detail the local cell distribution proving the advantage of our concept. The total DNA assay showed quantitatively the cell proliferation within the scaffolds, proving that 4 HF combined with flow through the scaffold achieves the best result.

Future work will focus on incorporation of biodegradable porous hollow fibers such as PLLA or PLGA [31] for permeation of nutrients in-vitro and implantation of the construct (in vivo). There, the hollow fibers could be connected to host vascular system until host vascular network infuses into the tissue engineered construct.

5 Acknowledgements

The authors would like to acknowledge the financial support from Technology Foundation STW (Project number – TKG. 6716). We also thank Gambro GmbH, Asahi Kasei Medical Co. Ltd. and Membrana GmbH for kindly providing the hollow fibers and Prof. Dr. C.A. van Blitterswijk (Tissue Regeneration (TR) group University of Twente, The Netherlands) for facilitating the bioreactor cell culture experiments in his lab. Thanks are also due to G.A. Higuera, J. Vicente and J.B. Bennink for assistance with bioreactor, HF characterization and set-up artwork respectively.

Abbreviations

3D	-	3 dimensional
3DF – HF	-	3D free form fabricated scaffold integrated with hollow fiber
C2C12	-	Mouse pre-myoblast cells
CAM	-	Computer aided machine program
CO₂	-	Carbon dioxide
D-MEM	-	Dulbecco's Modified Eagle's Medium
DNA	-	Deoxyribonucleic acid
ECM	-	Extra cellular matrix
EDTA	-	Ethylene-di-amine-tetra-acetate
FTS	-	Flow through scaffold

References

- [1] B. Burgarski, D. Jovanovic, G. Vunjak-Novakovic, Fundamentals of animal cell immobilization and microencapsulation - Bioreactor systems based on microencapsulated animal cell cultures, CRC press, Florida, 1993.
- [2] J.C.Y. Dunn, W.Y. Chan, V. Cristini, J.S. Kim, J. Lowengrub, S. Singh, B.M. Wu, Analysis of cell growth in three-dimensional scaffolds, *Tissue Engineering*, 12 (2006) 705-716.
- [3] C.K. Colton, Implantable biohybrid artificial organs, *Cell Transplantation*, 4 (1995) 415-436.
- [4] D. Wendt, S. Stroebel, M. Jakob, G.T. John, I. Martin, Uniform tissues engineered by seeding and culturing cells in 3D scaffolds under perfusion at defined oxygen tensions, *Biorheology*, 43 (2006) 481-488.
- [5] I. Martin, D. Wendt, M. Heberer, The role of bioreactors in tissue engineering, *Trends in Biotechnology*, 22 (2004) 80-86.
- [6] M. Pei, L.A. Solchaga, J. Seidel, L. Zeng, G. Vunjak-Novakovic, A.I. Caplan, L.E. Freed, Bioreactors mediate the effectiveness of tissue engineering scaffolds, *The FASEB journal : official publication of the Federation of American Societies for Experimental Biology*, 16 (2002) 1691-1694.
- [7] M.C. Lewis, B.D. MacArthur, J. Malda, G. Pettet, C.P. Please, Heterogeneous proliferation within engineered cartilaginous tissue: The role of oxygen tension, *Biotechnology and Bioengineering*, 91 (2005) 607-615.
- [8] J. Malda, T.B.F. Woodfield, F. Van Der Vloodt, F.K. Kooy, D.E. Martens, J. Tramper, C.A. Van Blitterswijk, J. Riesle, The effect of PEGT/PBT scaffold architecture on oxygen gradients in tissue engineered cartilaginous constructs, *Biomaterials*, 25 (2004) 5773-5780.
- [9] M. Radisic, W. Deen, R. Langer, G. Vunjak-Novakovic, Oxygen distribution in channeled cardiac constructs perfused with oxygen carrier supplemented culture medium, in, 2004, pp. 8757-8759.
- [10] S.J. Hollister, Porous scaffold design for tissue engineering, *Nature Materials*, 4 (2005) 518-524.
- [11] R. Langer, D.A. Tirrell, Designing materials for biology and medicine, *Nature*, 428 (2004) 487-492.

- [12] R.L.Y. Sah, Y.J. Kim, J.Y.H. Doong, A.J. Grodzinsky, A.H.K. Plaas, J.D. Sandy, Biosynthetic response of cartilage explants to dynamic compression, *Journal of Orthopaedic Research*, 7 (1989) 619-636.
- [13] R.L. Mauck, M.A. Soltz, C.C.B. Wang, D.D. Wong, P.H.G. Chao, W.B. Vallmu, C.T. Hung, G.A. Ateshian, Functional tissue engineering of articular cartilage through dynamic loading of chondrocyte-seeded agarose gels, *Journal of Biomechanical Engineering*, 122 (2000) 252-260.
- [14] H.J. Henzler, Particle stress in bioreactors, *Advances in biochemical engineering/biotechnology*, 67 (2000) 35-82.
- [15] M. Papadaki, T. Mahmood, P. Gupta, M.B. Claase, D.W. Grijpma, J. Riesle, C.A. Van Blitterswijk, R. Langer, The different behaviors of skeletal muscle cells and chondrocytes on PEGT/PBT block copolymers are related to the surface properties of the substrate, *Journal of Biomedical Materials Research*, 54 (2001) 47-58.
- [16] M.B. Claase, D.W. Grijpma, S.C. Mendes, J.D. De Bruijn, J. Feijen, Porous PEOT/PBT scaffolds for bone tissue engineering: Preparation, characterization, and in vitro bone marrow cell culturing, *Journal of Biomedical Materials Research - Part A*, 64 (2003) 291-300.
- [17] G.J. Beumer, C.A. Van Blitterswijk, M. Ponec, Biocompatibility of a biodegradable matrix used as a skin substitute: An in vivo evaluation, *Journal of Biomedical Materials Research*, 28 (1994) 545-552.
- [18] G.J. Beumer, C.A. Van Blitterswijk, D. Bakker, M. Ponec, Cell-seeding and in vitro biocompatibility evaluation of polymeric matrices of PEO/PBT copolymers and PLLA, *Biomaterials*, 14 (1993) 598-604.
- [19] R. Landers, R. Malhaupt, Desktop manufacturing of complex objects, prototypes and biomedical scaffolds by means of computer-assisted design combined with computer-guided 3D plotting of polymers and reactive oligomers, *Macromolecular Materials and Engineering*, 282 (2000) 17-21.
- [20] R. Landers, A. Pfister, U. Habner, H. John, R. Schmelzeisen, R. Malhaupt, Fabrication of soft tissue engineering scaffolds by means of rapid prototyping techniques, *Journal of Materials Science*, 37 (2002) 3107-3116.
- [21] R. Landers, U. Habner, R. Schmelzeisen, R. Malhaupt, Rapid prototyping of scaffolds derived from thermoreversible hydrogels and tailored for applications in tissue engineering, *Biomaterials*, 23 (2002) 4437-4447.
- [22] T.B.F. Woodfield, J. Malda, J. De Wijn, F. Paters, J. Riesle, C.A. Van Blitterswijk, Design of porous scaffolds for cartilage tissue engineering using a three-dimensional fiber-deposition technique, *Biomaterials*, 25 (2004) 4149-4161.

- [23] T.B.F. Woodfield, C.A. Van Blitterswijk, J. De Wijn, T.J. Sims, A.P. Hollander, J. Riesle, Polymer scaffolds fabricated with pore-size gradients as a model for studying the zonal organization within tissue-engineered cartilage constructs, *Tissue Engineering*, 11 (2005) 1297-1311.
- [24] L. Moroni, G. Poort, F. Van Keulen, J.R. De Wijn, C.A. Van Blitterswijk, Dynamic mechanical properties of 3D fiber-deposited PEOT/PBT scaffolds: An experimental and numerical analysis, *Journal of Biomedical Materials Research - Part A*, 78 (2006) 605-614.
- [25] L. Moroni, J.R. De Wijn, C.A. Van Blitterswijk, Three-dimensional fiber-deposited PEOT/PBT copolymer scaffolds for tissue engineering: Influence of porosity, molecular network mesh size, and swelling in aqueous media on dynamic mechanical properties, *Journal of Biomedical Materials Research - Part A*, 75 (2005) 957-965.
- [26] L. Moroni, J.R. De Wijn, C.A. Van Blitterswijk, 3D fiber-deposited scaffolds for tissue engineering: Influence of pores geometry and architecture on dynamic mechanical properties, *Biomaterials*, 27 (2006) 974-985.
- [27] K. Whang, T.K. Goldstick, K.E. Healy, A biodegradable polymer scaffold for delivery of osteotropic factors, *Biomaterials*, 21 (2000) 2545-2551.
- [28] N.S. Abdullah, D.B. Das, H. Ye, Z.F. Cui, 3D bone tissue growth in hollow fibre membrane bioreactor: Implications of various process parameters on tissue nutrition, *International Journal of Artificial Organs*, 29 (2006) 841-851.
- [29] H. Ye, D.B. Das, J.T. Triffitt, Z. Cui, Modelling nutrient transport in hollow fibre membrane bioreactors for growing three-dimensional bone tissue, *Journal of Membrane Science*, 272 (2006) 169-178.
- [30] J. Malda, J. Rouwkema, D.E. Martens, E.P. Le Comte, F.K. Kooy, J. Tramper, C.A. Van Blitterswijk, J. Riesle, Oxygen Gradients in Tissue-Engineered PEGT/PBT Cartilaginous Constructs: Measurement and Modeling, *Biotechnology and Bioengineering*, 86 (2004) 9-18.
- [31] G. Meneghello, D.J. Parker, B.J. Ainsworth, S.P. Perera, J.B. Chaudhuri, M.J. Ellis, P.A. De Bank, Fabrication and characterization of poly(lactic-co-glycolic acid)/polyvinyl alcohol blended hollow fibre membranes for tissue engineering applications, *Journal of Membrane Science*, 344 (2009) 55-61.

Chapter 4

Engineering multilayer tissue grafts capable of multi cellular organisation

N.M.S. Bettahalli ¹, N. Groen ¹, H. Steg ¹, H. Unadkat ², J. de Boer ²,

C.A. van Blitterswijk ², M. Wessling ^{1,3}, D. Stamatialis ^{1,*}

MIRA Institute for Biomedical Technology and Technical Medicine, University of Twente

¹ Membrane Technology Group, Faculty of Science and Technology, PO Box 217, 7500 AE Enschede, The Netherlands.

² Dept. of Tissue Regeneration , Faculty of Science and Technology, PO Box 217, 7500 AE Enschede, The Netherlands.

³ RWTH Aachen University, Chemische Verfahren Technik (CVT), 52064 Aachen, Germany

If you steal from one author, it's plagiarism; if you steal from many, it's research

(Wilson Mizner)

Abstract

The rapidly developing field of tissue engineering produces living substitutes that restore, maintain or improve the function of tissue or organs. In contrast to standard therapies, the engineered products become integrated within the patient, affording a potentially permanent and specific cure of the disease, injury or impairment. Despite the great progress in the field, development of clinically relevant size tissues with complex architecture remains a great challenge. This is mostly due to limitations of nutrient and oxygen delivery to the cells and limited availability of scaffolds which can mimic the complex tissue architecture.

This study presents the development of a multilayer construct produced by rolling pre-seeded electrospun sheets (C2C12 pre-myoblast cells were used) around a porous multibore hollow fiber (HF) to form an 8 layer tissue construct. The sheets were prepared from Poly (l-lactic acid) (PLLA). The multibore HF acts as a support for the electrospun layers and as additional source of nutrients and oxygen by permeating medium through the porous walls at low shear stress. In fact, the dynamic perfusion through the HF lumen and around the 3D scaffold led to massive cell proliferation with homogenous cell distribution across the layers. Cell viability, proliferation and migration within the multilayer sheets were examined by live dead assay, SEM, fluorescent staining and DNA quantification. Furthermore, dynamic culture of pre-labeled C2C12 cells with red (CM-DiI) and green (CM-DiO) lipophilic tracers, seeded in separate ES sheets, demonstrated that probably cell migration occurs within the multilayer ES construct illustrating the potential of using this construct for development of complicated tissues having different cell types per layer.

Taken together the present study reports a novel approach to develop 3D multilayer tissue using bottom-up process by rolling pre-seeded ES sheets. This approach has a marked potential to form functional tissue composed of multiple cell types, heterogeneous scaffold composition and customized dynamic culture conditions.

Adapted from NMS Bettahalli et.al, Engineering multilayer tissue grafts capable of multi-cellular organisation, Submitted.

1 Introduction

Currently, efforts to induce healing and regeneration of damaged tissue are being directed towards improving existing cell therapies and developing new tissue engineering strategies. Small defects can be successfully treated with autologous cells (autograft) [1-5]. However, large defects and most tissues and organs in our body are usually composed of multiple layers of various cell types and of varying extracellular matrix (ECM). The cells and ECM there are arranged in an elaborate and hierarchical order to achieve specific function and to mutually regulate the cellular activity by soluble bioactive molecules, cell–cell or cell– ECM interactions [6-8]. The elaborate structure also provides individual cells with a defined microenvironment, where the cells experience specific cues and show corresponding responses towards tissue function. To maintain the proper cell phenotype in 3D tissue engineering one needs to achieve biomimetic design to replicate the ECM, seeding/infiltration of cells onto a biomaterial scaffold and culturing the seeded scaffold with adequate nutrient supply [9-11].

The recent understanding that ECM is a natural 3D cell supporter with complicated ultra-structure [12, 13] often determines the direction for scaffold design. To this end, electro-spinning process (ESP) has been used to fabricate nonwoven mesh as scaffold to mimic collagen fibrils in natural tissue matrix [14] with fiber size in the micro/nanometer scale [15-18]. The fibrous mesh also attributes in spatial arrangement (random or aligned), high porosity, mechanical property and increased surface area [19, 20]. ESP utilizes an electrostatic field to control the formation and deposition of polymer nanofibers [21-23] and is efficient, reproducible, rapid and inexpensive. Synthetic polymers such as poly lactic acid (PLA), poly(lactic-co-glycolic acid) (PLGA), poly(capro-lactone) (PCL), poly(ethylene oxide terephthalate)-poly(butylene terephthalate) (PEOT-PBT) [21, 22, 24, 25], and natural macromolecules such as collagen and fibrinogen [13, 26, 27], or their hybrids have been processed into fibrous non-woven scaffolds with ESP and have also shown to support stem cell growth and induce differentiation [13, 27, 28]. Nonetheless, some challenges with the application of these mesh are recognized, especially the difficulty of cell infiltration into thick 3D nanofibrous meshes and of cellular spatial arrangement (for single or multiple cell type). Natural tissues vary from single cell type with rather uniform organization (muscle tissue [29], nerve conduits [30]) or gradient organization (cartilage [31]) to complex layer by layer

multi cellular organization (blood vessel [32, 33], skin [34]). Mimicking these multilayer multi cellular arrangements is a challenge for modern tissue engineers.

Besides the above the optimal supply of nutrients and oxygenation to the entire volume of the 3D structure is a major challenge. Media perfusion bioreactor systems have been developed to improve mass transport throughout 3D tissue engineered constructs cultured in-vitro [35-38]. However problems arise in big constructs where in order to achieve delivery of nutrients and oxygen into the interior of the scaffold, the medium perfusion occurs at high flow rates causing high shear stress to the cells in the periphery. New techniques are being developed to address this issue by incorporating porous hollow fiber membranes into the scaffold or fiber themselves as the scaffold [39-42]. In addition to the standard perfusion across the scaffold, additional perfusion occurs via the hollow fiber [40, 43, 44].

In this work we show the proof of concept of developing multilayered tubular construct by rolling electrospun PLLA sheets around a multibore hollow fiber membrane. The hollow fiber acts as a support for sheet rolling and most importantly additional nutrient supply to the cells. Different aspects such as ES sheet fabrication, hollow fiber characterization, and optimization of dynamic culture conditions are carefully studied. The multilayer constructs are cultured statically and dynamically to understand the time-resolved tissue development. The proof of concept of our approach is shown using combination of techniques: Scanning electron microscopy and cell staining for showing the cell distribution in the multilayer scaffold as well as DNA assay for quantitative determination of the cell proliferation within the scaffold. Besides, experiments with pre-labeled cells, demonstrate spatial multicellular arrangement and cell migration within the multilayered construct.

2 Materials and methods

2.1 Electro-spun sheet fabrication and characterization

Non-woven ES sheets were fabricated using Poly(L-lactic acid) (PLLA, Mol wt. 1.6×10^5 g/mol, kindly provided by Prof. Dr. D. Grijpma (Biomaterials Science and Technology (BST) group, University of Twente, The Netherlands), of different concentrations: 10, 12, 13 and 15 wt% dissolved in 1,3-dioxane (Sigma-Aldrich, 97% purity). The polymer solution was loaded into a 5ml syringe mounted on to a syringe pump and fed into a hypodermic metal needle (18G medical grade syringe needle) at constant rate ranging from 0.5 to 10 ml/h (see Figure 1). The needle was charged by connecting to 15KV generator source to initiate electrostatic field for electrospinning. Grounded aluminum foil of 10 cm x 10 cm was placed 10 to 25 cm apart from the tip of the needle to collect the fibers in the form of a non-woven mesh for 30min. The nonwoven fibers were then dried in air flow chamber to evaporate residual solvent. The setup was built inside a transparent box to maintain constant humidity.

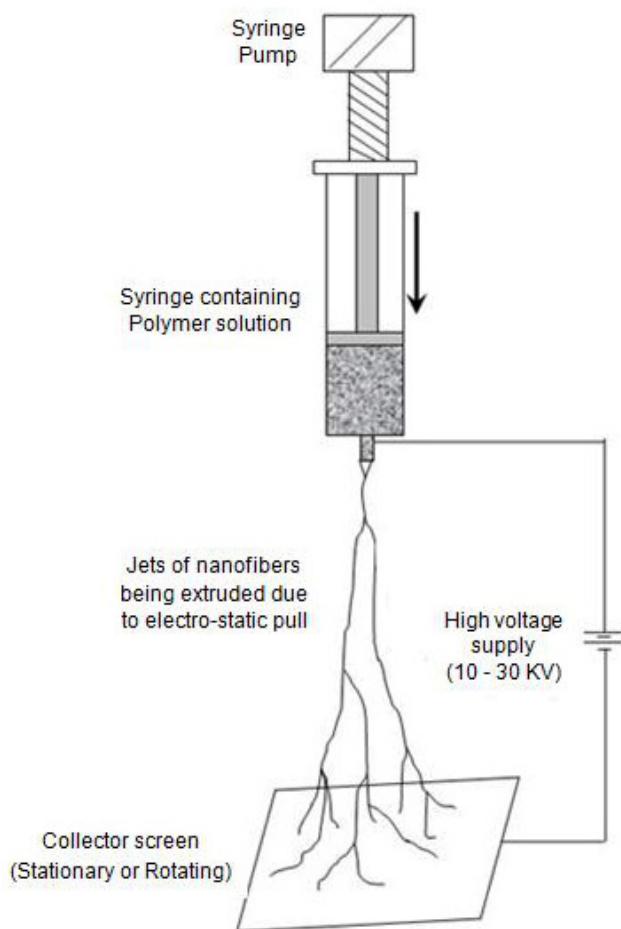


Figure 1. Schematic representation of electro spinning set-up

2.2 Multibore hollow fiber module assembly and treatment

The commercially available multibore HF membrane (Inge AG, Greifenberg, Germany) made of modified poly (ether sulfone) were used for medium permeation and support for ES sheets (details later). These fibers were selected because they have proven biocompatibility [43] and are expected to deliver efficiently nutrients to the cells via the multiple bores. Approximately 12cm long multibore HF modules were prepared manually by carefully inserting each end into 8mm polyethylene tube and sealed with polyurethane glue such that 2cm fiber surface is exposed for permeation at the middle of the module. The multibore HF modules were sterilized by pumping 70% ethanol at low pressure (~0.1bar) (in sterile environment) through the hollow fiber. Further, they were conditioned by pumping phosphate buffer solution (PBS) (pH=7.3) and proliferation medium correspondingly.

2.3 Characterization

2.3.1 Scanning electron microscopy (SEM)

SEM images of ES sheets and multibore hollow fibers were obtained using JEOL 5600LV scanning electron microscope at accelerating voltage of 5kV. Samples were dried in a vacuum oven at 30°C overnight and then used for surface scan, whereas samples for cross sectional observation were carefully fractured in liquid nitrogen. All samples were sputtered with gold (~15 to 20 nm-thick, Balzer-Union SCD-040) before imaging.

2.3.2 Multibore hollow fiber permeability

Water permeance

Pure water permeance of the multibore HF was determined by pressurizing ultrapure water (18.2 MΩcm, MilliQ) through the lumen of the HF (inside-out permeation). The experiments were carried out in glass encasing containing multibore HF module, each prepared using 8 mm polyethylene tube housing such that approximately 10 cm long HF is exposed for permeance (as explained above). The glass encasing had side ports to collect the flowing

permeate. Before measuring the clean water transport, the fibers were pre wetted by pumping water through the modules for at least 30 min. The flux (J in L/ (m².h)) through the membrane was measured at different trans-membrane pressures ranging between 0.02 to 0.3 bar at 20 ± 2°C. The flux at each pressure was successively measured by collecting the permeating water for at least 30 min. The pure water permeance (in L/ (m².h.bar)) was calculated using the slope of flux versus trans-membrane pressure plot. The data presented in this work is an average of four different hollow fiber modules.

Medium permeance

The proliferation medium permeance experiments were performed in sterile cross flow setup by pumping Dulbecco's Modified Eagle's Medium (D-MEM, Gibco) supplemented with 10% Fetal Bovine Serum (FBS, Cambrex), 100 U/ml penicillin (Gibco) and 100 µg/ml streptomycin (Gibco) through the lumen of the HF. The medium permeability was measured at trans-membrane pressure ranging between 0.02 to 0.1bar at 20±2°C. During the experiment the medium reservoir (feed) was stirred and pumped to the membrane module using a peristaltic pump with recirculation. The collected permeating medium and unfiltered medium was also used to statically culture mouse pre-myoblast (C2C12) cells in T-flask (T20) for comparison of cell proliferation rate.

2.4 ES sheet–multibore HF module assembly

Pre-seeded ES sheets

Mouse pre-myoblast, C2C12 cells were cultured in proliferation medium containing Dulbecco's Modified Eagle's Medium (D-MEM, Gibco) supplemented with 10% Fetal Bovine Serum (FBS, Cambrex), 100 U/ml penicillin (Gibco) and 100 µg/ml streptomycin (Gibco). Cells were initially plated in T-flask for expansion at 2000 cells/cm² until they reached 70-80% confluence, after which they were trypsinized using 0.05% Trypsin in 1mM EDTA. The obtained C2C12 cells were aggregated re-suspended in 200µl medium and 5 x 10⁵ cells were subsequently seeded onto 2cm x 6cm long ES sheet in a special culture plate which accommodates the ES sheet. The cells were allowed to attach for 1 day in a seeding box before rolling and subjecting to static or dynamic culture experiments.

Cell-ES sheet rolling

Two pre-seeded ES sheets cultured statically for one day were rolled around the multibore HF forming 4 layers each around the multibore HF. The sheets were rolled in such a way that the cell seeded surface faced the fiber surface. In total 8 layers of cell-ES sheet construct were formed by rolling two sheets of 2cm x 6cm. Sterile cotton thread (~10cm long for each end) were used to fasten the rolled sheets together and prevent unfolding of the layers (see Figure 2b). The whole construct was immediately placed in proliferation medium before further culturing under static or dynamic conditions. Hereafter these multilayer ES sheet-multibore HF constructs will be abbreviated as “MES construct”.

2.5 Cell culturing

2.5.1 Static culture

MES constructs were statically cultured in T-flasks containing proliferation medium by immersing the whole construct in the medium. The samples were cultured for 3 and 7 days in a sterile incubator with proliferation medium refreshed every alternate day. The resulting samples were analysed using light and fluorescent microscopy and were quantified by total DNA assay.

2.5.2 Dynamic culture

Dynamic cell culture within glass bioreactor was performed using a perfusion system consisting of a medium reservoir (Schott AG), FDA approved platinum cured silicon tubing (Masterflex), a multi-channel precision flow peristaltic pump (Watson-Marlow 205U), click connectors and a pressure sensor (see Figure 2). The whole perfusion bioreactor system was built within a temperature, humidity and CO₂-controlled sterile incubator. A reservoir containing 100ml of proliferation medium was re-circulated to feed the cells for 3 days before refreshing. The medium pumped from the reservoir was oxygenated before entering the bioreactor using long (~1.5m) gas permeable silicon tubing. The peristaltic pump used

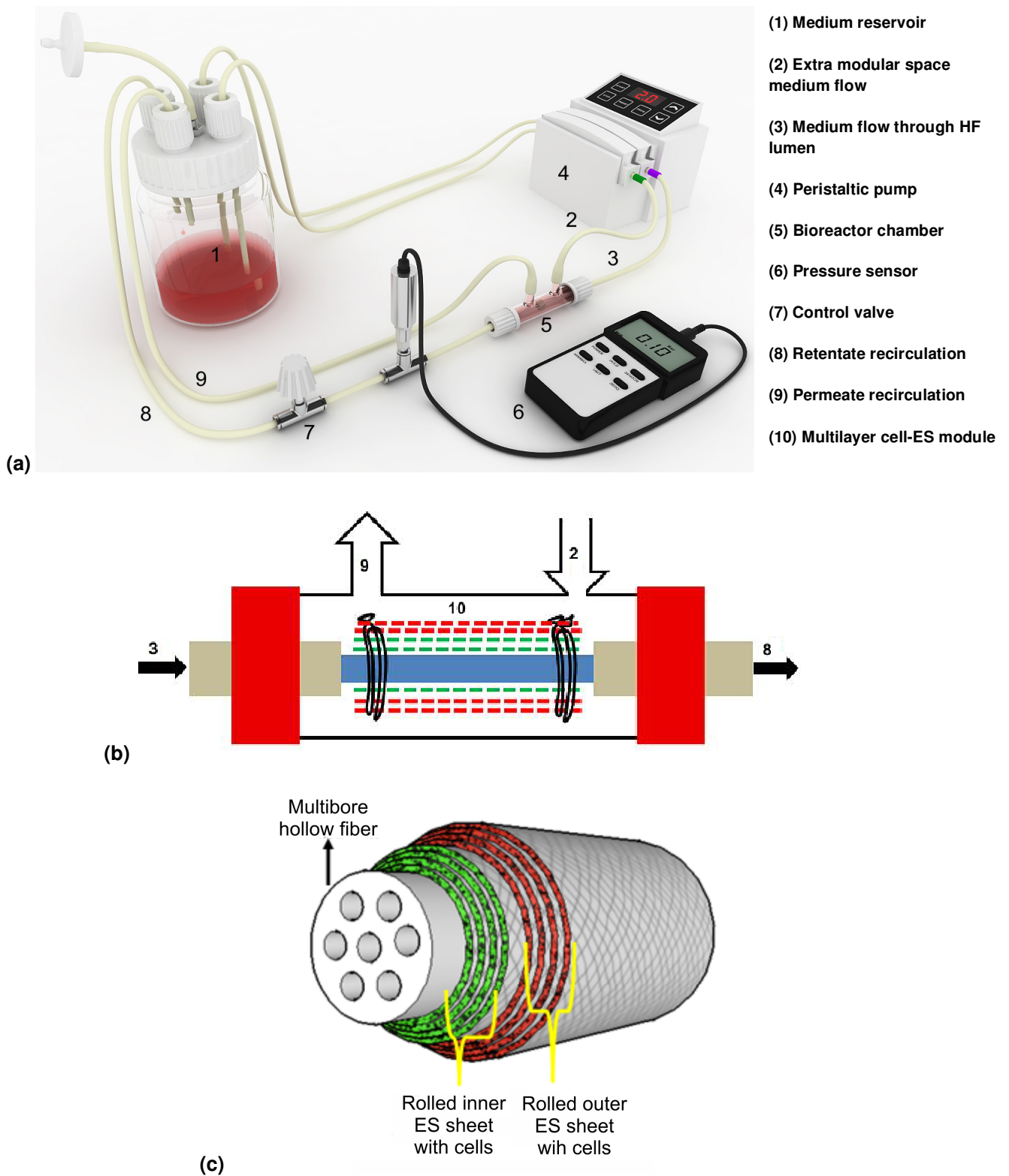


Figure 2. Scheme of the dynamic perfusion cell culture system (a) perfusion bioreactor setup with various components (b) cell-ES sheet rolled on multibore HF module mounted within glass bioreactor with side ports and (c) cross-section of multilayer MES construct.

different tube diameter for controlled medium volumetric flow rate. Pressure sensor and control valves were used to regulate the input trans-membrane pressure of the medium across the HF. The various parts of bioreactor were sterilized by autoclaving before each experiment. Fresh medium was perfused in single-pass and the stream leaving the bioreactor was collected as waste. When the system reached the steady state, the stream leaving the bioreactor was recycled. Medium samples were collected from the outlet stream to evaluate the glucose depletion and lactate formation using Vitros-DT60 diagnostic slides (**Ortho-Clinical Diagnostics**).

The glass bioreactor itself consists of a MES construct housed in a glass tube reactor of 1.5cm diameter and 5cm long with two side ports for medium flow and recirculation (Figure 2b). The module with the MES construct was held in the center of the glass reactor by a screw cap and silicon sealant rings mounted on the 8mm polyethylene tubing at both ends of the multibore HF module (Figure 2b). The construct was placed parallel within a glass reactor with medium flow through the fiber lumen as well around the construct. Two different medium perfusion flow configurations were investigated:

- Flow through multibore HF lumen only - In this configuration the pumped medium flows through the lumen of the multibore HF. The trans-membrane pressure across the fiber was monitored and kept constant at 50mbar with an average cross flow velocity of approximately 1ml/min. The permeating medium through the hollow fiber refreshes the medium in the bioreactor and exits through the side ports to the reservoir.
- Dual flow through multibore HF lumen and through the construct- Here, along with multibore HF lumen flow, flow was simultaneously charged in to the bioreactor from the side ports in counter current direction. For this, the pumped medium flows through one of the side ports and exited through the other side port of the glass bioreactor with an average flow rate of approximately 0.26ml/min. This flow continuously refreshes the medium in the glass tube and around the MES construct. The flow rates were maintained for both the flow system accordingly by using a peristaltic pump with different tube diameter. The same medium reservoir was used for both flows to pump medium to the proliferating cells in the bioreactor.

2.6 Scaffold-cell sample analysis

2.6.1 Viability staining

Cell viability on the ES sheets was examined using LIVE-DEAD staining assay. After unrolling the ES sheets in separate well plates, the sheets were incubated for 10 minutes with 6 μM Ethidium homodimer and 1 μM Calcein in PBS solution (LIVE-DEAD viability/cytotoxicity assay kit, Invitrogen - Molecular probes). Fluorescent microscopic images of the whole sheet were scanned in 64 (32 x 2) individual images using an automated confocal microscope (BD pathway 435, BD Biosciences) and collaged together to form a single image and visualize cell viability and distribution.

2.6.2 Fixation and staining for light microscopy

Cell-ES sheets were unrolled from the MES construct, samples were washed with PBS and incubated for 30 – 60 minutes in 10% neutral buffered formalin to fixate the cells and again washed with PBS. Subsequently the sheets were stained with few drops of 1% methylene blue staining solution prepared in borax solution for 3-5 minutes to stain the cells. Next, the sheets were washed with demineralized water to remove excess staining solution. The resulting stained samples were stored dry until further use for light microscopic analysis. The ES sheet was examined at different sections under light microscope (Nikon Eclipse E400) and representative images captured using a digital camera (Sony Corporation, Japan) and Matrix Vision software (Matrix Vision GmbH, Germany).

2.6.3 Cell proliferation assay

The concentration of DNA per ES sheet after 7 days was used as an indication for cell proliferation. The samples to be assayed were washed with PBS, cut in half and stored at -85°C. Before performing the DNA assay the samples were allowed to attain room temperature and sliced into small pieces and immersed completely in cell lysis buffer. Quantification of total DNA per sheet (standard deviation of 5 different MES samples) was measured according to the manufacturer's protocol (CyQuant Cell Proliferation Assay Kit, Invitrogen/Molecular probes) using a fluorescent plate reader (Perkin Elmer).

2.7 Pre- labelled multilayer MES construct

To study the migration of cells within the MES construct pre-seeded cells on the ES sheets were pre-labeled with lipophilic tracers (Molecular Probes, USA) for long term cellular labeling. The inner ES sheet (close to the HF) was seeded with cells labeled green using CM-DiO (3,3'-dioctadecyloxycarbocyanine per chlorate) and the outer sheet with cells labeled red using CM-DiI (1,1'-dioctadecyl -- 3,3,3',3'-tetramethylindocarbocyanine per chlorate) dyes. The cross-sectional scheme of the ES sheet rolling is as shown in Figure 2c. 3 and 7 days dynamic experiments were carried out in dual flow bioreactor as explained above. The cross sectional image of the MES construct at 3 and 7 days were taken using BD pathway 435 (BD Biosciences). 49 individual images (7 x 7) were taken and collaged together to form one complete image of the sectioned MES construct.

3 Results and discussion

3.1 Fabrication and characterisation electro-spun sheet

PLLA solution dissolved in 1,3 Dioxane was successfully electrospun into nanofibrous nonwoven mesh using the in-house built electrospinning set-up. SEM images were made to determine the surface topography and fiber diameter (see Figure 3). Nanofibers collected on collector (aluminum foil) were detached and viewed under SEM after sputter coating with gold. The influence of various spinning parameters such as polymer concentration, flow rate and distance between needle and collector were studied, whereas the applied voltage was kept constant at 15KV for all cases.

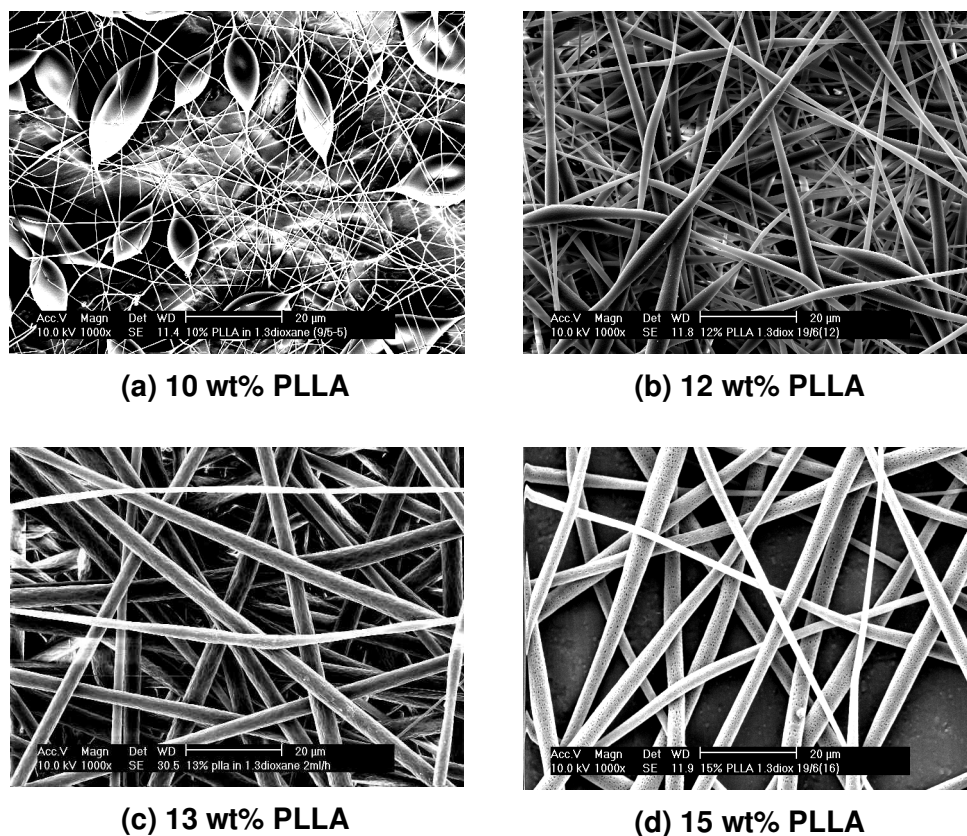
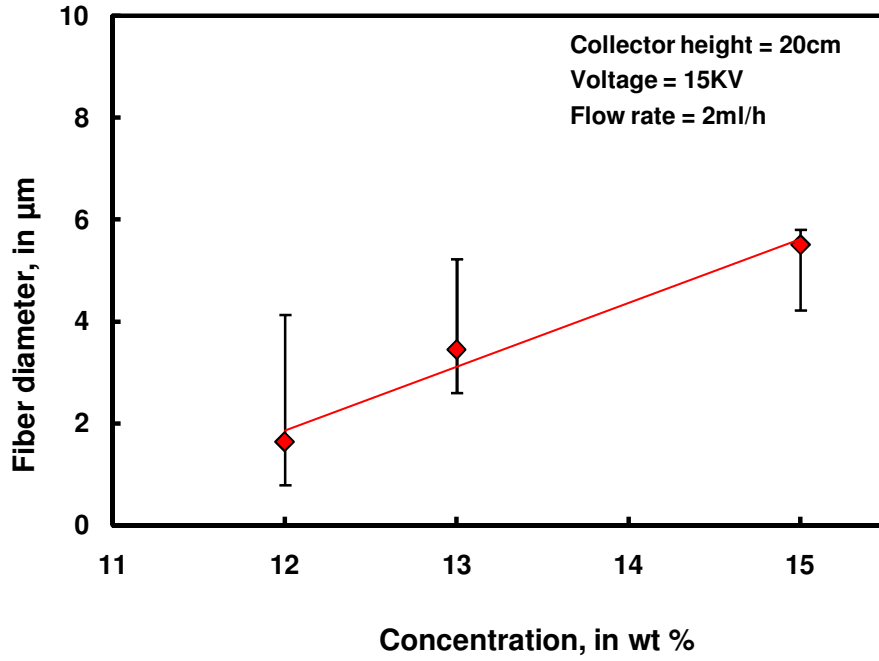


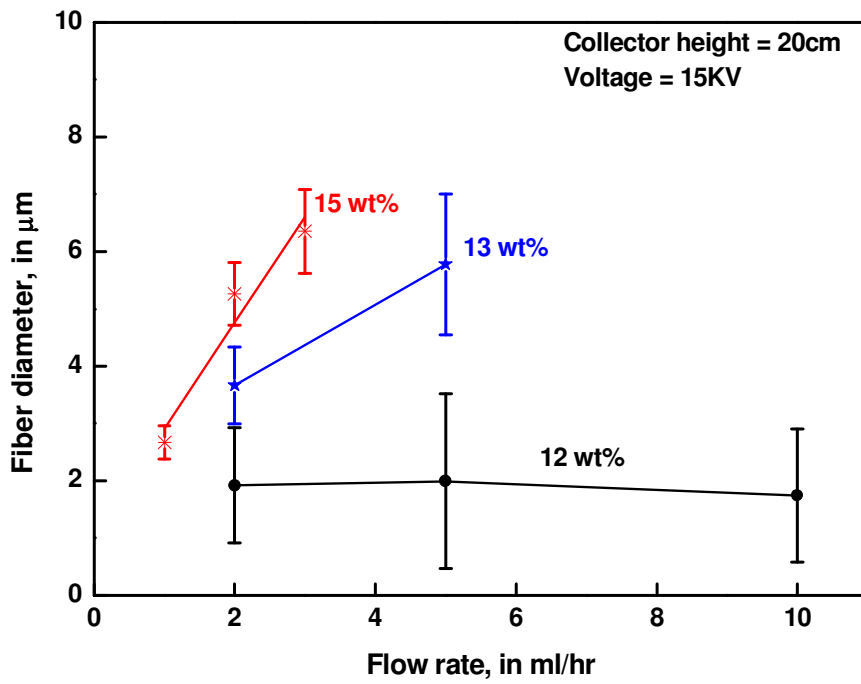
Figure 3. SEM images of ES sheet spun at different PLLA solution concentration (a) 10 wt%, (b) 12 wt%, (c) 13 wt%, and (d) 15 wt% dissolved in 1,3 dioxane (voltage = 15KV, height = 20cm, flow rate = 2ml/h)

The fabrication showed that below 12 wt% PLLA polymer concentrations, bead formation occurs (see Figure 3a). The range of fiber diameter deposited with respect to polymer concentration between 12 to 15 wt % is shown in Figure 4a (at constant flow rate – 2ml/hr, collector height – 20cm). The fiber diameter increases with increasing polymer concentration due to increasing viscosity and lower conductivity of the polymer solution.

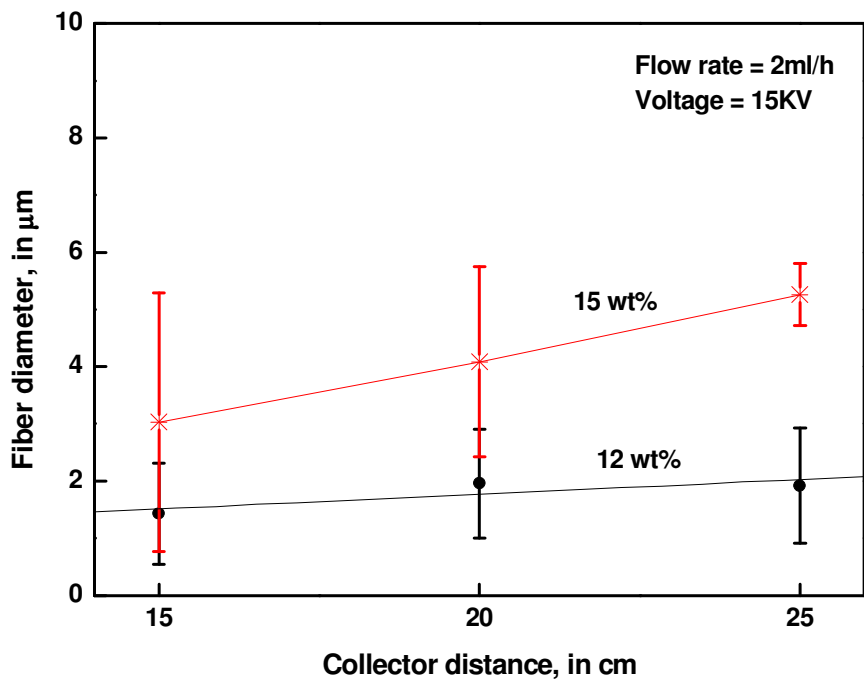
The influence of polymer flow rate through the capillary needle ranging between 0.5 to 10 ml/hr was also studied for different polymer concentrations at constant collector distance of 20 cm. The fiber diameter increases with increasing flow rate for 13 and 15 wt% PLLA solutions (Figure 4b), this effect is due to large droplet formation (also called Taylor cone) [45] at the tip of the capillary needle due to surface tension and the force of the electrostatic field. The fiber diameter of the mesh collected with 12 wt% PLLA solution is similar for all flow rates (Figure 4b), this effect is due to increased conductivity due to higher solvent concentration, but increasing flow rate influences beads formation within the mesh.



(a)



(b)



(c)

Figure 4. Plot of influence of electrospinning parameter on fiber diameter with respect to (a) Polymer concentration, (b) Flow rate and (c) Distance between needle tip and collector

Further, the influence of collector distance was tested for 12 and 15 wt% polymer concentration. Figure 4c represents the fiber diameter of ES meshes collected at 15, 20 and 25cm between needle tip and collector plate. Increasing collector distance influences solvent evaporation during the time of flight before collecting on the collector plate, hence smooth and round fibers are formed with increasing collector distance. For both polymer concentrations the standard deviation of fiber diameter collected decreases with increasing distance, but the average fiber diameter increases with increasing collector distance due to lower electro static force experienced by the Taylor cone to overcome the surface tension of the polymer solution.

Considering the above results with respect to various spinning parameter influencing fiber diameter and fiber morphology, the sheets prepared using 12 wt% PLLA solution concentration at 2 ml/h flow rate and 20cm air gap are considered the optimum with fiber diameter $2.5 \pm 2 \mu\text{m}$ and hence all the cell culture experiments were carried out on these meshes collected for 30 minutes on 10cm x 10cm electrically grounded collector (aluminium foil). The sheet thickness was approximately $200 \mu\text{m}$ with scaffold porosity of $71 \pm 3\%$ (measured using pycnometer).

3.2 Characterisation of multibore HF membrane

3.2.1 Scanning electron microscope

Figure 5 shows the SEM images of the multibore HF. It consists of 7 bores (0.9mm inner diameter) arranged symmetrically to form single fiber of 4 mm diameter.

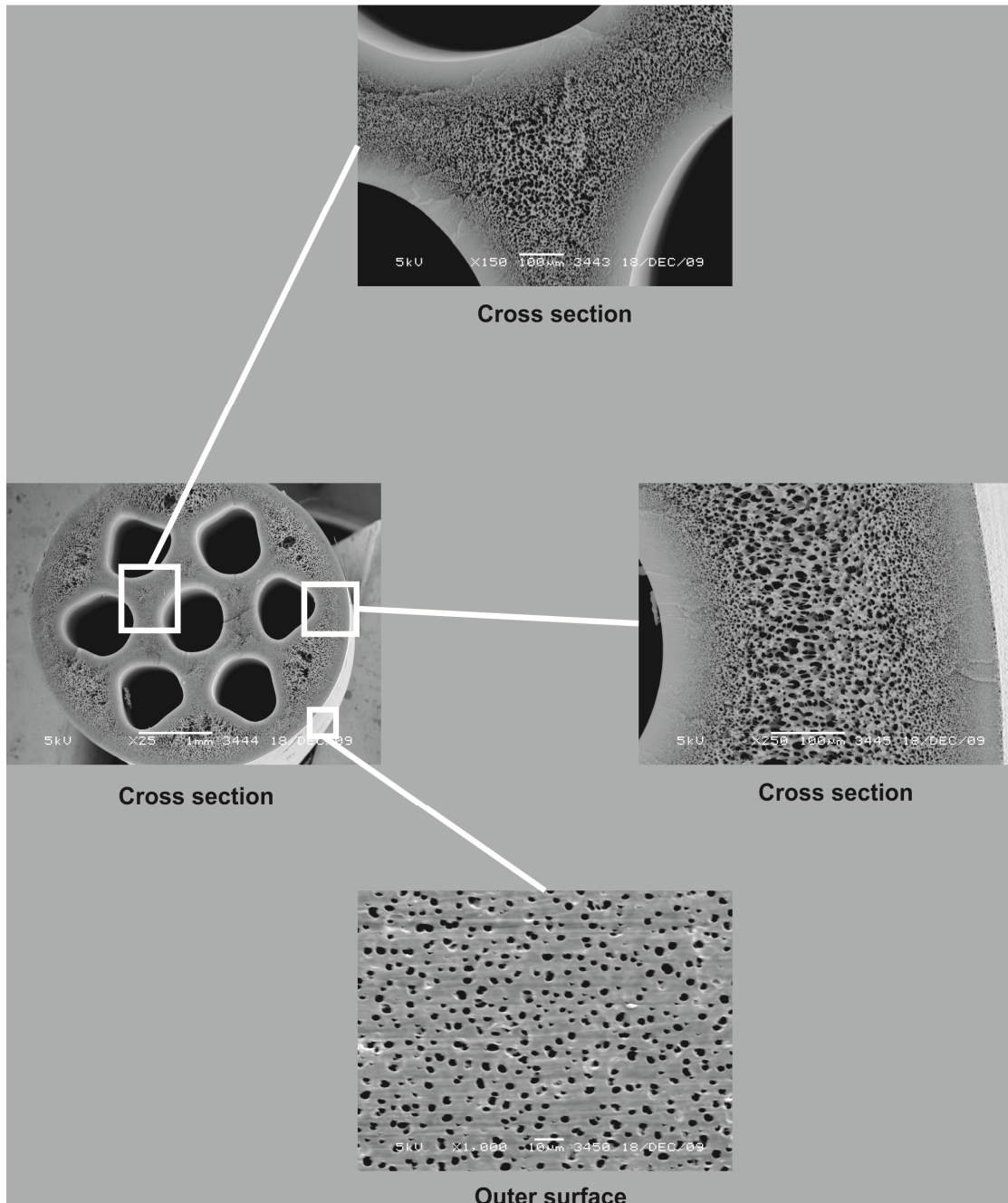


Figure 5. SEM images of multibore hollow fiber showing the symmetric arrangement of 7 bore in single fiber with open surface and porous support structure in-between

This arrangement significantly increases the mechanical stability of the interconnected porous structure. The cross sectional images also show that the membrane effective separation layer is present at the inner surface of the lumen supported by open porous support structure. The fiber surface images show that the pores on the outer surface of the hollow fiber are between 0.5 to 3 μm , so the fiber wall acts as a barrier and inhibits cell infiltration into the pores of the hollow fiber.

3.2.2 Clean water and medium permeation

Clean water transport through the fiber gives an indication of its porosity, pore connectivity and tortuosity. Figure 6 shows that the clean water flux at various trans-membrane pressures (0.1 – 0.25 bar) is linear with no compaction (several cycle of increasing and decreasing pressure flux were tested). The water permeance through the multibore HF is approximately 780 L / (m².h.bar) (calculated from the slope of the plot in Figure 6).

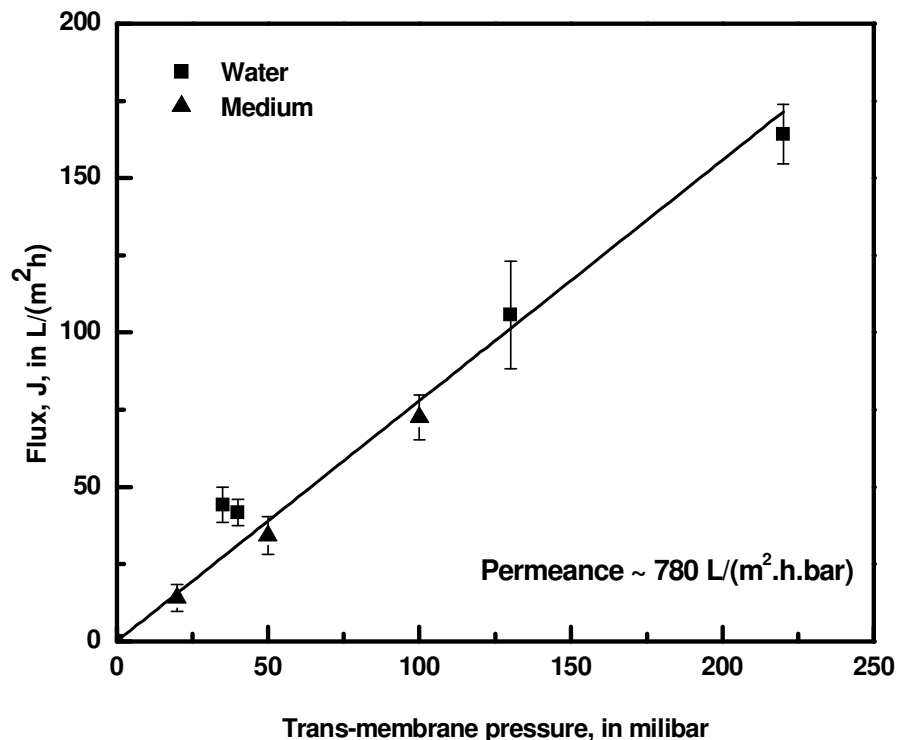


Figure 6. Flux of pure water and culture medium through multibore HF membrane with respect to applied trans-membrane pressure

For cell culturing, the fiber should deliver culture medium containing Fetal Bovine Serum (FBS) to the cells. FBS is a cocktail of 65% albumin (molecular weight ~ 66 kDa) and other small chain proteins [46, 47]. These proteins may negatively influence the medium permeation by fouling the HF. The maximum allowable pressure in a bioreactor system for tissue engineering application mimicking the physiological condition for cell culture is in between 0.1 to 0.15 bar corresponding to human diastolic and systolic blood pressure. Hence, we measured the medium permeation for trans-membrane pressure up to 0.1bar in sterile cross flow filtration set-up. The medium permeance of the multibore HF is almost identical to the clean water flux (~ 780 L/ (m².h.bar) see Figure 6). This illustrates that the pores of the hollow fiber do not foul by the medium proteins and medium transport is maintained. This result also suggests that the medium permeance through the multibore HF would be sufficient for multilayer tissue culture of approximately 10 layers of cells in confluence per unit active hollow fiber surface area at trans-membrane pressure of 0.05bar (calculated corresponding to the theoretical data for cell consumption [41, 48]). In fact, the medium permeated through the multibore HF at steady state was tested for C2C12 cells culture in (T-20) T-flask and the results were compared to cell culture with proliferation medium (positive control) and DMEM without FBS (negative control) to evaluate whether there is any difference in proliferation rate due to HF permeation. Figure 7 shows the light microscopic images of C2C12 cells cultured after 1 and 3 days with the respective media refreshed every alternate day. The images show that the proliferation of cells cultured with medium permeated through the HF after 15 and 60 minutes (Figure 7c and 7d) and standard proliferation medium (Figure 7a) is identical, proving that the fiber do not retain any valuable components of the medium. The rather lower cell proliferation with DMEM medium (without FBS, see Figure 7b) illustrates that FBS is essential for high C2C12 cell proliferation.

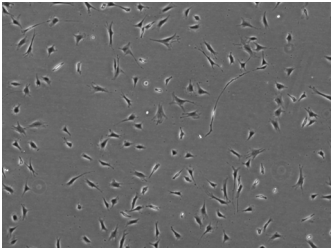
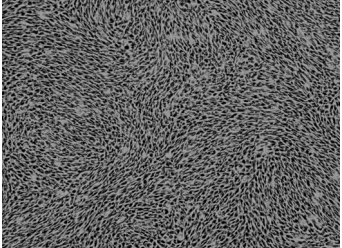
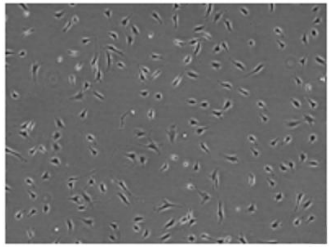
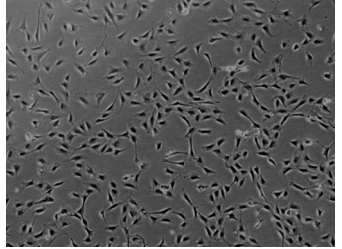
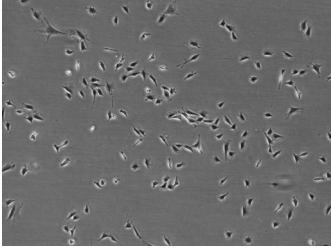
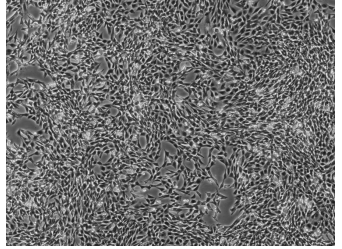
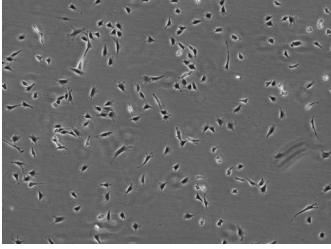
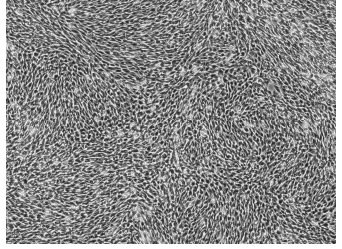
		1 day	3 days
(a)	DMEM + 10%FBS (Normal Medium)		
(b)	DMEM (No FBS)		
(c)	Medium filtered through HF (1st 15 min)		
(d)	Medium filtered through HF (After 60min)		

Figure 7. Light microscopic image of C2C12 cells cultured for 1 and 3 days with normal proliferation medium, DMEM (without FBS), and medium prefiltered through the multibore HF (seeding density – 3000 cells/cm²)

3.3 Bioreactor experiments

Perfusion bioreactor experiments were carried out with a construct containing approximately 8 layers of cell-ES sheet rolled around multibore HF module. For all bioreactor experiments the medium used in the reservoir was pre-conditioned by allowing medium gas exchange via pumping through gas permeable platinum cured silicon tubes built within temperature, CO₂ and humidity controlled incubator for at least 12 hours. During culturing, the medium was maintained with minimum glucose at $17\pm 0.5\text{mM}$ and maximum lactate at $6.5\pm 0.7\text{mM}$ concentration (compared to fresh medium concentration of $25.1\pm 0.4\text{mM}$ and $0.9\pm 0.3\text{mM}$ respectively) before refreshing in the reservoir for both static and dynamic culture to avoid the risk of recirculating toxic waste to the proliferating cells.

Two different configurations of medium flow through the bioreactor were assessed by carrying out cell culture experiments with medium flow through the multibore HF lumen and dual flow through the HF lumen and through the scaffold itself, see Figure 2). To compare with dynamic cultures, constructs were also cultured statically in T-flask as control.

Figure 8 shows the collaged (64 images, 10X magnification) fluorescent microscopic images of carefully unrolled ES sheet cultured under static (performed in T-flask) and dynamic (in the bioreactor, see Figure 2) conditions for 7 days and stained for cell viability (Live-dead assay, Invitrogen). The green colour in these images represents viable cells at different culture conditions.

For the statically cultured samples, cell proliferation varies largely within the outer and inner sheets (see Figure 8a). The outer sheet being directly in contact with medium has viable cells at the outer most edge whereas the cell number decreases as one looks towards the inner edge. The medium diffuses through the initial layers but probably the proliferating cells themselves become a barrier for medium diffusion, hence in the middle layers fewer cells are visible. Similar result with no viable cells can be observed at the outer edge of the inner sheet. Few viable cells at the innermost edge of the inner sheet (which is close to the fiber) are due to medium diffusion through the porous walls of the multibore HF (improves medium availability locally), which is in contact with the bulk medium. These results were also confirmed with staining the adherent cells using methylene blue and the cell distribution observed under light microscope. Most of the cells (stained blue) were located at outer most

(a) Static	Outermost edge	Outer sheet	Inner edge
	Outer edge	Inner sheet	Innermost edge
(b) HF perfusion	Outermost edge	Outer sheet	Inner edge
	Outer edge	Inner sheet	Innermost edge
(c) Dual flow perfusion	Outermost edge	Outer sheet	Inner edge
	Outer edge	Inner sheet	Innermost edge

Figure 8. *Fluorescent microscopic images of C2C12 cells stained with Live-dead assay, cultured under static and dynamic conditions for 7 days on MES construct. Each of these images is a collage of 64 images (2x32)*

edge of outer sheet (close to the medium) and innermost edge of the inner sheet (close to the HF) (see Figure 9a).

Images of constructs dynamically cultured with flow through multibore HF lumen samples show uniform cell proliferation on the inner sheet (that close to the HF, see Figure 8b), whereas viable cells on the outer sheet are mostly concentrated on the outermost edge (close to the medium). This may be due to irregular and slow refreshing of medium in the surface of the construct. Here, the medium permeated through the fiber may even experience channelling effect by which stagnant zones within the bioreactor/scaffold may be created influencing negatively the cell proliferation. These results were again confirmed with methylene blue stained images (Figure 9b). The intense blue stain observed at outermost edge of the outer sheet (close to the medium) and inner most edge of the inner sheet (close to the fiber) illustrates high cell proliferation. The gradient in dye intensity on the inner sheet (as we look from the centre to outer edge) suggests lower cell number in the inner sheet probably due to improper nutrient diffusion farther away from the permeating HF.

Finally, the images for the constructs cultured under dual flow show high cell proliferation on both inner and outer sheets. Higher intensity of green fluorescent colour indicates higher number of viable cells on both ES sheets. The flow through the scaffold via the side ports helps refreshing the medium around the construct and improves cell viability and proliferation on the outer sheet. This flow achieves uniform proliferation by refreshing the medium around the 3D construct (from outside) and conceals any channelling of HF permeated medium. The flow via the HF achieves uniform cell proliferation and distribution in the inner layer too. Methylene blue stained images of these samples (Figure 9c) show that the cells completely cover the surface of both the ES sheets and illustrate good cell culture environment across the multilayer 3D construct.

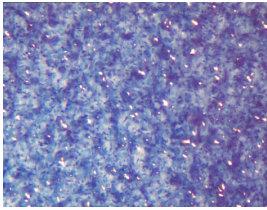
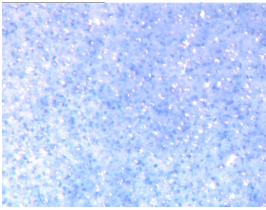
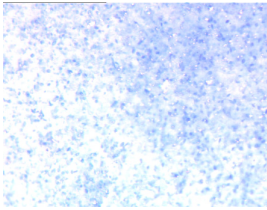
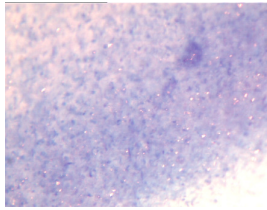
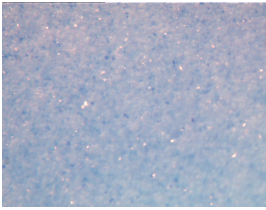
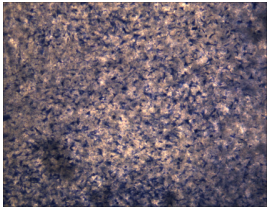
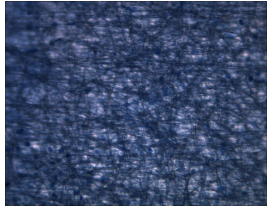
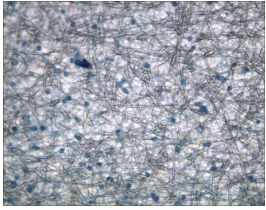
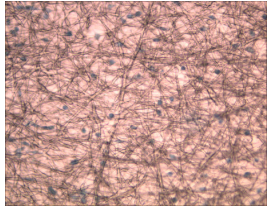
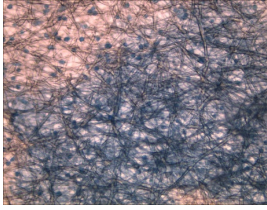
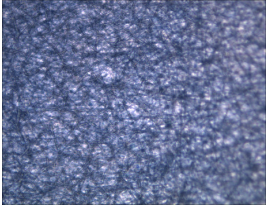
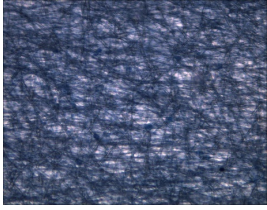
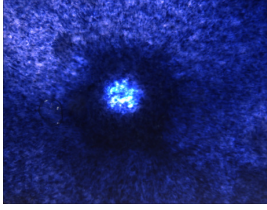
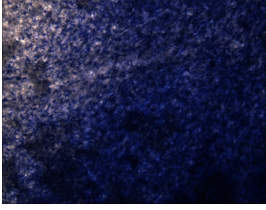
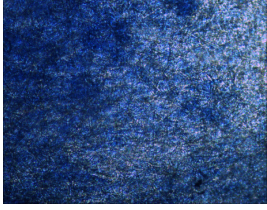
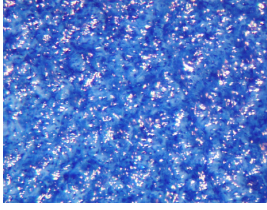
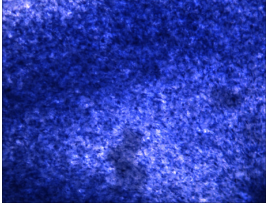
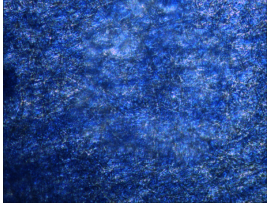
		Outer edge	Center	Inner edge
(a) Static	Outer sheet			
	Inner sheet			
(b) HF perfusion	Outer sheet			
	Inner sheet			
(c) Dual flow perfusion	Outer sheet			
	Inner sheet			

Figure 9. Light microscopic images of methylene blue stained C2C12 cells cultured under static and dynamic culture conditions for 7 days on MES construct (4x magnification)

Proliferation assay

The total DNA concentration (which corresponds to cell number) quantified over the rolled MES cultured for 7 days under static culture in petridish and dual flow dynamic culture in perfusion bioreactor is presented in Figure 10. An unrolled flat sheet was also cultured under static condition in petridish as positive control. To evaluate the cell distribution in different parts of the MES, each sheet (inner and outer) was cut in half and analysed separately using CyQuant Cell Proliferation Assay Kit. Therefore for each sheet, Figure 10 presents the DNA results (standard deviation of 5 different MES samples) of two pieces i.e. inner half and outer half sheet.

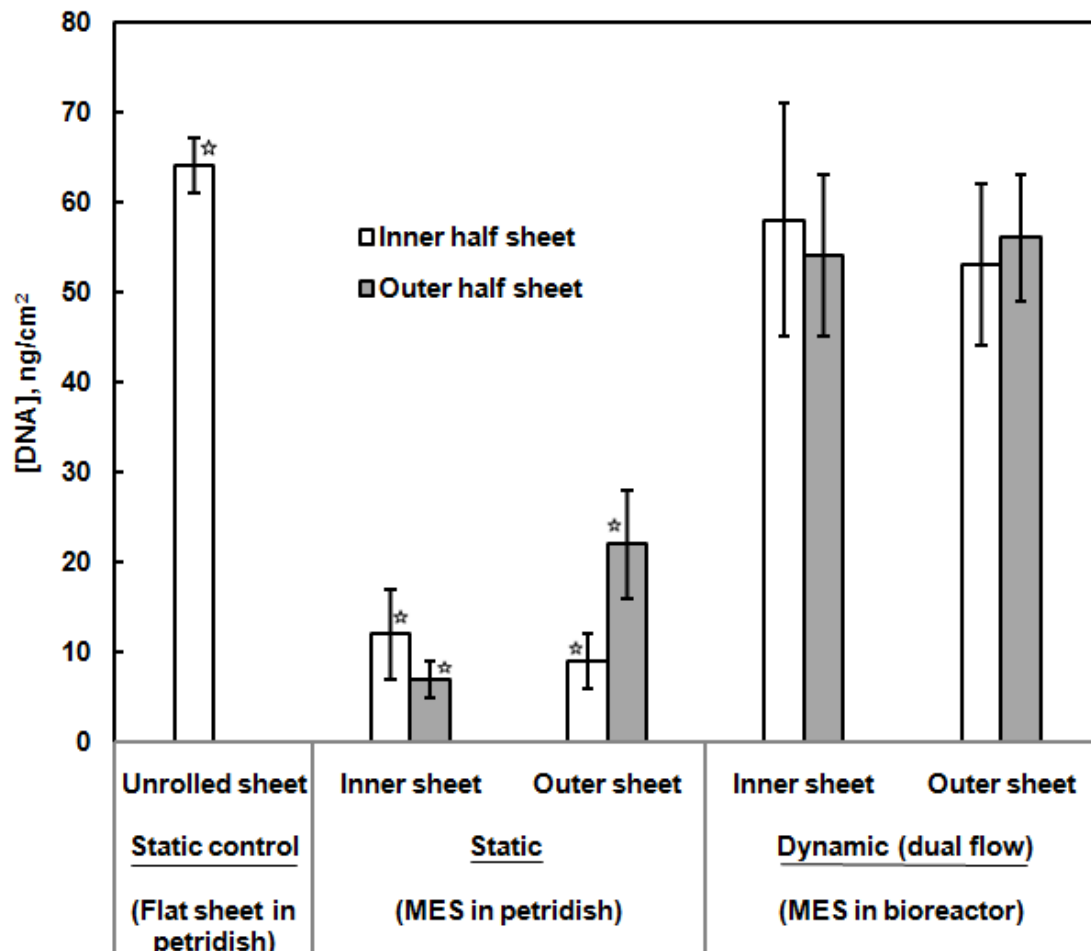


Figure 10. C2C12 cell proliferation within multilayer cell-ES sheet rolled on multibore HF module cultured statically and dynamically for 7 days. Control indicates the flat sheet (unrolled) sample cultured statically in petridish [\star = significant difference against control and statically cultured 3D construct ($p < 0.05$), error-bars indicate standard deviation]

For the unrolled ESP sheet cultured statically (positive control) the DNA values are high. In this case the cells cultured on the sheet are in direct contact with the medium and no oxygen or nutrient diffusion limitations occur. For the rolled MES construct cultured statically in the petridish, the DNA content is very low on both sheets (inner and outer sheet) in comparison to the unrolled positive control. This is due to nutrient and oxygen diffusion limitation in the MES construct. The outer sheet (that close to the medium) has higher DNA values than the inner sheet (consistent with the results of Figure 8, 9 presented earlier) showing that the proliferating cells in the outer layer act as barrier to medium or oxygen transport to the inner layer [49].

The results of the dynamic perfusion bioreactor show similar DNA content on all four parts of the ES sheets and comparable to the positive control. The medium perfusion via the HF enhances the nutrient diffusion through the multilayer construct from inside improving cell proliferation in the middle layers by convective diffusion of nutrients and oxygen. The flow from the side ports refreshes the medium around the multilayer construct and also influences the cell growth at the construct periphery. Overall, the DNA data for dynamic culture experiment proves once more that dual flow is the best option to achieve uniform cell growth across different layers of MES construct.

Cell migrations within MES construct

For the MES construct cultured in dual flow perfusion bioreactor, cell migration within multilayer ES sheets was studied by seeding pre-labeled C2C12 cells with 2 different lyophilic tracers CM-DiO – Green for the cells in the inner sheet and CM-DiI – red for the cells in the outer sheet. After culturing for 3 and 7 days, the samples were analysed using fluorescent microscopy. Images were made at corresponding excitation and emission filter wavelengths for each dye and finally merged to observe any cell overlapping, which would suggest cells migration.

Figure 11 presents a collage (7x7 or 49 images) of fluorescent images of MES construct in cross section and in section along the construct. Images of cells cultured for 3 days show distinct layers of red cells in the outer sheet and green cells in the inner sheet. (This assembly of 2 distinct dyed cells in different layers show the possibility of this model to incorporate

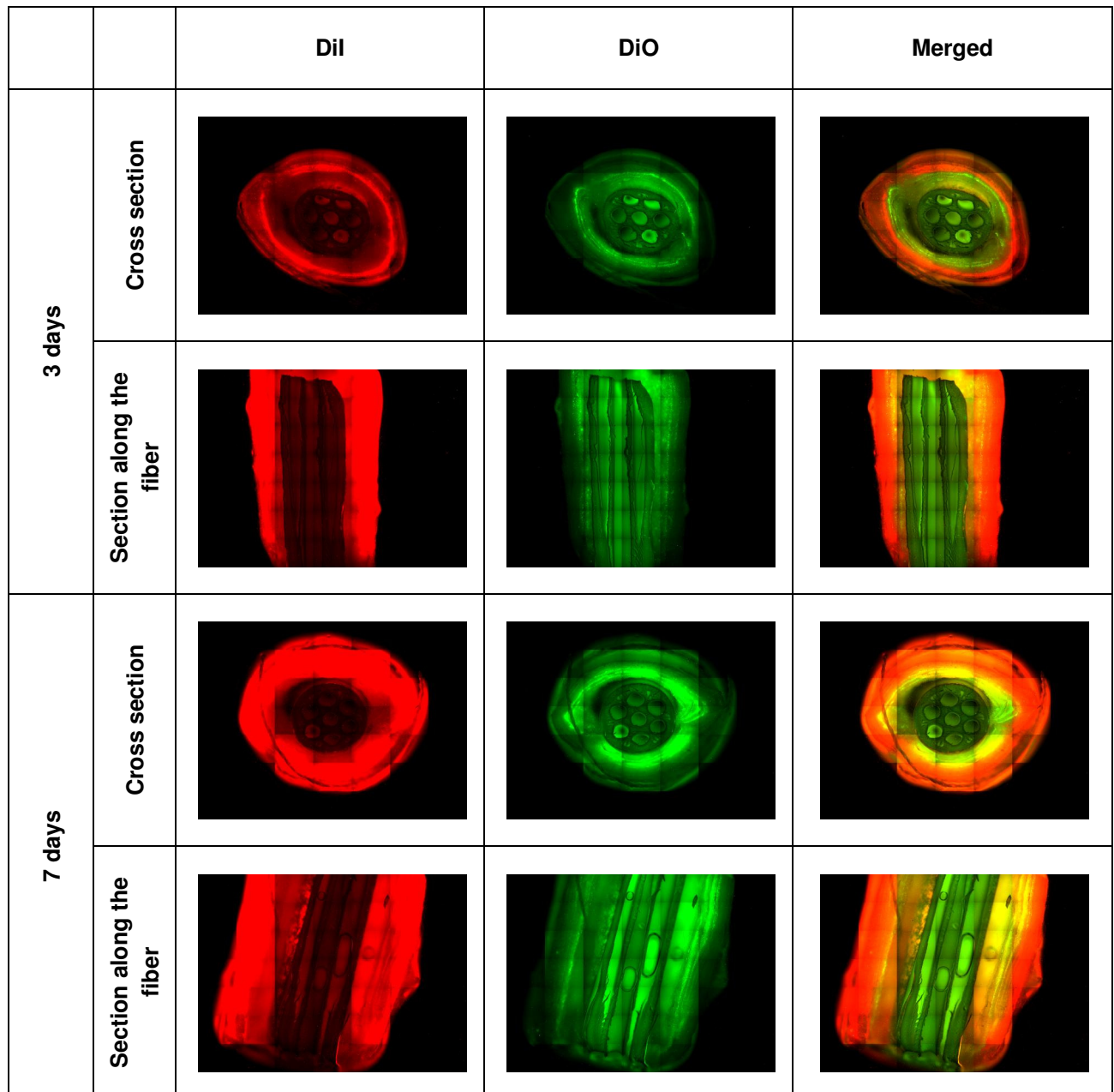


Figure 11. Fluorescent microscopic images of pre-labeled G2C12 cells cultured dynamically on MES in dual flow perfusion bioreactor for 3 and 7 days. Each of these images is a collage of 49 images (7x7). Yellow color in merged images is caused by overlapping of red and green labeled cells due to cell migration within the scaffold layers

multiple cell types in different layers. The thickness of each layer can be controlled by the length of the corresponding ES sheet). At 7 days, the images suggest migration of red-cells from the outer sheet to inner sheet illustrated by development of yellow colour when overlapping of red and green cells in merged image. This migration of cells within MES construct may be due to two reasons; (i) either small negative pressure difference is created

within the MES construct due to medium flowing through the multibore HF lumen or (ii) cell migration actually occurs towards the inner layer because of more refreshed medium available at fiber surface due to medium permeation. The pore size of ES sheet used in these experiments was approximately $30\pm 10\ \mu\text{m}$ which allows cell migration within the MES construct. Nonetheless, more experiments using different medium flow rates and medium concentration should be carried out to understand better the phenomena. Using different pore size sheets would give the flexibility to manipulate cell migration within layers and our concept could also be used to study cell- cell interaction in 3D environment.

Conclusion – Outlook

In this study a concept for developing multilayer ES scaffold and its culture in a perfusion bioreactor have been evaluated. The rolling of pre-seeded ES sheet to form multilayer constructs proposed in this work avoids the problem of cell infiltration and achieves uniform cell distribution in the scaffold. Static culture experiment showed that critical nutrient limitation occurs within the first 2 layers with the proliferating cells themselves acting as barrier for nutrient diffusion. The dynamic perfusion through the HF lumen and around the 3D scaffold led to massive cell proliferation with even cell distribution across the layers.

This concept can also be a useful tool for engineering tissues with complex cell architecture for in-vitro cell-cell and cell-substrate interaction studies. In fact, our future work will focus on development of specific multilayer tissues such as blood vessels using the proposed concept.

4 Acknowledgements

The authors would like to acknowledge the financial support from Technology Foundation STW (Project number – TKG. 6716). We also thank J.B. Bennink for assistance with the artwork.

Abbreviations

3D	-	3 dimensional
CM-DiI	-	1,1'-dioctadecyl -- 3,3',3'-tetramethylindocarbocyanine per chlorate
CM-DiO	-	3,3'-dioctadecyloxacarbocyanine per chlorate
D-MEM	-	Dulbecco's Modified Eagle's Medium
DNA	-	Deoxyribonucleic acid
ECM	-	Extra cellular matrix
ES	-	Electro spun sheet or mesh
ESP	-	Electro spinning process
FBS	-	Fetal Bovine Serum
HF	-	Hollow fiber
MES	-	Multilayer cell-electrospun construct
PBS	-	Phosphate buffer solution (pH=7.3)
PBT	-	Poly(butylene terephthalate)
PCL	-	Poly(caprolactone)
PEOT	-	Poly(ethylene glycol terephthalate)
PLLA	-	Poly (L lactic acid)
SEM	-	Scanning electron microscope

References

- [1] S. Baiguera, M.A. Birchall, P. MacChiarini, Tissue-engineered tracheal transplantation, *Transplantation*, 89 (2010) 485-491.
- [2] C. Brayfield, K. Marra, J.P. Rubin, Adipose stem cells for soft tissue regeneration, *Handchirurgie, Mikrochirurgie, plastische Chirurgie : Organ der Deutschsprachigen Arbeitsgemeinschaft für Handchirurgie : Organ der Deutschsprachigen Arbeitsgemeinschaft für Mikrochirurgie der Peripheren Nerven und Gefäße : Organ der Vereinigung der Deutschen Plastischen Chirurgen*, 42 (2010) 124-128.
- [3] L. Peterson, T. Minas, M. Brittberg, A. Nilsson, E. Sjögren-Jansson, A. Lindahl, Two-to 9-year outcome after autologous chondrocyte transplantation of the knee, *Clinical Orthopaedics and Related Research*, (2000) 212-234.
- [4] F.G. Sala, S.M. Kunisaki, E.R. Ochoa, J. Vacanti, T.C. Grikscheit, Tissue-Engineered Small Intestine and Stomach Form from Autologous Tissue in a Preclinical Large Animal Model, *Journal of Surgical Research*, 156 (2009) 205-212.
- [5] W. Zhang, H. Abukawa, M.J. Troulis, L.B. Kaban, J.P. Vacanti, P.C. Yelick, Tissue engineered hybrid tooth-bone constructs, *Methods*, 47 (2009) 122-128.
- [6] S. Fukuhara, S. Tomita, S. Yamashiro, T. Morisaki, C. Yutani, S. Kitamura, T. Nakatani, F.W. Sellke, H.M. Spotnitz, M. Scorsin, M.J.H. Hendrikx, Direct cell-cell interaction of cardiomyocytes is key for bone marrow stromal cells to go into cardiac lineage in vitro, *Journal of Thoracic and Cardiovascular Surgery*, 125 (2003) 1470-1480.
- [7] H.K. Kleinman, D. Philp, M.P. Hoffman, Role of the extracellular matrix in morphogenesis, *Current Opinion in Biotechnology*, 14 (2003) 526-532.
- [8] A. Stahl, A. Wenger, H. Weber, G.B. Stark, H.G. Augustin, G. Finkenzeller, Bi-directional cell contact-dependent regulation of gene expression between endothelial cells and osteoblasts in a three-dimensional spheroidal coculture model, *Biochemical and Biophysical Research Communications*, 322 (2004) 684-692.
- [9] A.S. Goldstein, G. Christ, Functional tissue engineering requires bioreactor strategies, *Tissue Engineering - Part A*, 15 (2009) 739-740.
- [10] I. Martin, D. Wendt, M. Heberer, The role of bioreactors in tissue engineering, *Trends in Biotechnology*, 22 (2004) 80-86.
- [11] D. Wendt, S.A. Riboldi, M. Cioffi, I. Martin, Potential and bottlenecks of bioreactors in 3D cell culture and tissue manufacturing, *Advanced Materials*, 21 (2009) 3352-3367.
- [12] M.M. Stevens, J.H. George, Exploring and engineering the cell surface interface, *Science*, 310 (2005) 1135-1138.
- [13] G.E. Wnek, M.E. Carr, D.G. Simpson, G.L. Bowlin, Electrospinning of nanofiber fibrinogen structures, *Nano Letters*, 3 (2003) 213-216.

- [14] Q.P. Pham, U. Sharma, A.G. Mikos, Electrospinning of polymeric nanofibers for tissue engineering applications: A review, *Tissue Engineering*, 12 (2006) 1197-1211.
- [15] D.H. Reneker, A. Yarin, E. Zussman, S. Koombhongse, W. Kataphinan, Nanofiber manufacturing: Toward better process control, in, 2006, pp. 7-20.
- [16] S.A. Theron, E. Zussman, A.L. Yarin, Experimental investigation of the governing parameters in the electrospinning of polymer solutions, *Polymer*, 45 (2004) 2017-2030.
- [17] K. Tuzlakoglu, N. Bolgen, A.J. Salgado, M.E. Gomes, E. Piskin, R.L. Reis, Nano- and micro-fiber combined scaffolds: A new architecture for bone tissue engineering, *Journal of Materials Science: Materials in Medicine*, 16 (2005) 1099-1104.
- [18] E. Zussman, A. Theron, A.L. Yarin, Formation of nanofiber crossbars in electrospinning, *Applied Physics Letters*, 82 (2003) 973-975.
- [19] N.M. Neves, R. Campos, A. Pedro, J. Cunha, F. Macedo, R.L. Reis, Patterned nanofiber meshes for biomedical applications, in, 2006, pp. 155-158.
- [20] Q.P. Pham, U. Sharma, A.G. Mikos, Electrospun poly(ϵ -caprolactone) microfiber and multilayer nanofiber/microfiber scaffolds: Characterization of scaffolds and measurement of cellular infiltration, *Biomacromolecules*, 7 (2006) 2796-2805.
- [21] A. Frenot, I.S. Chronakis, Polymer nanofibers assembled by electrospinning, *Current Opinion in Colloid and Interface Science*, 8 (2003) 64-75.
- [22] Z.M. Huang, Y.Z. Zhang, M. Kotaki, S. Ramakrishna, A review on polymer nanofibers by electrospinning and their applications in nanocomposites, *Composites Science and Technology*, 63 (2003) 2223-2253.
- [23] D.H. Reneker, A.L. Yarin, E. Zussman, H. Xu, Electrospinning of Nanofibers from Polymer Solutions and Melts, in, 2007, pp. 43-195,345-346.
- [24] S.J. Lee, S.H. Oh, J. Liu, S. Soker, A. Atala, J.J. Yoo, The use of thermal treatments to enhance the mechanical properties of electrospun poly(ϵ -caprolactone) scaffolds, *Biomaterials*, 29 (2008) 1422-1430.
- [25] L. Moroni, R. Licht, J. de Boer, J.R. de Wijn, C.A. van Blitterswijk, Fiber diameter and texture of electrospun PEOT/PBT scaffolds influence human mesenchymal stem cell proliferation and morphology, and the release of incorporated compounds, *Biomaterials*, 27 (2006) 4911-4922.
- [26] E.D. Boland, J.A. Matthews, K.J. Pawlowski, D.G. Simpson, G.E. Wnek, G.L. Bowlin, Electrospinning collagen and elastin: Preliminary vascular tissue engineering, *Frontiers in Bioscience*, 9 (2004) 1422-1432.
- [27] J.A. Matthews, G.E. Wnek, D.G. Simpson, G.L. Bowlin, Electrospinning of collagen nanofibers, *Biomacromolecules*, 3 (2002) 232-238.

- [28] R.J. Koch, G.K. Gorti, Tissue engineering with chondrocytes, *Facial Plastic Surgery*, 18 (2002) 59-68.
- [29] M.L.P. Langelaan, K.J.M. Boonen, R.B. Polak, F.P.T. Baaijens, M.J. Post, D.W.J. van der Schaft, Meet the new meat: tissue engineered skeletal muscle, *Trends in Food Science and Technology*, 21 (2010) 59-66.
- [30] J. Li, R. Shi, Fabrication of patterned multi-walled poly-l-lactic acid conduits for nerve regeneration, *Journal of Neuroscience Methods*, 165 (2007) 257-264.
- [31] T.B.F. Woodfield, C.A. Van Blitterswijk, J. De Wijn, T.J. Sims, A.P. Hollander, J. Riesle, Polymer scaffolds fabricated with pore-size gradients as a model for studying the zonal organization within tissue-engineered cartilage constructs, *Tissue Engineering*, 11 (2005) 1297-1311.
- [32] Y.M. Ju, J.S. Choi, A. Atala, J.J. Yoo, S.J. Lee, Bilayered scaffold for engineering cellularized blood vessels, *Biomaterials*, 31 (2010) 4313-4321.
- [33] C.M. Vaz, S. van Tuijl, C.V.C. Bouten, F.P.T. Baaijens, Design of scaffolds for blood vessel tissue engineering using a multi-layering electrospinning technique, *Acta Biomaterialia*, 1 (2005) 575-582.
- [34] X. Yang, J.D. Shah, H. Wang, Nanofiber enabled layer-by-layer approach toward three-dimensional tissue formation, *Tissue Engineering - Part A*, 15 (2009) 945-956.
- [35] M. Pei, L.A. Solchaga, J. Seidel, L. Zeng, G. Vunjak-Novakovic, A.I. Caplan, L.E. Freed, Bioreactors mediate the effectiveness of tissue engineering scaffolds, *The FASEB journal : official publication of the Federation of American Societies for Experimental Biology*, 16 (2002) 1691-1694.
- [36] B. Porter, R. Zauel, H. Stockman, R. Guldberg, D. Fyhrie, 3-D computational modeling of media flow through scaffolds in a perfusion bioreactor, *Journal of Biomechanics*, 38 (2005) 543-549.
- [37] F.W. Janssen, J. Oostra, A. Van Oorschot, C.A. Van Blitterswijk, A perfusion bioreactor system capable of producing clinically relevant volumes of tissue-engineered bone: In vivo bone formation showing proof of concept, *Biomaterials*, 27 (2006) 315-323.
- [38] F.W. Janssen, R. Van Dijkhuizen-Radersma, A. Van Oorschot, J. Oostra, J.D. De Bruijn, C.A. Van Blitterswijk, Human tissue-engineered bone produced in clinically relevant amounts using a semi-automated perfusion bioreactor system: A preliminary study, *Journal of Tissue Engineering and Regenerative Medicine*, 4 (2010) 12-24.
- [39] N.S. Abdullah, D.B. Das, Modelling nutrient transport in hollow fibre membrane bioreactor for growing bone tissue with consideration of multi-component interactions, *Chemical Engineering Science*, 62 (2007) 5821-5839.
- [40] L. De Bartolo, S. Salerno, E. Curcio, A. Piscioneri, M. Rende, S. Morelli, F. Tasselli, A. Bader, E. Drioli, Human hepatocyte functions in a crossed hollow fiber membrane bioreactor, *Biomaterials*, 30 (2009) 2531-2543.

- [41] H. Ye, D.B. Das, J.T. Triffitt, Z. Cui, Modelling nutrient transport in hollow fibre membrane bioreactors for growing three-dimensional bone tissue, *Journal of Membrane Science*, 272 (2006) 169-178.
- [42] D.F. Stamatialis, B.J. Papenburg, M. Girones, S. Saiful, S.N.M. Bettahalli, S. Schmitmeier, M. Wessling, Medical applications of membranes: Drug delivery, artificial organs and tissue engineering, *Journal of Membrane Science*, 308 (2008) 1-34.
- [43] L. De Bartolo, S. Morelli, M. Rende, C. Campana, S. Salerno, N. Quintiero, E. Drioli, Human hepatocyte morphology and functions in a multibore fiber bioreactor, *Macromolecular Bioscience*, 7 (2007) 671-680.
- [44] M.J. Ellis, J.B. Chaudhuri, Poly(lactic-co-glycolic acid) hollow fibre membranes for use as a tissue engineering scaffold, *Biotechnology and Bioengineering*, 96 (2007) 177-187.
- [45] L. Ni, Q. Xiao-Hong, L. Ling, W. Shan-Yuan, The effects of spinning conditions on the morphology of electrospun jet and nonwoven membrane, *Polymer Engineering & Science*, 48 (2008) 2362-2366.
- [46] H. Baker, B. DeAngelis, O. Frank, Vitamins and other metabolites in various sera commonly used for cell culturing, *Cellular and Molecular Life Sciences*, 44 (1988) 1007-1010.
- [47] X. Zheng, H. Baker, W.S. Hancock, F. Fawaz, M. McCaman, E. Pungor, Proteomic Analysis for the Assessment of Different Lots of Fetal Bovine Serum as a Raw Material for Cell Culture. Part IV. Application of Proteomics to the Manufacture of Biological Drugs, *Biotechnology Progress*, 22 (2006) 1294-1300.
- [48] N.S. Abdullah, D.B. Das, H. Ye, Z.F. Cui, 3D bone tissue growth in hollow fibre membrane bioreactor: Implications of various process parameters on tissue nutrition, *International Journal of Artificial Organs*, 29 (2006) 841-851.
- [49] B.J. Papenburg, J. Liu, G.A. Higuera, A.M.C. Barradas, J. de Boer, C.A. van Blitterswijk, M. Wessling, D. Stamatialis, Development and analysis of multi-layer scaffolds for tissue engineering, *Biomaterials*, 30 (2009) 6228-6239.

Chapter 5

Microstructured fibers for improving cell seeding and cell attachment in tissue engineering scaffolds

N.M.S. Bettahalli ¹, I.T.M. Arkesteijn ¹, M. Wessling ^{1,2}, D. Stamatialis ^{1,*}

MIRA Institute for Biomedical Technology and Technical Medicine, University of Twente

¹ Membrane Technology Group, Faculty of Science and Technology, PO Box 217, 7500 AE Enschede, The Netherlands.

² RWTH Aachen University, Chemische Verfahren Technik (CVT), 52064 Aachen, Germany

Men will not be content to manufacture life; they will want to improve on it.

(J.D. Bernal)

Abstract

The seeding of cells onto biocompatible and/or biodegradable scaffolds is a determinant step in the formation of in-vitro engineered tissues. Fast, efficient and spatially uniform cell seeding can improve the clinical potential of engineered tissue. One way to approach the cell seeding or adhesion requirements is through surface modification of traditional scaffold. 3D solid free form fabrication is one of the widely used scaffold fabrication technique today, due to its flexibility towards fabrication of scaffold with various porosity, 3D architecture and mechanical property by polymer/fiber deposition. An example for such scaffold production for tissue engineering is rapid prototyping or round fiber deposition technology.

In this present study, the fiber surface has been altered by incorporating grooves or channels by extruding through (precise through etched) silicon wafer inserts. Novel straight channel corrugated fibers of biodegradable polymer Poly (ethylene oxide) terephthalate-co-(butylene) terephthalate (300PEGT55PBT45) with 6 and 10 grooves on the fiber surface are compared with round fibers. Their efficiency towards mouse pre-myoblast (C2C12) cell adhesion or seeding and proliferation in static and dynamic culture conditions are evaluated by SEM, staining and DNA quantification. Seven days culture static and dynamic experiments showed that the DNA content in the corrugated fiber is almost double compared to round fiber. Under dynamic conditions the cells on the corrugated fibers seem to experience lower shear force and therefore adhere better than on the round fibers. This study suggests that the surface structure and curvature of the fiber plays a critical role influencing cell adhesion and proliferation and can be used as a tool to produce better scaffolds for tissue engineering.

1 Introduction

Tissue engineering techniques have been proposed for the functional repair of injured or degenerated tissue. A commonly used strategy for in-vitro generation of engineered tissue constructs typically starts with the attachment of isolated cells into three-dimensional (3D) porous scaffold. This stage is commonly referred as 'cell seeding'. The requirements for successful cell seeding include high efficiency, fast attachment of cells to scaffolds, high cell density and uniform spatial distribution of cells throughout the scaffold volume. Depending on the engineered tissue of interest the cells seeded is more or less fixed but scaffold design or surface morphology and seeding method can be altered to increase seeding efficiency.

In general, two methods of seeding cells into biomaterial scaffold are applied in tissue engineering: statically and dynamically. The static method may lead to highly efficient cell seeding and high cell viability, where freely suspended or encapsulated cells and scaffolds are brought into direct contact and allowed to sit, relatively undisturbed, with the intention of cellular attachment and migration into the scaffolds [1]. However, in relevance to large scale production, conventional static seeding of cells is very time consuming [2]. Furthermore, if the scaffold thickness exceeds 2mm, static seeding does not provide a high seeding efficiency or a homogenous cell distribution throughout the scaffolds [3]. Dynamic seeding, wherein medium flows under oscillatory pressures is used to mimic the desired arterial flow environment, provide a tool to achieve a higher seeding efficiency and a more homogeneous distribution of cells [4, 5] using either spinner flasks [6], flow seeding [7], or hydrodynamic loading [8]. This method has produced favorable results, but two potential weaknesses of the technique include the amount of time required for seeding (typically 24 h) and the fact that it is less efficient at low cell concentrations [6, 8].

Further, scaffold fabrication by rapid prototyping techniques has recently attracted more and more interest for applications in tissue engineering as powerful tools. These scaffolds are built layer by layer, through material deposition on a stage, having a defined structure and architecture to a customized shape using CAD-CAM techniques. This flexibility and versatility in creating scaffolds gives the opportunity to use rapid prototyping devices to generate improved scaffolds and to study the influence of different structural phenomena on tissue reconstruction. Among these devices 3D plotting [9, 10] and 3D fiber deposition (3DF) [11] has been recently developed and used for tissue engineering purposes, the latter being a

system for the extrusion of highly viscous polymers. 3DF is a fused deposition technique in which molten polymer is extruded through needle to form round fiber and deposited from a XYZ-axis motor driven syringe on a stationary stage by applying pressure [12, 13].

3DF scaffolds may vary in their composition depending on its final application for soft or hard tissue growth (polymer material, porosity or size), but the desirability of having high density cell adhesion to the scaffold material is a common goal. It is widely accepted that the efficiency and the spatial distribution of cell attachment to scaffolds during cell seeding influence the growth rate of tissue constructs. Cell density in turn impacts the kinetics of cell proliferation and extracellular matrix deposition, which increases construct functionality by tissue ingrowth. Hence surface topography of the scaffold plays an important role in cell adhesion. Cells on 3DF scaffold experience smooth and round fiber surface with certain angle of curvature dependent on fiber diameter which has negative effect for cell adhesion. Further due to smooth fiber surface the anchorage of the cell layer is weak and de-lamination occurs in dynamic culture conditions. To overcome this effect various surface modifications such as surface etching by plasma treatment [14], cell adhering protein coating [15], cell encapsulation [16], polymer surface functionalization etc.

This study investigates the effect of corrugations (grooves or channels) on the fiber surface with respect to cell seeding and cell proliferation. The corrugated fiber has higher surface area per unit volume and may also influence cell alignment or orientation [17]. Corrugated fibers with 6 and 10 channels running along the longitudinal axis and symmetrical over the axis of the fiber were fabricated. Individual strands of round (with different fiber diameter) and corrugated fibers were extruded and subjected to investigation for static seeding and subsequent cell culturing in static and dynamic culture conditions for up to 7days. Especially the effect of shear force acting on the proliferating cells in dynamic cell culturing was tested. The change in mechanical property of corrugated fibers with respect to round fibers is also measured.

2 Materials and Methods

2.1 Material

For this study Poly(ethylene glycol terephthalate)-poly(butylene terephthalate) (PEGT/PBT) block co-polymers was used, kindly provided by Prof. Dr. C.A. van Blitterswijk, Tissue Regeneration (TR) group, University of Twente, The Netherlands. Their chemical composition is represented by the notation aPEGTbPBTC, where a is the molecular weight of the starting poly(ethylene glycol) PEG segments used in the polymerization process, while b and c refer to the weight ratio between PEGT and PBT blocks, respectively. For this study, 300PEGT55PBT45 co-polymer was used due to their high mechanical stability, low swelling, good cell adhesion and suitability for tissue formation [18].

2.2 Corrugated fiber extrusion process

Corrugated and round fibers were fabricated using a Bioplotter device (Envisiontec GmbH, Germany), which is a XYZ plotter scaffold construction device [9, 11, 13, 19]. Few modifications were made before this device was used to extrude highly viscoelastic fibers. Briefly, Figure 1 illustrates the fiber extrusion process, wherein polymer granules were loaded in a stainless steel syringe and heated at a temperature T (180°-200°C), using a cartridge heating unit mounted on the device. When the polymer melted, a nitrogen pressure (P = 3bar) was applied to the syringe. Nitrogen was used in order to minimize the copolymer oxidation. The nozzle used to extrude round and corrugated fibers were made of silicon wafer (through etching technique) known as inserts [20, 21]. These inserts were placed in special insert holder connected to the syringe containing the molten polymer. The polymer was extruded as a fiber/filament into an ethanol bath kept at approximately -6°C with zero air gap, to immediately cool down. In this way the fiber retains its shape after extruded through the inserts.



Figure 1. Schematic of fiber extrusion set-up (blow-up shows silicon insert holder and various silicon inserts)

Gas Plasma (GP) treatment

For GP treatment fibers were placed on a glass plate which was placed inside the plasma chamber or radiofrequency glow discharge chamber. A vacuum was applied to the chamber (0.01 mbar), which was then four times flushed with argon (purity $\geq 99.999\%$). The fibers were treated under argon plasma (0.1–0.2mbar) for 10 min. After cooling the fibers were turned around and again treated for 10 min as explained above.

2.3 Characterization of fibers – *Round and Corrugated*

2.3.1 Scanning electron microscopy (SEM) sample preparation

SEM images of dry fibers were obtained using JOEL 5600LV scanning electron microscope at accelerating voltage of 5kV. Fibers dried in vacuum oven at 30C overnight were directly used for surface scan. For cross sectional observation samples were carefully fractured in liquid nitrogen. All the samples were sputtered with gold (~15 to 20 nm-thick, Balzer-Union SCD-040). Morphology and shrinkage, if any, were investigated using cross sectional images of the fiber.

2.3.2 Mechanical evaluation

The mechanical properties of fibers were measured using a tensile testing machine (Zwick, Static Material Prufung unit). The testing of fibers was carried out using an ISO standard specified for cylinders (ASTM D882-91). A dry 50mm long strand of fiber was clamped vertically between two holders of the Zwick test machine (Z020) separated by 25mm apart. 500N load cell was used to apply constant pressure on the hollow fiber elongated at a constant rate of 500mm/min until break point. The data presented here is an average of 5 difference samples. The E-modulus of the fiber is measured using the slope at the initial part of the stress strain curve. The maximum stress, stress at break and strain at break are noted from the stress - strain curve obtained correspondingly.

2.4 Cell culture and Analysis

2.4.1 Cell seeding and growth on fibers

Fiber conditioning: Gas plasma treated fibers subjected to analysis were cut 4cm long and sterilized in excess of 70% ethanol and iso-propanol, which were completely evaporated inside sterile flow-hood. Dried fibers were washed 3 times with PBS and finally neutralized in proliferation medium for hydration and serum protein adsorption prior to cell seeding. Six duplicates of each fiber type were kept separately inside the non treated 6 well plate culture plates for cell seeding.

Cell expansion: Mouse pre-myoblast, C2C12 cells were cultured in proliferation medium containing Dulbecco's Modified Eagle's Medium (D-MEM, Gibco) supplemented with 10% fetal bovine serum (FBS, Cambrex), 100 U/ml penicillin (Gibco) and 100 µg/ml streptomycin (Gibco). Cells were initially plated in T-flask for expansion at 2000 cells/cm² until they reached 70-80% confluence, after which they were trypsinized using 0.05% Trypsin contained in 1mM EDTA. Thus obtained C2C12 cells were subsequently seeded on to the outer surface of the fiber at 2×10^6 cells / well. The cells were allowed to attach for 6 hours before further use in static or dynamic culture conditions.

2.4.1.1 Static culture conditions

C2C12 cell seeded fiber samples were cultured in non treated petri dishes for 0, 3 and 7 days at 37°C in a humidified 5% CO₂ incubator. The proliferation medium was exchanged every alternate day. The resulting statically cultured samples were subjected to SEM and histological analysis after fixation.

2.4.1.2 Dynamic culture conditions

Dynamic culture condition was attained by placing the petri dishes containing fiber-cell samples on a XYZ axis movement shaker, which was kept inside a temperature controlled (37°C) humidified 5% CO₂ incubator. Experiments were carried out at different speed 2, 10, 15 rpm to compare the effect of shear force created by shaken/rotating culture medium within the petri dish. Proliferation medium was exchanged every alternate day and the resulting dynamic cultured samples after 3 and 7 days were subjected to further analysis.

2.4.2 Fiber-cell sample analysis

2.4.2.1 Critical point dried sample for SEM

Samples for SEM were washed with PBS to remove culture medium prior to fixation by incubating with freshly prepared 4% paraformaldehyde (Merck) for at least 1hr and again washed with PBS. Further the samples were dehydrated in 50%, 70%, 80%, 90%, 98% and 100% ethanol for 2hr each step. Dehydration in 100% ethanol was performed for two additional times to remove all the water. Dehydrated samples were critical point dried from liquid carbon-di-oxide using a Blazers CPD 030 Critical Point Drier. SEM images were taken as described above.

2.4.2.2 Fixation and staining for light microscopy

Samples were washed with PBS before incubating with freshly prepared 4% paraformaldehyde (Merck) for at least 1hr for fixation of cells and finally washed with de-mineralized water before staining. After fixation the C2C12 cultured samples were immediately stained with methylene blue for approximately 5 min, the samples were washed several times with de-mineralized water until the aspirated water run out clear. The resulting stained samples were kept hydrated in water until further use for light microscopy analysis.

2.4.2.3 Cell proliferation assay

The concentration of DNA per sample (at different culture time 1, 3 and 7days) was accounted to be an indication for cell proliferation. The samples to be assayed were washed with PBS and stored at -85°C for at least 1 day. The samples before subjecting to DNA assay were allowed to attain room temperature and sliced to small pieces and immersed in small quantity (0.5ml) of cell lysis buffer. Quantification of total DNA concentration per sample was measured according to the manufacturer's protocol (CyQuant Cell Proliferation Assay Kit, Invitrogen/Molecular probes) using a fluorescent plate reader (Perkin Elmer).

3 Results and discussion

3.1 Corrugated and round fiber extrusion

Corrugated fibers were uniquely designed with 6 and 10 symmetric channels running along the longitudinal axis of the fiber. Figure 1 show the insert design used to extrude corrugated and round fiber along with schematic illustration of the setup and insert holder. When the molten polymer leaves through the insert holder, extruded fiber takes the shape of the annular space/design of the silicon insert before it solidifies in ethanol bath kept at around -6°C. Both corrugated with 6 or 10 corrugations (indicated as C-6, C-10) and round fibers with different outer diameter ranging from 0.6 mm till 1.2 mm (indicated as R-0.6, R-0.8, R-1.0, and R-1.2, see Figure 1) were extruded through silicon inserts.

Figure 2 shows the SEM images of different fibers extruded. The channels were engraved on a fiber with 0.2mm arm length and 0.8mm outer diameter, which could directly be compared

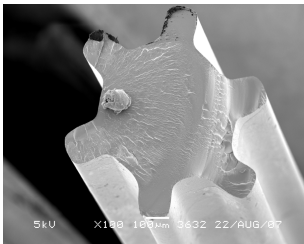
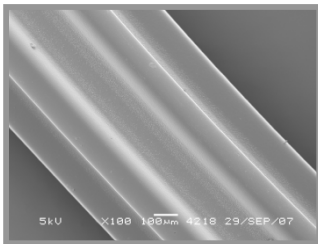
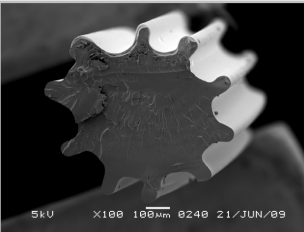
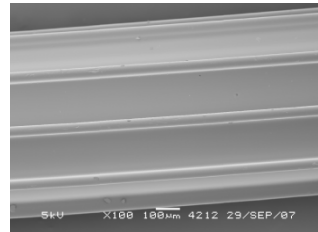
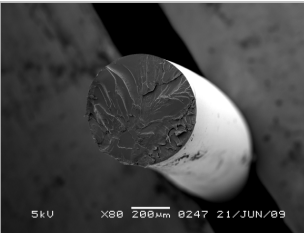
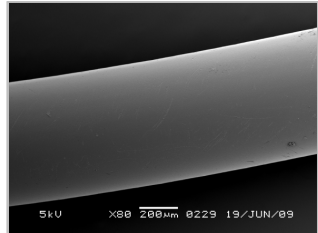
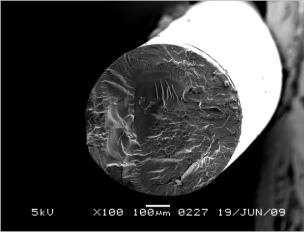
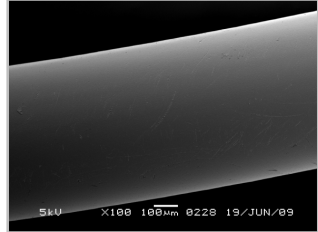
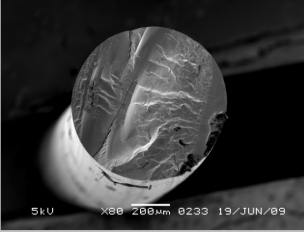
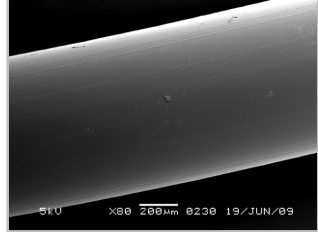
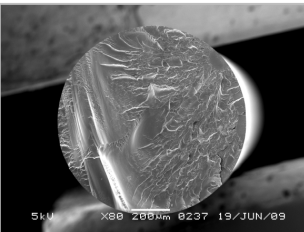
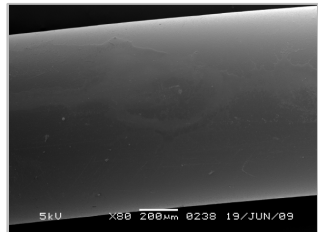
Type	Cross section	Surface
C - 6	 <p>5kV X100 100µm 3632 22/AUG/07</p>	 <p>5kV X100 100µm 4218 29/SEP/07</p>
C - 10	 <p>5kV X100 100µm 0248 21/JUN/09</p>	 <p>5kV X100 100µm 4218 29/SEP/07</p>
R - 0.6	 <p>5kV X80 200µm 0247 21/JUN/09</p>	 <p>5kV X80 200µm 0229 19/JUN/09</p>
R - 0.8	 <p>5kV X100 100µm 0227 19/JUN/09</p>	 <p>5kV X100 100µm 0228 19/JUN/09</p>
R - 1.0	 <p>5kV X80 200µm 0233 19/JUN/09</p>	 <p>5kV X80 200µm 0238 19/JUN/09</p>
R - 1.2	 <p>5kV X80 200µm 0237 19/JUN/09</p>	 <p>5kV X80 200µm 0238 19/JUN/09</p>

Figure 2. SEM images of corrugated and round fiber extruded of 300PEOT55PBT45 block co-polymer

with 0.8mm diameter round fiber for cell adhesion and proliferation. The fibers with 6 and 10 corrugations have 1.5 and 2 times higher surface area per unit volume compared to round fibers of same outer diameter (i.e. 0.8mm). The shrinkage observed after solidification with no air gap was approximately 5% (Table 1) whereas for air gaps of 0.5 to 2 cm shrinkage ranged between 10 to 20% (data not shown) due to polymer stretching before solidification. Severe deformation of channels was also observed due to viscous force acting on extruded molten polymer, which tends to form round fiber.

Table 1. Shows different types of inserts used to extrude round and corrugated fibers and their corresponding surface area per 4cm fiber sample, available for cell anchorage

Type	Insert outer Diameter, mm	Actual fiber diameter, mm	Shrinkage, %	Number of arms	Arm length, mm	Perimeter mm	Surface area, mm ²
R - 0.6	0.6	0.57 ± 0.01	5.3 ± 4.5	-	-	1.88	75.3
R - 0.8	0.8	0.77 ± 0.01	3.3 ± 1.1	-	-	2.51	100.5
R - 1.0	1.0	0.95 ± 0.01	4.8 ± 1.3	-	-	3.14	125.6
R - 1.2	1.2	1.16 ± 0.02	2.8 ± 1.8	-	-	3.77	150.8
C - 6	0.4	0.76 ± 0.02	5.5 ± 2.1	6	0.2	3.66	146.2
C - 10	0.4	0.76 ± 0.01	4.8 ± 1.6	10	0.2	5.26	210.2

3.2 Mechanical properties

Here we measured elastic modulus and tensile strength of the fiber as complete body force, applied externally over the cross-sectional area of the fiber. The initial linear slope of stress-strain curve is called young's or E-modulus which is unique to a material. Table 2 presents the values of E-modulus for the fibers produced in this work. The lower E-modulus in case of corrugated fibers is because the cross-sectional areas were calculated using the external diameter of the fiber.

Table 2. Mechanical property of round and corrugated fibers extruded of 300PEOT55PBT45 block copolymer (standard deviation $n = 5$)

Type	Arms	Actual fiber diameter, mm	E-modulus, MPa	Maximum stress σ_{max} , MPa	Stress at break ϵ_{max} , Mpa	Strain at break ϵ_{break} , %
R - 0.6	-	0.57 ± 0.03	123 ± 7	12.7 ± 0.57	12.5 ± 0.78	707.4 ± 36.8
R - 0.8	-	0.77 ± 0.01	119 ± 11	13.8 ± 0.82	13.7 ± 0.62	972.3 ± 37.8
R - 1.0	-	0.95 ± 0.01	122 ± 12	14.6 ± 0.35	14.2 ± 0.83	976.7 ± 49.1
R - 1.2	-	1.16 ± 0.02	126 ± 9	15.8 ± 0.42	15.5 ± 0.79	997.4 ± 64.2
C - 6	6	0.75 ± 0.02	107 ± 5	11.6 ± 0.68	11.3 ± 1.09	918.6 ± 61.4
C - 10	10	0.76 ± 0.01	89 ± 10	10.7 ± 0.93	10.6 ± 1.21	873.0 ± 73.7

Table 2 also presents the maximum stress and stress at break held by different fiber types. For the round fibers the maximum stress increases with increasing fiber diameter. Because the loaded deformable body is assumed as a continuum, the internal forces are distributed continuously within the cross-sectional volume of the fiber body, i.e. the stress distribution in the body is expressed as a continuous function of space coordinates and time. Hence, different fiber shape and diameter can be compared directly over differential cross-sectional area. The lower maximum stress of corrugated fibers with respect to round fiber (R-0.8) can be attributed to less internal forces due to lower material/polymer volume present. Nonetheless, the mechanical properties of PEGT/PBT corrugated fiber scaffold could be mimicked to that of round fiber scaffold simply by varying the copolymer composition, scaffold porosity and/or scaffold architecture.

3.3 Cell culture

3.3.1 Static culture

For all cases 6 fibers of 4cm long were sterilized and seeded statically with 2×10^6 cells in a tissue culture plate for 6 hours. Figure 3 shows the SEM images of cells with their extracellular matrix (ECM) adhering on its surface of the fiber after 7 days of culturing with medium exchange every alternate day. These images clearly show that the cells proliferate and cover entire surface of the fiber (the images were intentionally taken at defected spots for clear visualization of ECM on fiber surface). Seeding efficiency on the fiber was determined by the DNA assay of 1 day cultured samples.

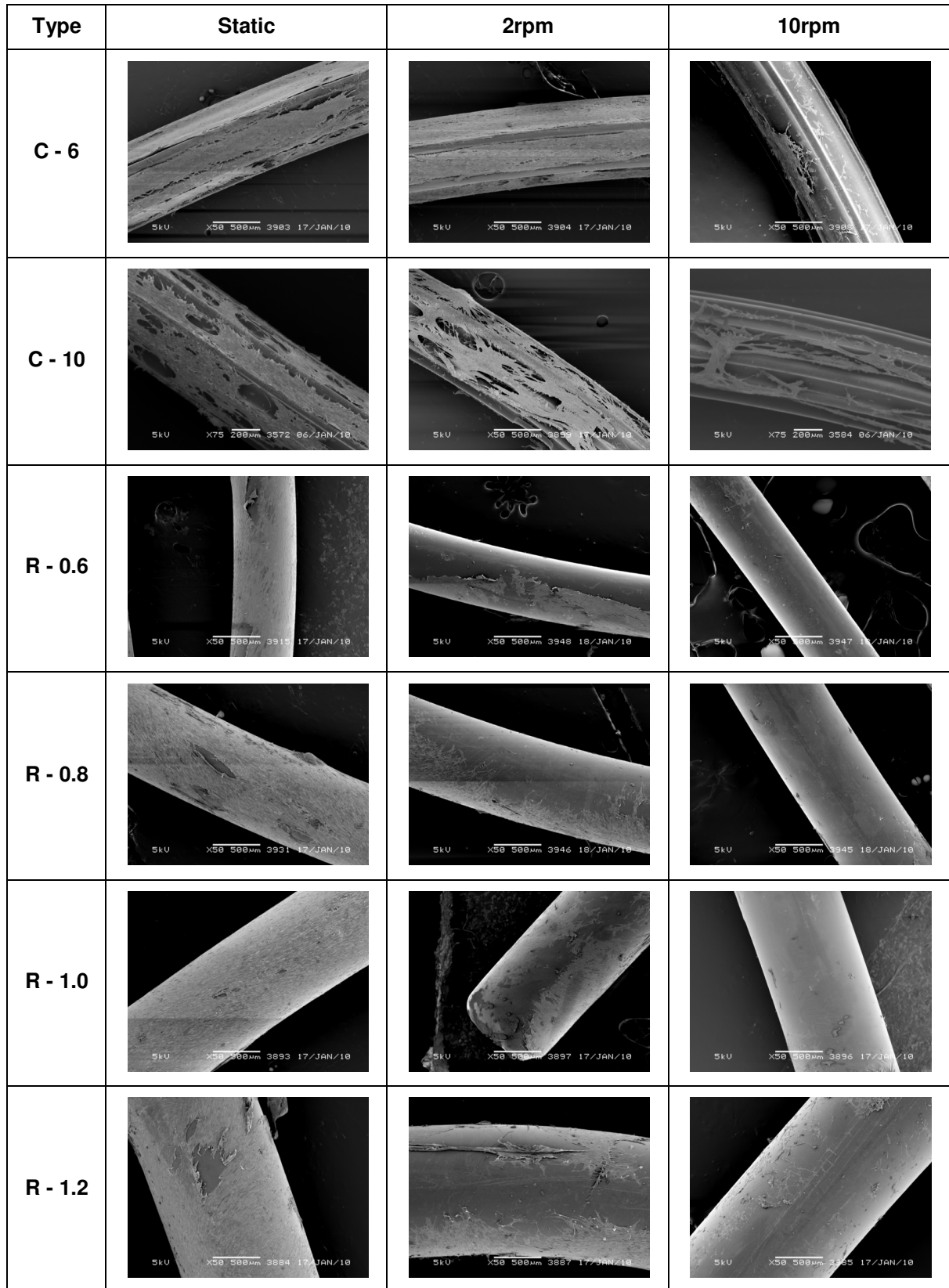


Figure 3. SEM images of ECM produced by C2C12 cells cultured for 7 days on corrugated and round fibers, statically and dynamically (2rpm and 10rpm)

The DNA data in Figure 4a shows that the number of cell seeded increases with increasing fiber diameter (R-0.6 to R-1.2), as the surface area for cell adhesion increases. However, when the DNA data is normalized per unit surface, there is no significant difference between the round fibers of various diameters (See Figure 4b). Similar results with respect to seeding were obtained in the case of corrugated fibers. But the seeding efficiency increases for corrugated fibers because the cell adhesion per unit volume increases as the surface area per unit volume increases.

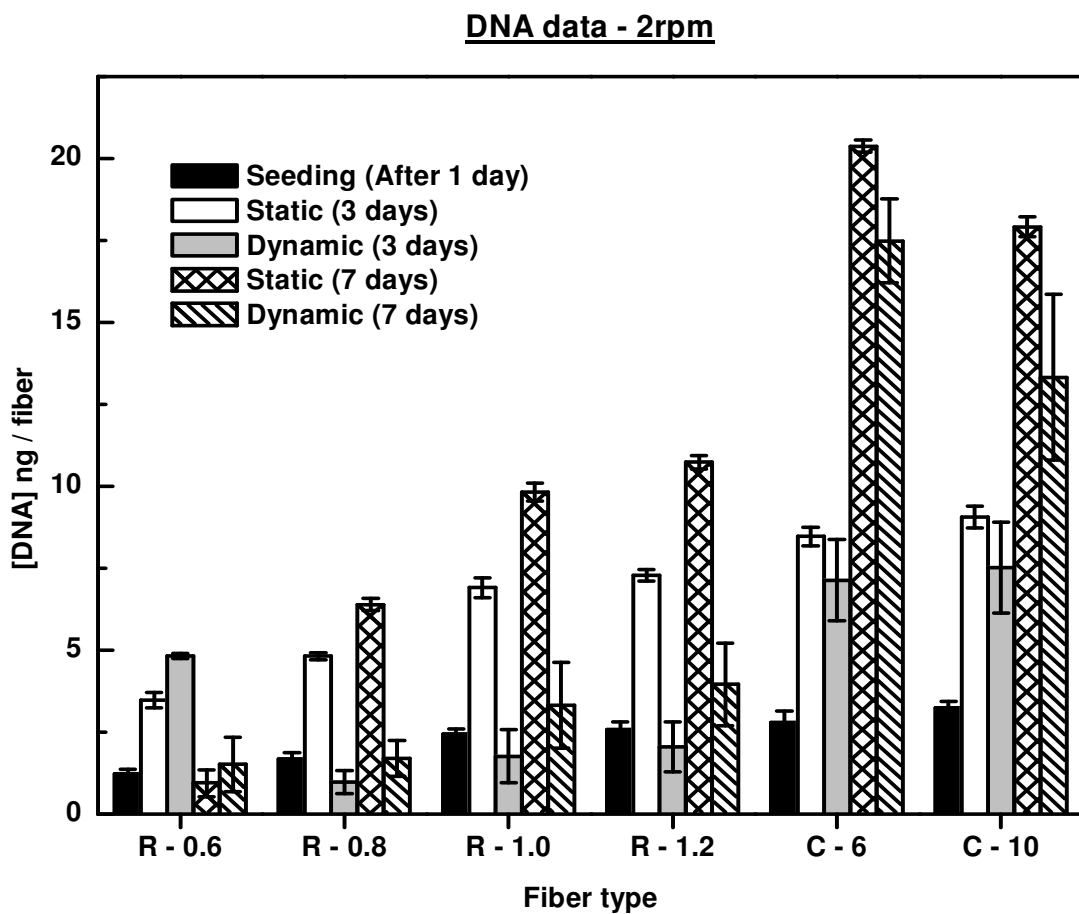


Figure 4a. DNA assay data for C2C12 cells cultured on round and corrugated fibers under static and dynamic culture conditions (2rpm) at 1, 3 and 7 days. Data represented is for 4cm long fiber available for cell adhesion, error-bar indicates standard deviation evaluated for 6 samples

Proliferation of C2C12 cells on all types of fibers was almost similar per unit surface area after 3 days static culturing (Figure 4b). At 7 days static culturing, the total cell number drastically increased in case of corrugated fibers per unit surface area. This increase in cell number may be due to better cell-anchorage to the walls of the channel and multilayer cell

growth within the channels of the corrugated fiber. The above result can also be visualised in SEM images of 7 days statically cultured corrugated fiber samples in Figure 3 shows cell and ECM filled completely within the channels. Thus corrugated fiber improves cell seeding efficiency and induces multilayer cell/tissue development.

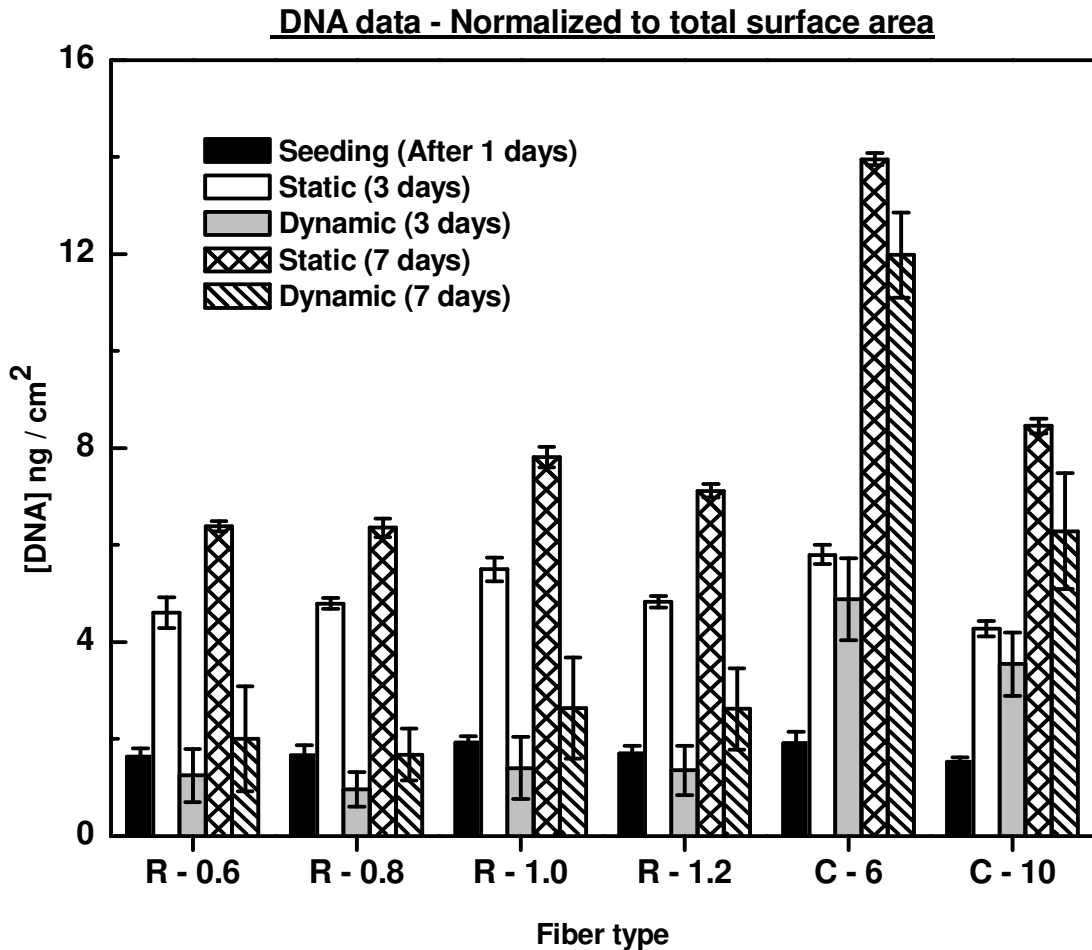


Figure 4b. DNA assay data for C2C12 cells cultured on round and corrugated fibers under static and 2rpm dynamic culture conditions at 1, 3 and 7 days. Data represented is normalized for total surface area available for cell adhesion; error-bar indicates standard deviation evaluated for 6 samples

3.3.2 Dynamic culture

Six fiber samples seeded with cells were cultured in non-treated petri dishes placed over a XYZ axis movement constant speed shaker platform. Three shaker rates of 2, 10 and 15 rpm were compared to static culture. Figure 3 shows the SEM images of 7 days static and dynamic cultured samples (2 and 10 rpm). The images clearly indicate that ECM and cell numbers are

lower as speed increases. In fact, for 15 rpm dynamic culture samples a negligible amount of cell or DNA data were measured probably due to shear force induced by the rotating culture medium. The SEM images also confirmed the above result for 15 rpm samples with no ECM deposition on fiber surface. C2C12 cells can handle shear stress of about $1-5 \text{ dyn.cm}^2$, but above this force the cells might experience harsh conditions [22]. Although shear forces acted upon the fiber-cell sample was not assessed, optimization with lower speed rate produced remarkable output.

Comparing the SEM images of 7 days dynamically cultured round fiber (Figure 3) at 2 and 10 rpm show very little ECM and/or cell proliferation with respect to static culture. But, for corrugated fibers, dynamic culture at 2 rpm show similar ECM deposition within the channels comparable to that of static culture and cell aggregates formation were found within the fiber channels of 10 rpm samples. The cell aggregates found for the corrugated fibers at 10 rpm suggest partial cell detachment due to shear stress, too. Figure 5 shows methylene blue stained light microscopy pictures of dynamic culture samples which confirm the above observation of uniform cell distributed proliferation at 2 rpm and cell aggregate formation (dark blue spots) at 10 rpm. Thus indicating that high shear stress (shaking speed more than 10 rpm), induces complete detachment of cells.

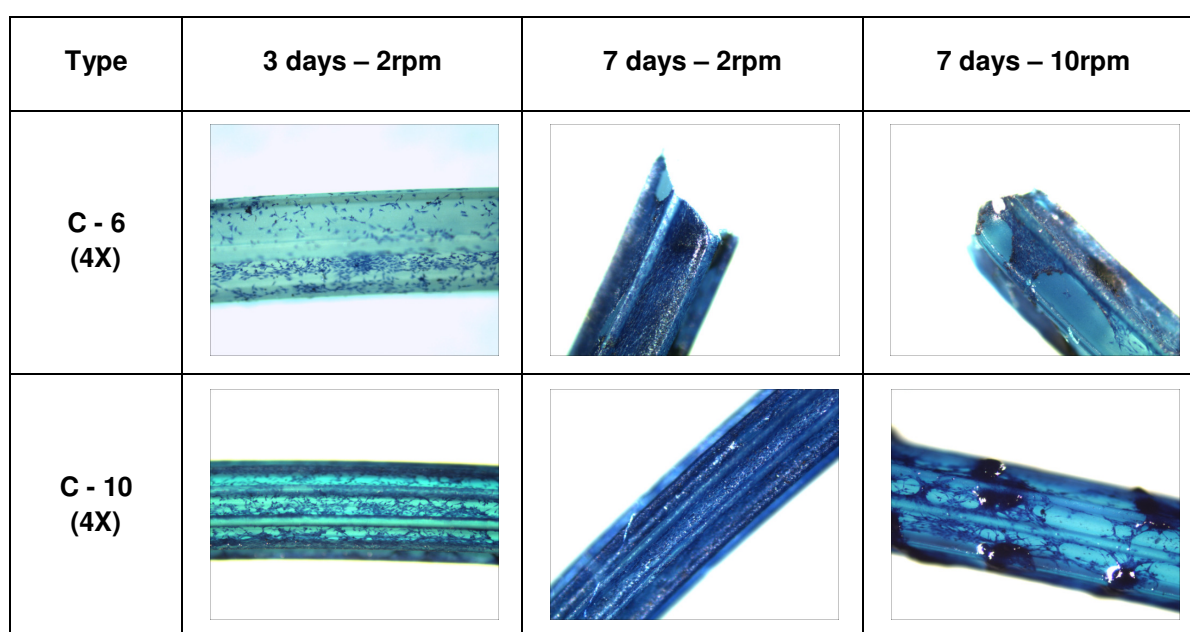


Figure 5. Light microscopic images of C2C12 cells cultured dynamically for 3 and 7 days on corrugated fiber, stained with methylene blue dye

The DNA data for 2 rpm speed dynamic culture on round fibers (Figure 4b) at 3 and 7 days shows very little cells compared to static culture respectively, which can be attributed to the lower cell adhesion on the round fiber due to curvature and direct influence of shear stress on to the anchored cells. But, corrugated fiber show good cell proliferation may be due to lower shear stress experienced within the channels and better anchorage of cells to the walls of the channel. Thus, indicating that the corrugated fibers are well suited in bioreactor culture system for tissue regeneration.

Finally, Figure 4b also shows that the DNA content per unit surface area is almost twice on corrugated fiber compared to round fiber after both 3 and 7 days of dynamic culture. This suggests that in the corrugations multilayer cell growth occurs and perhaps there the shear stress to the cell is lower. Further it can be observed that fibers with 6 corrugations have more cells (higher DNA values) compared to fibers with 10 corrugations. More experiments have to be carried out to understand the effect of corrugation dimensions to the cell attachment and proliferation.

4 Conclusion

Microstructured corrugated fibers developed in this work improve seeding efficiency and cell attachment and reduce the effect of shear stress to the cells in dynamic culture conditions. Thus, the modification in the fiber structure might accelerate the 3D tissue regeneration in large scaffolds cultured in bioreactors.

This study constitutes an important step towards the effects of fiber surface modification by (i) increasing our understanding of the influence of channels/grooves on the efficiency of cell attachment to fiber surface and the production of extracellular matrix and (ii) introducing a comprehensive approach to the investigation of the effects of bio-processing conditions on cell proliferation and fiber morphology. Taken together, the results obtained in this study motivate further investigation for fabrication of 3D corrugated fiber scaffold for tissue engineering.

5 Acknowledgements

The authors would like to acknowledge the financial support from Technology Foundation STW (Project number – TKG. 6716). We also thank Prof. Dr. C.A. van Blitterswijk, Tissue Regeneration (TR) group, University of Twente, The Netherlands, for allowing us to use the bioplotter and perform cell culture experiments in his lab.

References

- [1] F. Oberpenning, J. Meng, J.J. Yoo, A. Atala, De novo reconstitution of a functional mammalian urinary bladder by tissue engineering, *Nature Biotechnology*, 17 (1999) 149-155.
- [2] Y. Wang, U.J. Kim, D.J. Blasioli, H.J. Kim, D.L. Kaplan, In vitro cartilage tissue engineering with 3D porous aqueous-derived silk scaffolds and mesenchymal stem cells, *Biomaterials*, 26 (2005) 7082-7094.
- [3] M.B. Claase, D.W. Grijpma, S.C. Mendes, J.D. De Bruijn, J. Feijen, Porous PEOT/PBT scaffolds for bone tissue engineering: Preparation, characterization, and in vitro bone marrow cell culturing, *Journal of Biomedical Materials Research - Part A*, 64 (2003) 291-300.
- [4] J. Van Den Dolder, P.H.M. Spauwen, J.A. Jansen, Evaluation of various seeding techniques for culturing osteogenic cells on titanium fiber mesh, *Tissue Engineering*, 9 (2003) 315-325.
- [5] R. Sodian, T. Lemke, M. Loebe, S.P. Hoerstrup, E.V. Potapov, H. Hausmann, R. Meyer, R. Hetzer, New pulsatile bioreactor for fabrication of tissue-engineered patches, *Journal of Biomedical Materials Research*, 58 (2001) 401-405.
- [6] G. Vunjak-Novakovic, B. Obradovic, I. Martin, P.M. Bursac, R. Langer, L.E. Freed, Dynamic cell seeding of polymer scaffolds for cartilage tissue engineering, *Biotechnology Progress*, 14 (1998) 193-202.
- [7] S.S. Kim, C.A. Sundback, S. Kaihara, M.S. Benvenuto, B.S. Kim, D.J. Mooney, J.P. Vacanti, Dynamic seeding and in vitro culture of hepatocytes in a flow perfusion system, *Tissue Engineering*, 6 (2000) 39-44.
- [8] S. Saini, T.M. Wick, Concentric cylinder bioreactor for production of tissue engineered cartilage: Effect of seeding density and hydrodynamic loading on construct development, *Biotechnology Progress*, 19 (2003) 510-521.
- [9] R. Landers, A. Pfister, U. Habner, H. John, R. Schmelzeisen, R. Malhaupt, Fabrication of soft tissue engineering scaffolds by means of rapid prototyping techniques, *Journal of Materials Science*, 37 (2002) 3107-3116.
- [10] R. Landers, U. Habner, R. Schmelzeisen, R. Malhaupt, Rapid prototyping of scaffolds derived from thermoreversible hydrogels and tailored for applications in tissue engineering, *Biomaterials*, 23 (2002) 4437-4447.
- [11] T.B.F. Woodfield, J. Malda, J. De Wijn, F. Peters, J. Riesle, C.A. Van Blitterswijk, Design of porous scaffolds for cartilage tissue engineering using a three-dimensional fiber-deposition technique, *Biomaterials*, 25 (2004) 4149-4161.
- [12] L. Moroni, J.R. De Wijn, C.A. Van Blitterswijk, Three-dimensional fiber-deposited PEOT/PBT copolymer scaffolds for tissue engineering: Influence of porosity, molecular network mesh size, and swelling in aqueous media on dynamic mechanical properties, *Journal of Biomedical Materials Research - Part A*, 75 (2005) 957-965.

- [13] L. Moroni, J.R. De Wijn, C.A. Van Blitterswijk, 3D fiber-deposited scaffolds for tissue engineering: Influence of pores geometry and architecture on dynamic mechanical properties, *Biomaterials*, 27 (2006) 974-985.
- [14] M.B. Olde Riekerink, M.B. Claase, G.H.M. Engbers, D.W. Grijpma, J. Feijen, Gas plasma etching of PEO/PBT segmented block copolymer films, *Journal of Biomedical Materials Research Part A*, 65A (2003) 417-428.
- [15] C.M. Hwang, A. Khademhosseini, Y. Park, K. Sun, S.-H. Lee, Microfluidic Chip-Based Fabrication of PLGA Microfiber Scaffolds for Tissue Engineering, *Langmuir*, 24 (2008) 6845-6851.
- [16] D. Hamann, Comparison of seeding methods as the critical factor for cartilage tissue engineering utilizing mesenchymal stem cells on 3D fiber-deposited scaffolds, *"Osteochondral tissue engineering for total joint repair - Critical steps towards cell-based constructs"* - PhD thesis, (2008) 15 - 29.
- [17] B.J. Papenburg, L. Vogelaar, L.A.M. Bolhuis-Versteeg, R.G.H. Lammertink, D. Stamatialis, M. Wessling, One-step fabrication of porous micropatterned scaffolds to control cell behavior, *Biomaterials*, 28 (2007) 1998-2009.
- [18] M. Papadaki, T. Mahmood, P. Gupta, M.B. Claase, D.W. Grijpma, J. Riesle, C.A. Van Blitterswijk, R. Langer, The different behaviors of skeletal muscle cells and chondrocytes on PEGT/PBT block copolymers are related to the surface properties of the substrate, *Journal of Biomedical Materials Research*, 54 (2001) 47-58.
- [19] T.B.F. Woodfield, C.A. Van Blitterswijk, J. De Wijn, T.J. Sims, A.P. Hollander, J. Riesle, Polymer scaffolds fabricated with pore-size gradients as a model for studying the zonal organization within tissue-engineered cartilage constructs, *Tissue Engineering*, 11 (2005) 1297-1311.
- [20] W. Nijdam, J. De Jong, C.J.M. Van Rijn, T. Visser, L. Versteeg, G. Kapantaidakis, G.H. Koops, M. Wessling, High performance micro-engineered hollow fiber membranes by smart spinneret design, *Journal of Membrane Science*, 256 (2005) 209-215.
- [21] P.Z. Culfaz, E. Rolevink, C. van Rijn, R.G.H. Lammertink, M. Wessling, Microstructured hollow fibers for ultrafiltration, *Journal of Membrane Science*, 347 (2009) 32-41.
- [22] E. Figallo, C. Cannizzaro, S. Gerecht, J.A. Burdick, R. Langer, N. Elvassore, G. Vunjak-Novakovic, Micro-bioreactor array for controlling cellular microenvironments, *Lab on a Chip - Miniaturisation for Chemistry and Biology*, 7 (2007) 710-719.

Chapter 6

General conclusions and outlook

*What we call the beginning is often the end,
And to make an end is to make a beginning,
And the end is where we start from.*

(T.S.Eliot)

Conclusions and discussion

Limited or no vascularization in 3D tissue engineered constructs is recognized as one of the main hurdles that have to be overcome to translate tissue engineering research to clinical application. This is especially the case for large tissue engineered constructs containing active cells, since proliferating cells at the outer surface themselves act as barrier for nutrient transport in to the core of these constructs [1-5]. Moreover, nutrient and oxygen gradients will be present in the outer regions of the tissue, which could result in non-uniform cell proliferation, differentiation and integration.

In **Chapter 1**, apart from general criteria related to culturing/engineering large tissue constructs we reviewed the nutrient limitations related to the development of clinical relevant size tissue constructs. . We emphasize there that one of the challenges in tissue engineering is the nutrient supply through the scaffolds which are “essential” for uniform cellular growth across the construct. Literature has shown that cell densities decrease with distance from the construct surface and no cells within a tissue mass can survive being more than approximately 200 μ m away from a source of oxygen or nutrients [6, 7]. In adopting conventional approach such as forced nutrient diffusion into the construct in bioreactor systems, we started with the question:

How can we mimic the capillary network present in almost every tissue?

To address this question, we had to understand the principle of nutrient supply in nature. The branched capillaries facilitate the actual distribution of nutrients to the tissues in the body, which are in-turn connected with micro vessels (arterioles and venules) and macro vessels (arteries and veins) that carry fresh blood and form complete closed vascular circulatory system [5]. These capillaries distribute the blood over the tissue while lowering the pressure head, allowing blood to diffuse into the tissue. Its disruption and disorganization is a hallmark of injuries and diseases and it plays a central role during regeneration and healing.

In order to mimic this system we proposed the use of semi-permeable hollow fiber membrane integrated within the porous scaffold, designed and evaluated in *in-vitro* experimental model system. The main results presented in different chapters of this thesis are hereafter discussed.

Development and characterization of biodegradable semi-permeable membrane

Semi-permeable membrane forms the backbone for the proposed concept to overcome nutrient diffusion limitations. In order to develop a tissue construct implantable directly, biodegradable semi-permeable hollow fibers have to be incorporated. Although polymeric hollow fibers are commercially available for various other applications, only few recent publications deal with biodegradable fibers. Hence, **chapter 2** deals with the fabrication of Poly lactic acid (PLLA) fibers. There, since PLLA was rather expensive and ethanol was the non-solvent for phase separation, a miniaturized spinning setup was developed to extrude the hollow fiber. Various fiber spinning parameters like air gap, polymer concentration, addition of non-solvent (ethanol) were tailored and porogens (like Poly-vinylpyrrolidone (PVP) and Poly (ethylene-glycol) (PEG)) were added to the dope solution to develop porous fibers with high porosity and pore-interconnectivity. Post treatment with sodium hypochlorite produced open fiber surface and increased pore interconnectivity. The cell culture medium contains essential proteins (like FBS - a cocktail of 65% albumin (~ 66 kDa) and other small chain proteins), but the produced microfiltration hollow fiber is capable of delivering all the components of the medium to the cells in in-vitro perfusion bioreactor systems. The high transport properties and the low fouling properties of these fibers demonstrate their suitability for in-vitro tissue engineered constructs.

Chapter 2 showed that biodegradable PLLA hollow fiber can permeate nutrients for long period in vitro under physiological conditions mimicking the vascular network

“Combination” of technologies to create uniform 3D tissue constructs

Chapter 3 illustrates the proof of concept of improving nutrient transport within a tissue construct. Free form fabricated (FFF) scaffolds integrated with different number of hollow fibers were developed such that tissue can be cultured in closed bioreactor system. A new hollow-fiber bioreactor system of small volumes (up to 5 ml) was developed. There cells and medium were separated by hollow fiber membrane (by Gambro) and oxygenation of medium was accomplished by special oxygen permeable tubing used to feed bioreactor and open filter placed on the medium reservoir. A constant flow through the scaffold (FTS) mimics the rotating flask bioreactor by refreshing the medium continuously around the construct with low shear stress at the periphery of the scaffold. Perfusion via the hollow fiber lumen flow mimics conventional perfusion bioreactor system by permeating medium directly inside the porous space of the scaffold reducing the distance of nutrient source. Growth and viability of the cells in the bioreactor were the same or better, and the viable cell count was always higher compared to culture in static petri-dish. Optimization of operating conditions for specific scaffold architecture and cell type is feasible by simply controlling the trans-membrane pressure of the recirculating medium. This study provides a basis for development of new hollow fiber perfusion bioreactor culture methodology to overcome the limitations of passive nutrient diffusion in 3D cell-scaffold system for in-vitro tissue engineering.

Mimicking multicellular tissue organization

Most tissues and organs in our body are usually composed of multiple layers of various cell types and of varying extracellular matrix (ECM). The cells and ECM are arranged in an elaborate and hierarchical order to achieve specific function and to mutually regulate the cellular activity. The cells experience specific cues and show corresponding responses towards tissue function when in specific architecture. To maintain the proper cell phenotype in 3D tissue engineering one needs to achieve biomimetic design to replicate the multicellular organization. **Chapter 4** illustrates an approach towards such layer by layer organization by rolling pre-seeded electrospun sheets around a hollow fiber membrane which acts as a support and permeates nutrients to the cells when connected to a perfusion bioreactor system. This bottom-up approach may have a marked potential to form functional tissue composed of multiple cell types, heterogeneous scaffold composition and customized dynamic culture conditions.

Chapters 3 and 4 showed that integration of hollow fiber membranes with scaffolds is a promising approach to improve nutrient supply to the cells inside large tissue engineered constructs

Influence of fiber dimensions and texture on cell seeding and culture

Apart from optimal physiochemical properties, research has suggested that the introduction of surface topography into the scaffold improves tissue organization leading to increased tissue function [3, 8, 9]. **Chapter 5** illustrates the fabrication of round and corrugated fibers from the biodegradable polymer 300PEGT55PBT45 polymer. Static culture experiments showed higher seeding efficiency for the corrugated fibers due to surface pattern and increased surface area per unit volume. Besides, for the corrugated fibers with 6 and 10 grooves, multilayer cell growth and ECM deposition within the channels was observed. Further when subjected to shear stress during dynamic culture in a shaker flask, the cellular adhesion within the channels was higher compared to cell layers on round fibers. Extensive study has to be carried out to optimize the dimensions of channel structure which is in turn dependent on cell type.

Chapter 5 showed that the surface topography and curvature of the fiber plays a critical role influencing cell adhesion and proliferation, which can be used as a tool to produce better scaffolds

Future directions

Even though the result of this thesis show drastic improvement in cell growth and ECM deposition within 3D tissue constructs, further optimization is required for each specific cell type to culture functional tissue. Some suggestions are:

Focus on implanting in-vitro matured tissue constructs that can be micro-surgically anastomosed to host blood vessels

Although chapter 3 results suggest uniform cellular growth of 3D tissue construct, further study with integration of biodegradable hollow fiber (PLLA) is required for possible direct implantation of in-vitro matured construct. An important factor for the application of an *in vitro* matured tissue construct is its ability to connect to the host vasculature after implantation. Literature studies suggest that by co-culturing endothelial cells with the cell type of interest, one can induce capillary growth within the specific tissue of interest [10, 11]. Hence study with seeding endothelial cells into the inner wall of the fiber lumen may allow connection to the host vasculature upon implantation. Vascularization may even be better when the hollow fiber can be micro-surgically connected to the host blood system. Studies in this direction are worthwhile and can yield clues on possible lining of the endothelial cells on the walls of the fiber lumen.

Study to fabricate FFF scaffold with porous full fibers

Literature has shown that plotting of 3D FFF scaffolds inside a liquid medium is possible [12]. Hence, there might be a possibility to phase separate the plotted scaffold fiber by plotting the spinning dope solution in a non-solvent. Fabrication of FFF scaffold with interconnected porous fiber (full or hollow) would increase the medium transport in the scaffold without the need of integrating hollow fibers and preparing modules for perfusion bioreactor. For such studies, PEGT-PBT might be a suitable polymer. Figure 1 shows the SEM pictures of full fibers of 300PEGT55PBT45. For this, this polymer was dissolved in chloroform along with PVP as leachable material and extruded into ethanol at 5°C. The surface roughness of these fibers is very high which may induce better cell adhesion. However, the produced fibers have pores which are not interconnected and further optimization is required to obtain highly porous fibers.

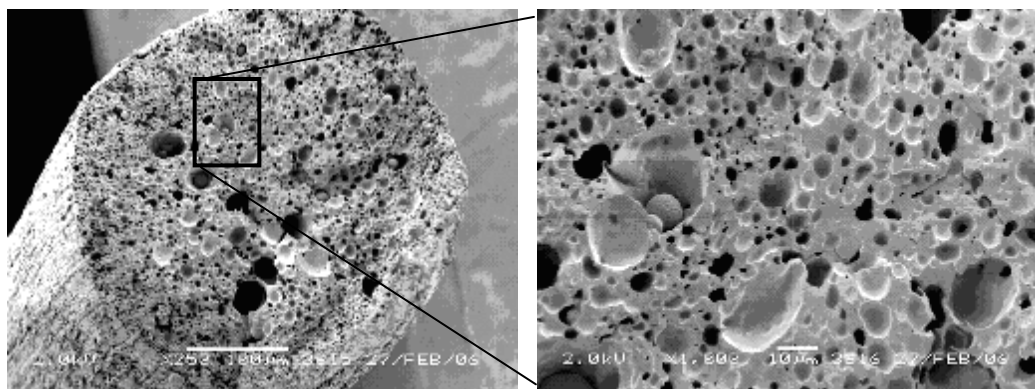
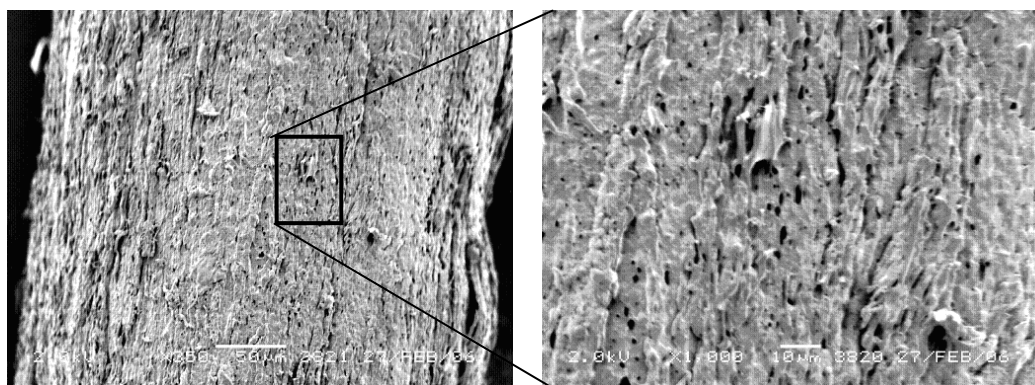
**Cross section****Surface**

Figure 1. SEM images of full fiber spun using dope solution containing 17.5wt% 300PEGT55PBT45 + 7.5wt% PVP (K-30) + 10wt% Ethanol dissolved in chloroform (non-solvent = ethanol)

Study by incorporation of multiple cell type to mimic functional tissue

It is evident from literature that cell-cell or cell– ECM interactions and co-culture of different cell type plays a crucial role in formation of functional tissue [11, 13]. **Chapter 3** illustrates the possible layer-by-layer cellular organization with control over thickness of particular cell type. Future research should focus on development of specific tissue with distinct layer-by-layer cellular organization like blood vessel, skin etc. where different cell types can be arranged by density, position and thickness. By controlling the pore size of the electrospun sheet, the degree of cellular interaction and the migration of cells or bioactive molecules could be manipulated. Further co-culture experiments in 3D environments can be easily studied in this model.

Study to investigate the effect of nano and micro surface architecture on cell culture

Literature and results of **chapter 5** shows that applying surface topography in the form of a micropattern can control the behavior of attached cells, improve seeding efficiency and tailoring the architectural design of the micropattern can have an impact on cell proliferation [3, 8, 9]. Mimicking the collagen fibrils present in natural tissue ECM, electro-spinning process (ESP) has emerged as a method to fabricate nonwoven mesh as scaffold with fiber size in the micro/nanometer scale. Introducing micro scale corrugated topography (as in **chapter 5**) within ES sheets underlined with nanofibers would be an interesting behavioral study for cell culture. Preliminary results to fabricate such Microstructures Electro Spun Sheet (MESS) are shown in Figure 2. These MESS sheets were prepared by using a micro-structured conductive collector.

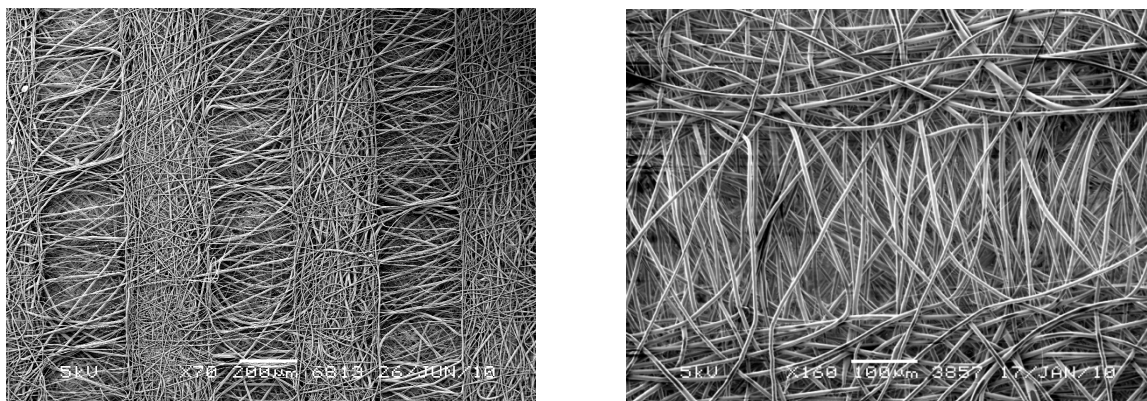


Figure 2. SEM images of MESS samples fabricated with PLLA dissolved in 1,3 dioxane (500 μ m channel width, 300 μ m channel depth, 500 μ m distance between channels)

Preliminary results of C2C12 cell culture study on these MESS samples reveal that the cells align within the channel, adhering to the ES nanofibers which are perpendicular to the channel length (see Figure 3).

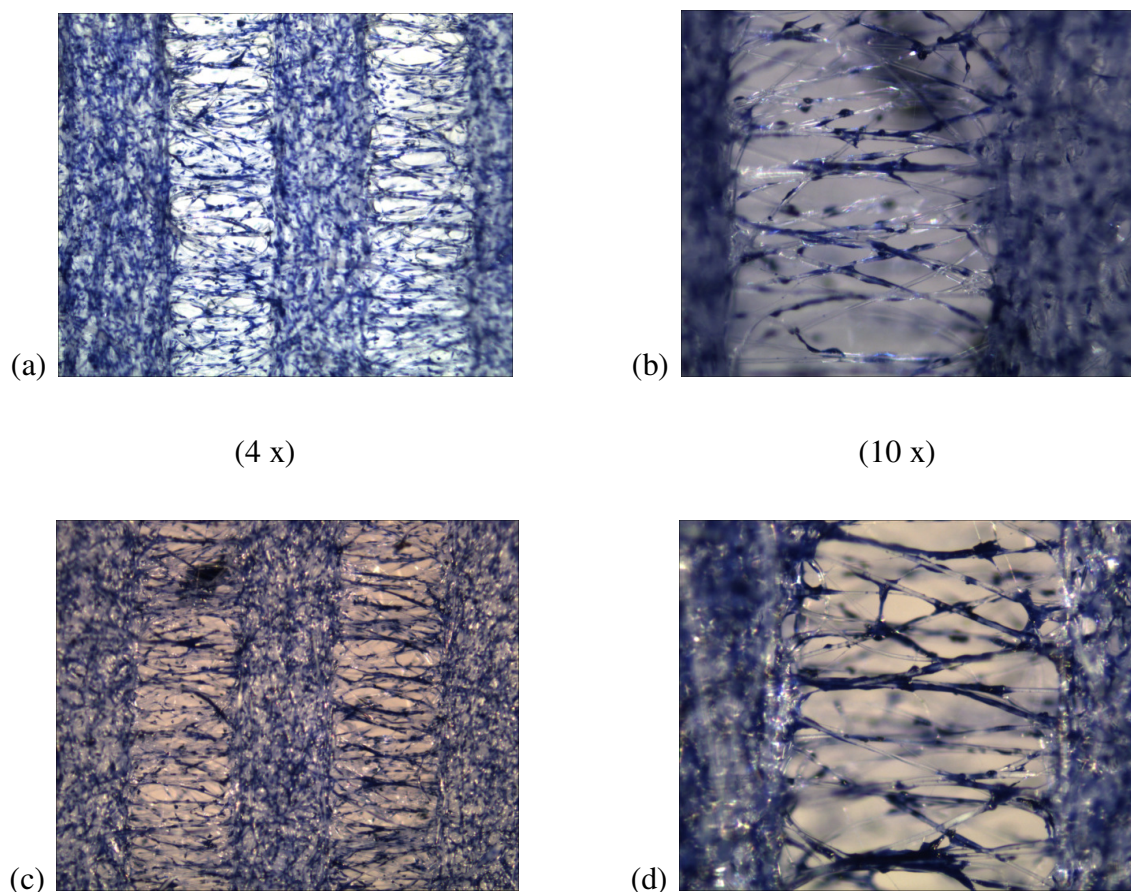


Figure 3. Light microscopy images of methylene blue stained MESS samples (500 μm channel width) cultured statically with C2C12 cells, (a) and (b) after 1 day culture (c) and (d) after 3 days, seeding density 4,000 cells/cm²

Study to develop online analysis of cell proliferation

Bioreactor systems for cell based processes resulting in clinical and commercial viable products need automation and reproducibility in addition to being cost-effective and safe. To scrutinize various parameters and reduce the number of experiments and contamination, it is advantageous to have online analysis of cell proliferation. Alamar blue dye assay is a method for monitoring cell proliferation in-vitro. Alamar BlueTM is a non-fluorescent compound which yields a fluorescent product after reduction e.g. by living cells. In contrast to the MTT-assay or CyQuant proliferation assay kit, the Alamar BlueTM-assay does not lead to cell death rather the cells can be cultivated further. However, when not removed from the cells, the Alamar BlueTM shows a reversible, time- and concentration-dependent growth inhibition (as observed for leukemic cell lines). When applied in the medium reservoir of a hollow-fiber bioreactor system, the dye can be delivered to the cells across the hollow-fiber membrane, reduced by the cells and released from the cell into the medium reservoir back again. Thus,

fluorescence intensity can be measured in medium samples reflecting growth of the cells in the cell compartment. Here, the handling steps would be minimized since no cells need to be taken for readout. Moreover, after exchange with normal medium, the cells can be cultivated further which could be a major advantage of this system.

References

- [1] Burgarski B, Jovanovic D, Vunjak-Novakovic G. Fundamentals of animal cell immobilization and microencapsulation - Bioreactor systems based on microencapsulated animal cell cultures. Florida: CRC press; 1993.
- [2] Colton CK. Implantable biohybrid artificial organs. *Cell Transplantation*. 1995;4:415-36.
- [3] Dunn JCY, Chan WY, Cristini V, Kim JS, Lowengrub J, Singh S, et al. Analysis of cell growth in three-dimensional scaffolds. *Tissue Engineering*. 2006;12:705-16.
- [4] Malda J, Rouwkema J, Martens DE, le Comte EP, Kooy FK, Tramper J, et al. Oxygen gradients in tissue-engineered Pegt/Pbt cartilaginous constructs: Measurement and modeling. *Biotechnology and Bioengineering*. 2004;86:9-18.
- [5] Ko HCH, Milthorpe BK, McFarland CD. Engineering thick tissues - the vascularisation problem. *European Cells and Materials*. 2007;14:1-19.
- [6] Carmeliet P, Jain RK. Angiogenesis in cancer and other diseases. *Nature*. 2000;407:249-57.
- [7] Hassan KA, Mervat El A, Nadia M, Mohsin B. Intercapillary distance measurement as an indicator of hypoxia in carcinoma of the cervix uteri. *International journal of radiation oncology, biology, physics*. 1986;12:1329-33.
- [8] Martínez E, Engel E, Planell JA, Samitier J. Effects of artificial micro- and nano-structured surfaces on cell behaviour. *Annals of Anatomy - Anatomischer Anzeiger*. 2009;191:126-35.
- [9] Papenburg BJ, Vogelaar L, Bolhuis-Versteeg LAM, Lammertink RGH, Stamatialis D, Wessling M. One-step fabrication of porous micropatterned scaffolds to control cell behavior. *Biomaterials*. 2007;28:1998-2009.
- [10] Madri JA, Pratt BM, Tucker AM. Phenotypic modulation of endothelial cells by transforming growth factor-beta depends upon the composition and organization of the extracellular matrix. *The Journal of Cell Biology*. 1988;106:1375-84.

- [11] Rouwkema J, Boer JD, Blitterswijk CAV. Endothelial Cells Assemble into a 3-Dimensional Prevascular Network in a Bone Tissue Engineering Construct. *Tissue Engineering*. 2006;12:2685-93.
- [12] Landers R, Pfister A, Hubner U, John H, Schmelzeisen R, Mulhaupt R. Fabrication of soft tissue engineering scaffolds by means of rapid prototyping techniques. *Journal of Materials Science*. 2002;37:3107-16.
- [13] Papenburg BJ, Liu J, Higuera GA, Barradas AMC, de Boer J, van Blitterswijk CA, et al. Development and analysis of multi-layer scaffolds for tissue engineering. *Biomaterials*. 2009;30:6228-39.

Summary / Samenvatting

Great things are not done by impulse, but by a series of small things brought together.

(V. van Gogh)

Summary

Tissue engineering aims at restoring or regenerating a damaged tissue. Often the tissue recreation occurs by combining cells, derived from a patient biopsy, onto a 3D porous matrix, functioning as a scaffold. After isolation and eventual in-vitro expansion, cells are seeded on the scaffolds and depending on the strategy, implanted directly or at a later stage (after in-vitro maturation) in the patient's body. Although tissue engineering is promising and has been an active field of research for several decades now, the number of successful clinical applications is rather limited and are mostly limited to thin or avascular tissues like skin and cartilage. One of the current limitations of tissue engineering is the inability to provide sufficient nutrient and oxygen supply in developing 3D in-vitro culture.

In human body the vasculature is, along with the lymphatic and the nervous system, embedded into almost every tissues and organs. Large blood vessels (arteries, veins) and smaller vessels (capillaries) are part of the vascular circulatory system. They transport blood, and thus nutrients and waste products, to and from almost any part of the body. It is a critical template for the exchange of gas, nutrients, cells or molecules and a regulator of tissue development. Insufficient vascularization within the construct results in nutrient limitations, which in-turn results in suboptimal integration of, and cell death in tissue engineered constructs. Several strategies to overcome this limitation have been studied in the past. These include biological stimuli like dosing angiogenic growth factor, scaffold design to facilitate angiogenesis, prevascularization and physical strategies like highly porous interconnected scaffold design and bioreactor culture system for convective diffusion across the construct. In 3D in-vitro tissue engineered constructs, the formation of vessels takes time, diffusion through the tissue is confined to 100-200 μm from source and proliferating cells themselves act as barrier for convective transport. **Chapter 1** (introduction of the thesis) discusses those issues in more detail.

This thesis explores a new approach by integrating semi-permeable porous hollow fiber membrane in to tissue engineered scaffolds to mimic capillary network. The rationale of this method is that the hollow fibers integrated within the tissue engineered scaffolds would supply required nutrients and gases through the walls of the fiber during in-vitro perfusion

bioreactor culture. After implantation of the resulting mature construct, the hollow fiber network could be connected to the vasculature of the host and thus become a functional, perfused vascular network that provides the construct with nutrients and thus a better survival of the implant.

Chapter 2 describes the development of bio-degradable porous Poly lactic acid (PLLA) hollow fiber using a miniaturized spinning setup. Various fiber spinning parameters (air gap, polymer concentration, addition of non-solvent (ethanol) are tailored and porogens (like Polyvinylpyrrolidone (PVP) and Poly (ethylene-glycol) (PEG)) are added to the dope solution to develop porous fibers with high porosity and pore interconnectivity. The produced fiber have high clean water, BSA and FBS protein permeation which are suitable for delivering medium to the cells in perfusion bioreactor systems. Furthermore, the good cell (C2C12) adhesion and proliferation on the fiber surface in static culture system shows the cytocompatibility of the fiber, whereas dynamic cell culture results demonstrate the suitability of the produced fiber for mimicking vascularization in-vitro for tissue engineering applications.

Chapter 3 illustrates the proof of concept of integration of 3D tissue engineering scaffold with hollow fibers to improve nutrient supply in-vitro. The bioreactor system developed is highly flexible since several systems can be run in parallel with ease in controlling. It is shown that, convective transport through the porous walls of the hollow fiber is crucial to reduce mass transfer limitations and nutrient gradients within the scaffold. However the distance between the hollow fibers or number of fibers integrated depends on scaffold type (specificity) and size.

In nature most tissues are made of multiple cell types in specific organization to perform particular function. Hence, development of clinically relevant size tissues with complex architecture remains a great challenge. **Chapter 4** reports a novel approach to develop 3D multilayer tissue using bottom-up process by rolling pre-seeded ES sheets around multibore hollow fiber. The rolling of pre-seeded ES sheet to form multilayer constructs achieves uniform cell distribution in the scaffold. This approach has a marked potential to form functional tissue composed of multiple cell types, heterogeneous scaffold composition and customized dynamic bioreactor culture conditions.

The study in **chapter 5** suggests that the surface structure and curvature of the fiber plays a critical role in cell adhesion and proliferation and can be used as a tool to produce better

scaffolds for tissue engineering. In this study, corrugated fibers (with grooves or channels) were produced by extruding polymer solutions through spinnerets with suitable inserts. Novel straight channel corrugated fibers of biodegradable polymer with 6 and 10 grooves on the fiber surface were compared with round fibers. An improved efficiency of cell seeding and proliferation in static and reduced effect of shear stress to the cells in dynamic culture conditions has been observed. The results obtained in this study motivate future investigation for possible cell alignment within the channels and fabrication of 3D corrugated fiber scaffold for tissue engineering.

In **Chapter 6**, the main conclusions of the thesis are discussed and most importantly an outlook for future studies is given.

Samenvatting

Met Tissue engineering probeert men beschadigd weefsel te repareren of zelfs te regenereren. Dit gebeurt vaak door een combinatie te gebruiken van cellen, die worden geïsoleerd uit een biopsie van de patiënt, op biomateriaal te zaaien dat als steigermateriaal (scaffold) werkt. Na de isolatie van de cellen en de eventuele expansie in vitro worden de cellen gezaaid op de scaffold en afhankelijk van de strategie direct of in een later stadium teruggeplaatst in het lichaam. Hoewel tissue engineering al tientallen jaren een veelbelovend veld van onderzoek lijkt, staat het klinische gebruik van de technieken nog in de kinderschoenen. Wat er van de technieken gebruikt wordt is meestal in dun of niet-doorbloed weefsel, zoals kraakbeen of huid, inzetbaar. Dit komt doordat in het gebruik van tissue engineering voornamelijk zuurstof en voedingsstoffen beperkende factoren zijn in groeiende 3D in vitro kweken.

In het menselijk lichaam zijn vaten, samen met het lymfestelsel en het zenuwstelsel, ingebed in bijna elk weefsel of orgaan. Grote bloedvaten (aderen en slagaderen) en kleinere vaten (capillairen) zijn een deel van dat systeem. Ze transporteren het bloed en daarmee voeding- en afvalstoffen van en naar elk deel van het lichaam. Dit systeem is een perfect voorbeeld van een uitwisseling van gas, voedingsstoffen, moleculen en cellen die de groei van het weefsel sturen. Wanneer er te weinig vascularisatie is leidt dat direct tot een gebrek aan voedingsstoffen, wat daarbij weer zorgt voor celdood of slechte integratie van het nieuwe weefsel in het lichaam. Verschillende strategieën om dit probleem aan te pakken zijn door de jaren heen bestudeerd. Er is bijvoorbeeld geprobeerd om vasculatuur sneller te laten ontstaan door groeifactoren te verstrekken of door veranderingen aan te brengen in de vorm van de scaffold; en er zijn pogingen gedaan tot prevascularisatie. Ook fysische manieren zijn geprobeerd door erg interconnectieve scaffolds te maken of bioreactoren te gebruiken. In een in vitro gekweekte 3D structuur kost de formatie van aderen tijd. De diffusie door weefsel is vaak beperkt tot 100-200µm. Daarbij zorgt groei van weefsel meestal voor een grote barrière in het transport. **Hoofdstuk 1** (de introductie van het proefschrift) bediscussieert deze problemen.

In dit proefschrift is een nieuwe manier van voedingsstoffentransport beschreven. Hierbij wordt een semidoorlatende poreuze holle vezel membraan gebruikt om een capillair netwerk

te vormen in een tissue engineering scaffold. Het oorspronkelijke idee voor deze manier is dat de holle vezels in het tissue engineering systeem voedingstoffen en zuurstof kunnen leveren tijdens het *in vitro* kweken van het weefsel in de bioreactor. Na implantatie van het gevormde weefsel zouden de holle vezels gebruikt kunnen worden om de verbinding te vormen tussen het nieuwe weefsel en het lichaam, waardoor het weefsel beter doorbloed wordt en er meer van het weefsel gebruikt kan worden door de patiënt.

Hoofdstuk 2 beschrijft de ontwikkeling van een biodegradabele poreuze holle vezel gemaakt uit polimelkzuur. Verschillende parameters van het spinproces (hoogte van de spinaret tot de nonsolvent, polymeerconcentratie, ethanol toevoeging aan de oplossing, porogenen) zijn toegevoegd en aangepast zodat er poreuze vezels zijn gevormd met hoge interconnectiviteit. Deze vezels zijn erg permeabel voor water. Ook BSA en FBS permeatie is mogelijk en voldoende om de vezels te kunnen gebruiken voor celkweek met bioreactor systemen. Er zijn met deze vezels meer testen uitgevoerd om te bekijken of ze daadwerkelijk gebruikt kunnen worden voor celkweek. Uit deze testen blijkt dat cellen er goed op kunnen hechten en ook prolifereren in statische systemen. Dynamische kweken met deze vezels laten zien dat de vezels goed te gebruiken zijn om vascularisatie te vormen in *in vitro* applicaties van tissue engineering.

In **hoofdstuk 3** wordt het bewijs geleverd voor het principe van het gebruik van de holle vezels voor de verbetering van het leveren en afvoeren van voeding- en afvalstoffen. Het bioreactorsysteem dat is gevormd is erg flexibel omdat er meer systemen parallel aan elkaar kunnen worden geschakeld en gecontroleerd. Het is bewezen dat transport door de vezels cruciaal is om voedingstoffen in het hele 3D construct te brengen. De afstand van de vezels tot elkaar en de hoeveelheid vezels in een construct zijn afhankelijk van de scaffold die wordt gebruikt en de interconnectiviteit van het weefsel.

In de natuur zijn de meeste weefsels gemaakt uit verschillende typen cellen met een specifieke organisatie. In tissue engineering blijkt dit nog een grote moeilijkheid. Voor het maken van grotere weefsels is het wel nodig om verschillende celtypen te gebruiken om de voedingstoffen bij het weefsel te brengen. In **hoofdstuk 4** wordt een nieuwe aanpak beschreven waarbij verschillende, met cellen voorgezaaide, electrogesponnen lagen om een holle vezel heen worden gedraaid, zodat een uniforme verdeling van cellen in de scaffold wordt bewerkstelligd. Deze aanpak heeft toekomst in het gebruik voor functionele weefsels, gemaakt uit verschillende celtypen.

Het onderzoek in **hoofdstuk 5** laat zien dat het oppervlak en de structuur van de vezels een rol speelt in cel adhesie en proliferatie. Dit zou gebruikt kunnen worden om betere scaffolds te vormen. In dit onderzoek is gebruik gemaakt van holle vezels met vormen of kanaaltjes aan het oppervlak. Deze worden gemaakt door een spinaret te gebruiken met verschillende vormen. Vezels met 6 tot 10 kanaaltjes werden vergeleken met gladde vezels. Er blijkt een betere efficiëntie van het zaaien van cellen te worden bewerkstelligd op deze manier en in dynamische kweken blijken de cellen ook minder hinder te ondervinden van schuifkrachten. Van deze techniek zou in de toekomst ook gebruik kunnen worden gemaakt bij het vormen van weefsels waarbij de cellen in dezelfde richting moeten groeien.

In **hoofdstuk 6** worden de belangrijkste conclusies van dit proefschrift bediscussieerd. En, belangrijker, er wordt gekeken naar mogelijkheden voor toekomstig onderzoek.

Acknowledgements

Think where mans glory most begins and ends, And say my glory was I had such friends.

W.B. Yeats

Personally this thesis has provided me with a great experience in approaching multi-disciplinary research. Preparation, patience, patience, patience and a bit of luck are the known important factors in achieving quality research and so it was no surprise that these were also experienced during the course of this thesis. I have enjoyed the experience though many things may have gone wrong in some way or other, however I do feel as though I have learnt the most by being as independent as possible. Hopefully this will help me in the future assignments of the sort.

These years have been an incredible journey of personal and professional discovery. I want to thank Prof. Dr.-Ing. Matthias Wessling for giving me the opportunity to do my PhD research in your laboratory. I have nothing but admiration for you, both as a person and as a budding scientist. I thank you for the freedom and trust you kept in me. Hope I can follow your foot steps in my career.

I would like to thank my daily supervisor Dr. Dimitris Stamatialis. I sincerely appreciate your time, guidance and feedback throughout my PhD study (also for all sorts of crazy ideas). I have learned a lot and gained many positive experiences during this period, experiences which will hopefully allow me to tackle even bigger challenges in the future. Your contribution at the end was immense, Just thank-you would be an understatement for your contribution, anyway thanks....

At this moment I would like to remember and thank Prof. Dr.-Ing. Volkmar Jordan of FH-Munster university and Dr. Christiane Richard-Elsner of Cognis GmbH, Germany, for recognizing the research ability in me and advising me to pursue this PhD. I am also indebted to Prof. Ananthram, Dr. M. V. Ramani and Prof. Shiney of India, Prof. Büttner and Prof. Korff of Germany who laid a strong foundation for my scientific career. My special thanks to my back home friends Deepak, Shridhar, Manjunath, Ravisha, Girish, LNGupta and lot more.

Greet and John Heeks you are exceptional persons in the group who constantly help with patience (especially the foreigners). It's a privilege to all of us, you being a part of the group. Dank-u-wel

Many thanks to Nathalie (dutch-Pele), Irene (laughter girl), Joao (junior) and Hilde (special thanks to you and Paul for translating the summary to dutch) for working with me and helping me to achieve this work. I (mostly) liked working together with you and it wouldn't have been the same without you guys.

Standing to my sides (as always) are two of my best friends as paranymphs. Thank you guys you made my life easier by taking all the responsibility, starting with reading and printing this book till arranging the defense party, while I was enjoying back home in India.

I cannot forget the sweet memories shared with lots of officemates starting with Magda, Mariam, Saiful, Katja, Clara, Szymon (in Langezijds) and Alisha, Can, Kishore (in Meander). Thank you guys for the nice atmosphere and the friendly talks/discussions.

Thanks to all the dutch colleagues Rob, Kitty, Antoine, Zandrie, Herman, Harmen, Eric, Ineke, Lydia, Marcel, Tymen, Hilke, Wika, Jorrit, Paul, Sander, Annacoline, Marlon . . . for letting me know the dutch culture and showing me around Enschede and other parts of Netherlands. Thanks for persuading me to take part in Batavieren race twice running 8kms (I don't think I will ever even dream of doing it again).

The international atmosphere in MTG was stimulating in all corners, thanks once again to Matthias for including me in this pool. Of-course I want to thank all the membraniacs for including me as one of it, especially Jens, Maik, Hakan, Nilesh (Nillu), Joao, Gor, Al-Hadidi, Ikenna, Matias, Jorg, Dana, David, Zynep, Izabela, Gor, Hans, Schwan, Geraldine, Nicolas, Jumeng, Giri, Ana, Magda, Olga, Enver, Elif, Sreenath I would miss the most important socializing coffee and rauchen breaks (although I do not smoke) which were required at times thanks to all the members of MTG. Heartfelt thanks to Katja-Christoph, Szymon-Danuta and Agata-Wilco for inviting me to your wedding.

This thesis being a multidisciplinary topic, I spent half the time in TR group, thanks to Prof. Clemens van Blitterswijk for letting me use his lab. Thanks to Lorenzo, Jeroen, Ram, Nico, Gustavo, Hemanth, Anand, Hugo, Ananditha, Jacqueline and Anouk (thanks for your efforts to find the cause for infection).

I cannot forget the mini India in enschede, without you I would forget all Indian festivals and miss delicious Indian food. Thanks to Seshan-Jayanthi, Pramod-Vishaka, Chandu-Meenakshi, Ambati-Sangeetha, Ram-Veda, Mayur-Shradha, Jigar-Phalguni, Srihari-Lakshmi, Giri-Varsha, Kishor-Hema, Dhaval-Hinal, Digvijay-Abba, Mustafa-shahina, Babu-Indu, Vinay, Tony, Manish, Sameer, Amol, Raghav, Vishnu, Andy, Shanker, Ashok (Mottu), Anand (chakki), Shashank, Raja, Rani, Hrudya, Jalaja, Lavanya, Kotti, Raghu (DB), and many more. Also, Thanks for believing in me and giving financial responsibility for both Indian Student Association (ISA@UT) and AADHAAR (an NGO at UT), I really enjoyed serving for good cause. Hope I can continue this good work.

I have no words to express my gratitude to the most important persons during this PhD. Jitu, Sandeep and KK, without you, I wouldn't have had energy and enthusiasm to do this work. I hope you would forgive me for all the ups and down during our stay together. I wish you all a bright future in professional and personal life.

I know I have missed lot of you guys, but you know when it comes to names I have a very bad memory, but that does not make my appreciation to you any less, SO

Dhanyawaadagalu, Anugurihiitosmi, Bedankt, Shukriya, Dziekuje, Efharisto poli, Danke, Merci, Obrigado, Grazie, Çok sagolun, Shukran, Imena, Dêkuji, Makasih, Padiux, Multumesc, Komapsumnida, Mersie, Gracias,
THANK YOU ALL!!!

Lastly, Big thanks to Amma and Anna (mom and dad) not only this PhD thesis, but anything and everything I achieve will be dedicated to you (it's all because of lord Narasimha and your ashirvada). Thank-you for your confidence in me and all the freedom. I would also like to thank my uncle Appannaiah (big-dad) for his elderly advices throughout my accomplishments. A bulk of credit also goes to my brothers (3 Sri bro's), sister-in-laws, cousins and to my nephews and niece for your support and cheering me up always. As this life chapter comes to a close, I look forward to the start of new chapters and adventures.

श्री

Sri

If the only prayer you ever say in your entire life is 'thank you,' it will be enough.

(Meister Eckhart)

Curriculum vitae

NM Srivatsa Bettahalli was born on 31st of March 1978 in Bangalore, India. He finished the bachelor degree in chemical engineering at BMS Engineering College (Bangalore, India) in 1999. He did his bachelor thesis at the company United breweries (UB-group), Bangalore, India on *'Estimation of steam consumption & beer losses in the process of production of a particular beer brand'*. Further, he started studying Master of Science in chemical engineering at the Münster University of Applied Sciences (Steinfurt, Germany) in 2002 and finished his study in 2005. He did his master thesis at the company Cognis Deutschland GmbH, Düsseldorf, Germany on *'Removal of Maillard compounds from protein products'* for this he received outstanding performance award. After the graduation in 2005 he started as a PhD student in the multidisciplinary field of tissue engineering in the *Membrane Technology Group* at the University of Twente (Enschede, The Netherlands). The research was performed on reducing in-vitro mass transfer limitation present in 3D tissue engineering scaffolds by using polymeric membranes, under the supervision of Prof. M Wessling, Prof. CA van Blitterswijk and Dr. D Stamatialis, the results of which are described in this thesis *'Membrane supported scaffold architectures for tissue engineering'*. On a personal level, he loves traveling around the world, adventurous sports, cooking, and family & friends.



Notes

Notes

Notes

Notes